The regulatory properties of the PII-like protein SbtB on the CO_2-concentrating mechanism in cyanobacteria

Die regulatorischen Eigenschaften des PII-ähnlichen Proteins SbtB auf den CO_2-Konzentrationsmechanismus in Cyanobakterien

---

Kumulative Dissertation
zur Erlangung des akademischen Grades
doctor rerum naturalium (Dr. rer. nat.)
der Mathematisch-Naturwissenschaftlichen Fakultät
der Universität Rostock

vorgelegt von
Oliver Mantovani
geb. am 06.05.1995 in Tradate (Italien)

Rostock, 2024

https://doi.org/10.18453/rosdok_id00004846

Gutachter:

Prof. Dr. Martin Hagemann, Universität Rostock, Institut für Biowissenschaften

Prof. Dr. Dr. Annegret Wilde, Universität Freiburg, Institut für Biologie III

Jahr der Einreichung: 2024

Jahr der Verteidigung: 2024

Table of contents

Zusammenfassung

Cyanobakterien sind die „Erfinder“ der sauerstoffhaltigen Photosynthese und können CO_2 durch die Carboxylierungsreaktion von RuBisCO im Calvin-Benson-Bassham-Zyklus binden. Aufgrund der modernen niedrigen CO_2- und hohen O_2-Konzentrationen in der Atmosphäre, bindet RuBisCO manchmal fälschlicherweise O_2 durch die Oxygenierungsreaktion, was zu einer Energieverschwendung für die Zellen führt. Um das Problem zu lösen, haben Cyanobakterien den anorganischen Kohlenstoffkonzentrationsmechanismus (CCM) entwickelt, der es der Zelle ermöglicht, die CO_2-Konzentration um RuBisCO herum zu erhöhen, um das Auftreten der Oxygenierungsreaktion effektiv zu reduzieren.

Einer der Hauptbestandteile des CCM ist der Bikarbonattransporter SbtA, der durch SbtB reguliert wird, einem kleinen Proteinteil der PII-ähnlichen Superfamilie. Mit der Fähigkeit, eine Vielzahl von Adenylnukleotiden zu binden, ist SbtB in der Lage, die Energie-, anorganischen Kohlenstoff- und Lichtzustände der Zelle zu erfassen, die Aktivität mehrerer Komponenten des CCM und des Kohlenstoffstoffwechsels zu modulieren und es Cyanobakterien so zu ermöglichen, sich effizient an schwankenden Kohlenstoff anzupassen Bedingungen. Seine Hauptregulierungsfunktion übernimmt die T-Schleife, ein Bestandteil des Proteins, der je nach Ligand an der Bindungsstelle unterschiedliche Strukturen annimmt. Sein Hauptinteraktionspartner ist der Transporter SbtA, mit dem es auf unterschiedliche Weise interagiert, um entweder den Transport zu hemmen, wenn er nicht benötigt wird, oder um das Austreten von Bikarbonat zu verhindern und so Energieverschwendung zu vermeiden. Die Interaktion mit dem Transporter wird durch zwei einzigartige Funktionalitäten von SbtB beeinflusst, nämlich seine ATP/ADPase-Aktivität und seine C-terminale redoxempfindliche Schleife. Beide werden von der Lichtphase beeinflusst, sodass SbtB die CCM entsprechend dem zyklischen Licht des Tagesrhythmus regulieren kann. Zusätzlich zur Regulierung von SbtA ist das Protein in der Lage, durch die c-di-AMP-abhängige Interaktion mit dem Glykogen-Verzweigungsenzym den Glykogenstoffwechsel direkt zu beeinflussen, um die Glykogensynthese während des Tages zu fördern. Darüber hinaus erweitert SbtB seine regulatorische Funktion auf die Genexpression beider Komponenten der CCM- und Ci-regulierten Gene.

Daher eröffnete die Entdeckung und hier durchgeführte Charakterisierung der SbtB-Funktionalität ein neues Paradigma für die Regulierung der Aufnahme und des Einbaus von anorganischem Kohlenstoff in Cyanobakterien.

Summary

Cyanobacteria are the “inventors” of oxygenic photosynthesis and are able to fix CO_2 through the carboxylation reaction of RuBisCO in the Calvin-Benson-Bassham cycle. With the modern low CO_2 and high O_2 concentrations in the atmosphere, RuBisCO sometimes erroneously fixes O_2 through the oxygenation reaction, causing the cells an energy wastage. To solve the issue, cyanobacteria evolved the inorganic carbon-concentrating mechanism (CCM), which allows the cell to increase the concentration

of CO_2 around RuBisCO to effectively reduce the occurrence of the oxygenation reaction.

One of the main components of the CCM is the bicarbonate transporter SbtA that is regulated by SbtB, a small protein part of the PII-like superfamily. With the ability to bind a variety of adenyl nucleotides, SbtB is capable of sensing the energy, inorganic carbon and light states of the cell, to modulate the activity of multiple components of the CCM and carbon metabolism, allowing cyanobacteria to efficiently adapt to fluctuating carbon conditions. Its main regulatory function is carried out by its T-loop, a component of the protein which assumes different structures depending on the ligand in the binding site. Its main interaction partner is the transporter SbtA, which it interacts with in different ways to either inhibit transport when not needed or to prevent leakage of bicarbonate to avoid energy waste. The interaction with the transporter is affected by two unique functionalities of SbtB, namely its ATP/ADPase activity and its C-terminal redox-sensitive loop. Both are affected by the light phase, allowing SbtB to regulate the CCM according to the cycling light of the diurnal rhythm. In addition to the regulation of SbtA, the protein is capable of directly influencing glycogen metabolism through the c-di-AMP-dependent interaction with the glycogen branching enzyme, to promote glycogen synthesis during the day. Furthermore, SbtB extends its regulatory function to the gene expression of both components of the CCM and C_i-regulated genes.

Hence, the discovery and here performed characterization of the SbtB functionality opened a new paradigm for the regulation of the inorganic carbon acquisition and incorporation among cyanobacteria.

Introduction

Changes in atmospheric CO_2 and O_2 due to the evolution of cyanobacteria

During the course of Earth history, the composition of the atmosphere underwent significant changes. Before 2.4 billion years ago, the concentration of O_2 never surpassed 0.001%, while the CO_2 concentration fluctuated between 15 and 30% (Berner, 2006; Lyons *et al*., 2014). However, this changed greatly after the appearance of oxygenic photosynthesis that evolved in ancient cyanobacteria, which caused the “great oxidation event”, greatly increasing the concentration of O_2 until today’s concentration of ~21%, with virtually all of the oxygen in the atmosphere coming from photosynthesis. Cyanobacteria appeared around 2.7 billion years ago and after their proliferation and the spread of photosynthesis into Eukaryotes, through the years, the concentration of CO_2 also showed a sharp decline, reaching the modern levels of 0.04% (Hohmann-Marriott & Blankenship, 2011).

Photosynthesis, carbon fixation and photorespiration

While the process of photosynthesis refers to harvesting of physical light energy into chemical energy in the light process that is mainly used for the reduction of CO_2 to produce organic carbon for biomass, this process differs among photosynthetic

organisms. In cyanobacteria, the light, harvested by the photosystems I and II (PSI and PSII), is used to split water, to generate O_2, released in the environment, and protons (H^+), and to generate an electron transfer chain. Powered by the movement of electrons, protons are used to produce chemical energy under the form of adenosine triphosphate (ATP) and the reducing agent $NADPH_2$ (Bryant & Frigaard, 2006) The chemical energy is then utilized by the cell to fix CO_2 through the Calvin-Benson-Bassham (CBB) cycle. The CBB cycle catalyses the fixation of 3 CO_2 molecules, by consuming ATP and $NADPH_2$, to produce one molecule of the primary organic compound 3-phosphoglycerate (3PGA). (Hagemann *et al*., 2016; McFarlane *et al*., 2019) The key enzyme of this reaction is ribulose 1,5-bisphosphate carboxylase/oxygenase (RuBisCO), the most abundant enzyme on Earth and the enzyme used by all oxygenic phototrophs for the fixation of CO_2. The main reasons behind its abundance, outside of the relevance of the reaction it catalyses, is the relatively low kinetics and low specificity. This enzyme, in fact, instead of the intended carboxylation reaction of CO_2 fixation, can incorrectly perform the oxygenation reaction, binding and fixing O_2 instead, leading to the production of the intermediate 2-phosphoglycolate (2PG). To get rid of this molecule, oxygenic phototrophs evolved the metabolic process known as photorespiration, as both 2PG and its subsequent products are intracellular toxins, known to inhibit key enzymes of different vital metabolic pathways such as the CBB cycle. Photorespiration, a process present with many variations in all oxygenic phototrophs, allows the conversion of two molecules of 2PG into one 3PGA, with the cost of one ATP, one $NADPH_2$, one CO_2 and causing the release of one NH_3. Despite wasteful, photorespiration is an essential process that allows oxygenic phototrophs to survive in the modern atmosphere, by preventing the operation of photosynthesis and of the CCB cycle to be interrupted. The ratio of carboxylation/oxygenation reaction is affected mainly by CO_2 and O_2 concentrations at the active site of RuBisCO, but also by temperature, with higher temperatures favouring the oxygenation reaction. (Hagemann *et al*., 2016; Orf *et al*., 2016) With the increased levels of O_2 and decreased levels of CO_2 in the modern atmosphere, this issue was exacerbated, leading to a rate of around 1 oxygenation reaction for every 4 carboxylation reactions in land plants. (Sharkey, 1988) Oxygenic phototrophs have evolved different mechanisms to reduce the rate of the oxygenation reaction, such as the evolution of RuBisCO enzymes with higher specificity towards CO_2 than O_2, compromising with an even lower reaction rate. Among the different adaptations, however, the most efficient is the inorganic carbon-concentrating mechanism (CCM) in cyanobacteria and many algae, which allows the rate of oxygenation reactions to decrease to around 1%. (Raven *et al*., 2017; Young *et al*., 2011)

Cyanobacteria

Cyanobacteria, formerly called blue-green algae, are a phylum of Gram-negative bacteria, characterized by the vast majority of them being capable of performing photosynthesis. They are evolutionarily closest to the cyanobacteria-like prokaryotes responsible for the transfer of oxygenic photosynthesis to the eukaryotic ancestors of algae and land plants through primary endosymbiosis, leading to the formation of chloroplasts. (Eisenhut *et al*., 2008; Hohmann-Marriott & Blankenship, 2011; Sukenik *et al*., 2009) In modern days, cyanobacteria have become ubiquitous. Though they

appear more frequently in water bodies, both fresh water and marine bodies, they can be found in every photic environment on Earth, ranging from tropics to deserts. Because of this, they now represent the largest and most varied group of photosynthetic prokaryotes. (Monchamp *et al*., 2019; Sukenik *et al*., 2009)

The great variety of cyanobacteria is also reflected in their morphology, starting from the cells size, which ranges between 0.5 to 100 µm. Cyanobacteria can be unicellular, colonial or form multicellular filaments, showcasing different cell shapes in each case. Some show cell differentiation, such as heterocysts, responsible for nitrogen fixation, or akinetes, acting as spore-like cells, with both being more common among filamentous cyanobacteria. Moreover, some filamentous strains are capable to form true branches (Dvořák *et al*., 2015; Mehdizadeh Allaf & Peerhossaini, 2022) Many cyanobacteria also possess pili as extracellular appendages, which mainly facilitate the uptake of genetic material and allow some cyanobacteria to possess a gliding type of motility. (Schuergers & Wilde, 2015) The thylakoid membrane, the intracellular folding of the plasma membrane where the photosynthetic complexes are located, also show a large diversity in architecture among the different groups of cyanobacteria.(Mareš *et al*., 2019)

The vast variety in the morphology and environmental habitat of cyanobacteria is mirrored by the complexity of their metabolism. Outside of photosynthesis and carbon fixation, and with some are capable of nitrogen fixation, hundreds of bioactive compounds have been discovered to be produced by cyanobacteria. Among these, there are also many toxins, mostly comprising of neurotoxins, hepatotoxins and endotoxins. (Calteau *et al*., 2014) Furthermore, all these metabolic processes possess complex regulation, due to the constantly changing conditions in their environments. Outside of the adaptation to the diurnal light rhythm, with the presence of a circadian clock, cyanobacteria, requiring a liquid media to live in, face significant changes in their environment such as variations in metabolites and ionic concentrations in the water. Therefore, cyanobacteria evolved regulatory systems that allows them to adapt their metabolism to constant environmental changes. One example of such a system is the CCM. (Cohen & Golden, 2015; Mehdizadeh Allaf & Peerhossaini, 2022)

CO_2-concentrating mechanism in cyanobacteria

Outside of the changes in inorganic carbon (C_i) availability on a large time scale, cyanobacteria face fluctuations of C_i on a short time scale. In fact, the solubility of CO_2 in the water is subjected to rapid changes, being affected by temperature, pH and salt content. High temperature reduces the solubility of CO_2, which, once dissolved, can be present as either CO_2, bicarbonate (HCO_3^-) or carbonate (CO_3^{--}), depending on the pH. This greatly affects the availability of C_i, as CO_2 possesses a low solubility, representing less than 1% of the C_i in the water, with most being in the form of carbonate or bicarbonate. Acidic waters contain mostly CO_2, shifting to mostly bicarbonate in slightly alkaline conditions or carbonate under higher pH. (DiMario *et al*., 2018) First appearing between 400 and 2000 million years ago, the CCM, evolved by cyanobacteria, not only very efficiently increases the rate of the carboxylation reaction and reduces the oxygenation reaction of RuBisCO, but also allows them to

acclimate to fluctuating C_i concentrations. (Badger & Price, 2003; Kupriyanova *et al*., 2013)

The cyanobacterial CCM is a biophysical system that achieves its efficiency thanks to different components (Fig. 1), which allow the cells to accumulate bicarbonate instead of CO_2, since this ion more easily dissolves in water, can be actively transported and cannot escape from the cell. The CCM utilizes three bicarbonate transporters located in the plasma membrane. The primary active transporter is the ABC-type transporter BCT1 (Omata *et al*., 1999) that works conjunctively with two Na^+-bicarbonate symporters SbtA (Shibata *et al*., 2002) and BicA. (Price *et al*., 2004) While BCT1 is constitutively expressed in many cyanobacteria such as in the model strain *Synechocystis* sp. PCC 6803 (henceforth *Synechocystis*), SbtA and BicA are induced under low-C_i conditions (LC) conditions. (Mantovani *et al*., 2022) The transporter BCT1 is regulated by the transcription factor CmpR that activates with the binding of the metabolites ribulose 1,5 bisphosphate and 2PG, which accumulate under LC conditions. (Nishimura *et al*., 2008)

The second component of the CCM are carboxysomes, polyhedral protein microcompartments in which RuBisCO is located. Two phylogenetically distant variants of carboxysomes and RuBisCO exist in cyanobacteria, sharing a similar function and distinguishing the β-cyanobacteria, which include most of the cyanobacterial phylum, from the α-cyanobacteria, mainly composed by picoplanktonic cyanobacteria. These microcompartments, outside of RuBisCO, contain the enzyme carbonic anhydrase (CA), which efficiently converts HCO_3^- to CO_2, greatly enriching the carboxysomal environment with CO_2 and thereby reducing the occurrence of the oxygenation reaction. (Hagemann *et al*., 2021; Kaplan & Reinhold, 1999; Melnicki *et al*., 2021; Rae *et al*., 2013)

The third component of the CCM is the CO_2 hydration system, composed of two specialized NAD(P)H dehydrogenase complexes, $NDH1_3$ and $NDH1_4$, which uses reduced ferredoxin, the last product of the photosynthetic electron transfer chain, to reduce CO_2 to HCO_3^-. Both are located at the thylakoid membrane, but $NDH1_4$ is constitutive and has low CO_2 affinity, while $NDH1_3$ is induced under LC-conditions and has high CO_2 affinity. (Hagemann & Kaplan, 2020; Shibata *et al*., 2001) Not all the CO_2 released by the CA in the carboxysomes is fixed and some escapes into the cytoplasm and flows out of the cells, as the gas is capable of freely diffusing through carboxysome and cell membrane alike. The conversion of CO_2 to HCO_3^- by the hydration system not only allows the prevention of the loss of the non-fixed CO_2, but also reduces its intracellular concentration, promoting its inward diffusion. In addition to the CCM, the canonical NDH1 complex is involved in respiration and the cyclic electron transport around PSI. (Hagemann *et al*., 2021; Tchernov *et al*., 2001)

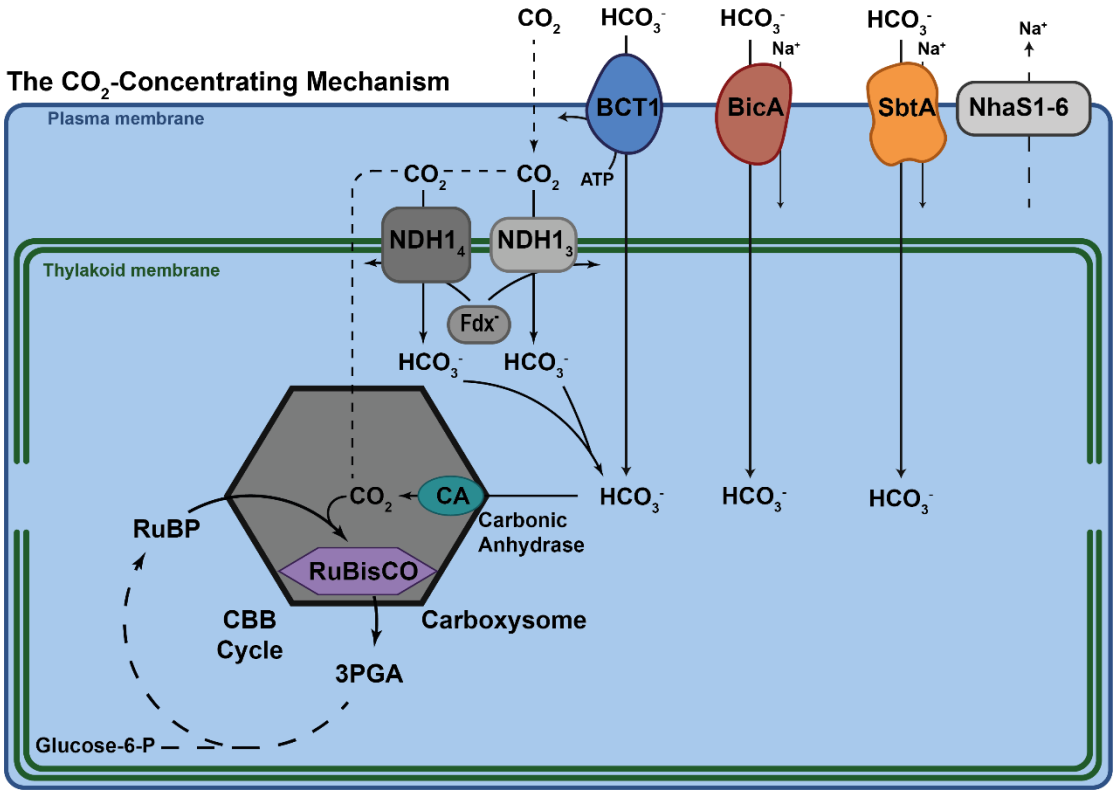

Figure 1: Schematic illustration of the cyanobacterial inorganic carbon-concentrating mechanism (CCM). Three bicarbonate transporters (SbtA, BicA, and BCT1) and the Na^+-gradient restoring proteins NhaS1-6 representing different Na^+/H^+ antiporters, are located at the plasma membrane. Together with the two CO_2-hydrating systems on thylakoid membranes, using reduced ferredoxin (Fdx^-), they achieve high intracellular HCO_3^- concentrations. Bicarbonate diffuses into the carboxysomes, in which it is converted to CO_2 by the carbonic anhydrase (CA), thereby promoting the carboxylation reaction of RuBisCO.

The bicarbonate transporter SbtA and the PII-like protein SbtB

Among the bicarbonate transporters, one of great interest in the acclimation to fluctuating C_i concentrations is the sodium-dependent bicarbonate transporter A (SbtA). First identified in the model β-cyanobacterium *Synechocystis* (Shibata *et al*., 2002), this transporter is highly conserved among cyanobacteria, and homologs appear even among heterotrophic bacteria. (von Rozycki *et al*., 2004). The expression of SbtA is highly induced under LC conditions, where it acts as the main transporter, possessing the highest flux rate. (Du *et al*., 2014) The regulation of its expression is mediated via the $NADPH_2$ dehydrogenase transcriptional repressor NdhR, which, inactivated under LC conditions by releasing the co-repressing metabolite 2-oxoglutarate (2-OG) and binding 2PG, is responsible for the transcription control of different components of the CCM. (Jiang *et al*., 2018; Klähn *et al*., 2015)

In *Synechocystis*, the gene coding for SbtA is *slr1512*, found in an operon together with the gene *slr1513*, which encodes the small, conserved protein SbtB. In the initial investigation of this protein, it was annotated as a protein of unknown function that, however, possess a structure very similar to the nitrogen metabolism regulating

protein PII, suggesting a function as a regulator protein for the carbon concentrating mechanism. (Selim *et al*., 2018)

SbtB is part of the PII superfamily

The structural and biochemical investigation of SbtB confirmed the protein to be part of the PII superfamily. These are small regulatory proteins present in bacteria, archaea and plastids, capable of a vast regulatory activity on both carbon and nitrogen metabolism and constitute one of the largest signalling protein families. Their regulatory activity is exercised through protein-protein interactions with multiple partners, and is modulated by a variety of cellular signals, sensed by PII proteins thanks to their ability to bind different regulatory metabolites including second messengers. (Forchhammer & Lüddecke, 2016; Selim *et al*., 2018) Second messengers define a class of ions and small molecules, capable of rapid diffusion inside the cells, which produce a specific response by transducing extra- and intra-cellular signals to the effector protein(s). By action of enzymes producing and disposing of second messengers, their homeostasis is tightly controlled, allowing quick fluctuations in their concentrations in response to specific signals. (Newton *et al*., 2016)

The canonical PII protein in cyanobacteria, GlnB, is characterised by a highly conserved homo-trimeric structure. Each subunit presents a ferredoxin-like $(\beta\alpha\beta)_2$ fold, presenting three main loop regions, the T- B- and C- loops. Together, the tree loops form a ligand binding pocket in the cleft between subunits, formed by the B-loop and the basal part of the T-loop of one subunit, together with the C-loop of the neighbouring subunit. Among the three, the T-loop is the most relevant for the function of the protein, as it not only strongly influences the affinity of each ligand for PII, but it is the main mediator of the interaction capabilities of the protein. (Forchhammer & Lüddecke, 2016; Kaczmarski *et al*., 2019; Xu *et al*., 2003) Contrary to the other two loop regions, in fact, the T-loop is mostly disordered when no ligand is bound, but it can assume different conformations depending on the second messenger bound to the protein, modulating its activity. In such a manner PII can sense the energy state of the cell via ATP/ADP interaction and the carbon/nitrogen balance through 2-OG, the carbon skeleton for nitrogen assimilation, thereby sensing nitrogen and carbon availability to regulate multiple aspect of the central nitrogen metabolism. (Fokina *et al*., 2010; Forchhammer *et al*., 2022) Among the identified regulation targets of PII in cyanobacteria are the transporters Amt, Nrt and Urt, responsible for the uptake of ammonia, nitrate and urea, respectively, which PII is able to inhibit. The signal transduction of the protein extends to arginine biosynthesis, by activating the key enzyme N-acetylglutamate kinase (NAGK), and nitrogen-starvation-induced glycogen formation, modulating the flow of carbon from glycogen to anabolic pathways by interacting with phosphoglycerate mutate (PGAM). Furthermore, outside direct protein activity, PII is capable of modulating gene expression levels, affecting the expression of multiple components of nitrogen metabolism. It achieves this by modulating the activity of the two-component transcription regulator NtrB-NtrC, responsible for the expression of proteins involved in nitrogen assimilation and glutamine synthesis, and the transcription factor NtcA, the key transcription regulator of nitrogen-controlled gene expression. (Forchhammer *et al*., 2022; Forchhammer & Selim, 2020)

SbtB is a major receptor for adenyl-nucleotides

As part of the PII superfamily, SbtB presents the same structural characteristic as PII proteins, but it is categorized as a non-canonical member of the family. The main reason for this is that while PII proteins are able to bind 2-OG, ATP, ADP and glutamine, SbtB can only bind to the adenyl nucleotides ATP, ADP, AMP, cAMP and c-di-AMP and to the Ca^{2+} ion. (Kaczmarski *et al*., 2019; Selim *et al*., 2018, 2021)

ATP-ADP-AMP

Among all organisms, adenosine triphosphate (ATP) is used in the majority of cellular processes that require energy, as it is the most common energy-carrying molecule. The chemical energy is released by the hydrolysis of the γ- or β-phosphate groups, yielding ADP or AMP, respectively, which are then used as substrate to regenerate ATP. With the synthesis of ATP being performed both during the day, powered by photosynthesis, and night, powered by respiration, and with the presence of adenylate kinase, which performs the reversible reaction 2 ADP ↔ 1 ATP + 1 AMP, the concentrations of the three energy molecules are subjected to significant fluctuations. (Mantovani *et al*., 2023; Nitschmann & Peschek, 1986; Song *et al*., 2022) Due to these factors, the ratios of ATP/ADP and more importantly ATP/AMP represent a signal for the energy state of the cell, acting in a manner similar to second messengers, by influencing many regulatory proteins such as SbtB. This is particularly the case for photoautotrophic organisms such as cyanobacteria, where the ratios of ATP, ADP and AMP, strongly dependent on light availability, exert a large influence on anabolic metabolism, especially carbon and nitrogen assimilation. (Mantovani *et al*., 2022; Selim *et al*., 2018)

cAMP

Adenosine 3’5’-cyclic AMP (cAMP) is one of the most common second messengers among all organisms. cAMP is produced by the enzyme adenylate cyclase from one molecule of ATP and is degraded by phosphodiesterases (PDE). Multiple adenylate cyclases exist in each organism, either soluble or associated to the membrane, and in the model organism *Synechocystis*, the most important one is the soluble Cya1 (*slr1991*). (Mantovani *et al*., 2022; Terauchi & Ohmori, 1999) Due to the important role cAMP plays in many regulatory mechanisms, its levels are affected by a large variety of environmental factors, such as light, pH, nitrogen, oxygen and C_i levels. (Mantovani *et al*., 2023; Yoshimura *et al*., 2000) Among its identified roles are the regulation of phototaxis (Wallner *et al*., 2020), the signaling for nutrient deficiency (Francko & Wetzel, 1981) the sensing of the carbon status through binding with SbtB (Selim *et al*., 2018) and the regulation of the CCM. (Bantu *et al*., 2022) In bacteria, most of the cAMP-mediated cellular signals are transduced by the cAMP receptor protein (CRP), a transcription factor capable of affecting the expression of a large number of genes. (Görke & Stülke, 2008)

c-di-AMP

Di-cyclic AMP (c-di-AMP) is an adenyl nucleotide-type second messenger produced from two molecules of ATP through the di-adenylate cyclase (Dac) and is degraded by specific PDEs. In bacteria, usually only one Dac and one PDE are present and in

Synechocystis, the only Dac is DacA (*sll0505*). No protein effectors for c-di-AMP have been identified yet, but c-di-AMP can transduce its signal through riboswitches, metabolite binding components of non-coding portions of mRNA. (Agostoni *et al*., 2018; Mandal & Breaker, 2004; Mantovani *et al*., 2022) In *Synechocystis*, the currently known roles of c-di-AMP are the regulation of potassium homeostasis, osmotic stress acclimation, glycogen metabolism during day/night acclimation (Agostoni *et al*., 2018; Selim *et al*., 2021) and exopolysaccharide secretion (Peng *et al*., 2016).

Ca^{2+}

Calcium ions act as an important second messenger among bacteria. Its concentration is tightly controlled by Ca^{2+} transport and Ca^{2+} binding proteins, which ensure very low intracellular concentration to allow for very fast signaling upon Ca^{2+} release. In cyanobacteria, Ca^{2+} concentration is a signal for nitrogen and C_i levels and a variety of environmental stresses. (Agostoni & Montgomery, 2014) It regulates heterocysts differentiation, C/N homeostasis, photosynthesis and motility. (Hu *et al*., 2011; Mantovani *et al*., 2023)

The second-messenger regulation of SbtB

With the ability of SbtB to bind such a variety of second messengers, the possible regulatory functions of SbtB are also similarly varied. The main component of the protein that allows the changing function of SbtB is the large T-loop which, like in PII proteins, can adopt different conformations depending on the adenyl nucleotide bound to SbtB. The adenosine moiety binding mode is also almost identical compared to canonical PII proteins, showing only slight differences in regard to the aminoacidic side chains involved. The solved structures of SbtB bound to the different adenyl nucleotides revealed that the T-loop is completely structured only when ATP is bound. (Fig. 2) The binding of c-di-AMP, however, causes a partial structuring of the T-loop, while AMP, ADP and cAMP cause it to be completely disordered. (Fang *et al*., 2021; Selim *et al*., 2018, 2021) The binding of Ca^{2+} complements the binding of ATP, further stabilizing the structured T-loop. (Kaczmarski *et al*., 2019)

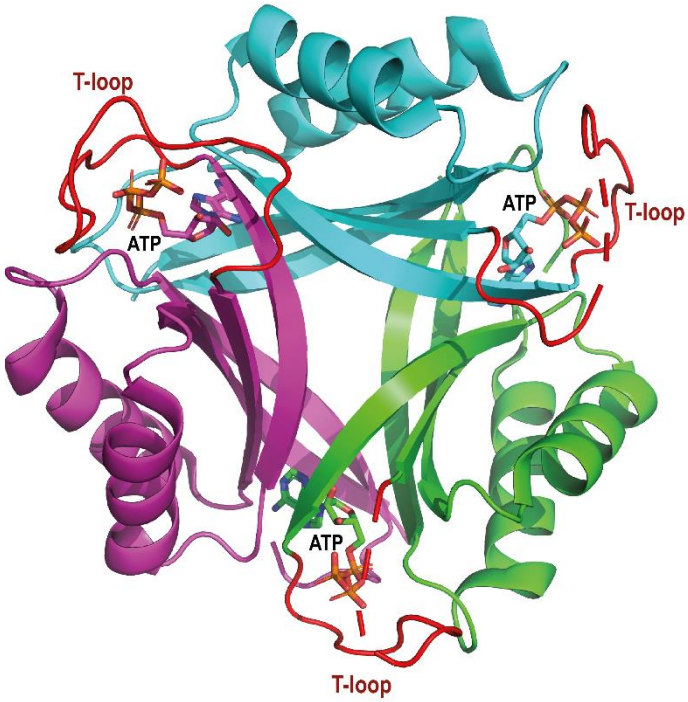

Figure 2: Tri-dimensional structure of the protein SbtB bound to ATP. The three sub-units of the trimer are shown in magenta, cyan and green. The T-loops of each subunit are highlighted in red. Each subunit shows a molecule of ATP in the binding site.

The regulation of SbtB is further affected by its di-phosphohydrolase (apyrase) activity, which causes the hydrolysis of the β- and γ- phosphates of ATP and ADP, leading to AMP remaining in the binding pocket of SbtB. Not only is this a novel function not yet identified in PII proteins, but it is also affected by another non-canonical component of SbtB, the C-terminal redox-regulated loop (R-loop). The R-loop can form a structured hairpin through the formation of a disulphide bridge between two cysteine residues, thereby functioning as a redox sensor for the cell. The basal part of the T-loop, mostly involved in the binding of ATP and ADP, sterically communicates with the R-loop. When the R-loop is in a reduced and disordered state, the T-loop assumes an ATP-protecting conformation, coordinating with the β- and γ- phosphates of ATP and ADP. When the R-loop is oxidised, however, the T-loop adopts a conformation clashing with the β- and γ- phosphates of ATP and ADP, forcing them in a strained conformation and facilitating hydrolytic attack. (Selim *et al*., 2023) Mn^{2+} and Mg^{2+} ions also participate in the modulation of the apyrase activity, with both promoting it by coordinating with the β- and γ- phosphates of the adenyl nucleotides. (Selim *et al*., 2023) Furthermore, as the binding of Ca^{2+} ions affects the coordination between the γ- phosphate of ATP and the T-loop, it might also influence the apyrase activity of SbtB, but this has not been verified yet. (Kaczmarski *et al*., 2019)

SbtB interacts with SbtA and modulates bicarbonate uptake

While the regulatory functions of SbtB are believed to be as wide as PII proteins, the main and best characterized interaction partner of SbtB remains the bicarbonate

transporter SbtA. Not only co-expressed in the same operon, the membrane association of SbtB is highly dependent on the presence of SbtA, which, when absent, causes SbtB to be found only in the soluble cytosolic fraction of *Synechocystis*. (Selim *et al*., 2018)

The structural investigation of the co-crystallization of SbtAB showed that both possess a trimeric structure. Each subunit of SbtA possesses an immobile gate domain, facing towards the middle of the SbtA trimer, and a mobile core domain, capable of binding one HCO_3^- molecule and one Na^+ ion and transport them through an elevator-like mechanism, by alternating outwards and inwards facing conformations. Each subunit of SbtB can bind to one subunit of SbtA in a monomer-monomer interaction. While multiple structural components of both SbtA and SbtB are involved in the interaction, the most important one is the T-loop of SbtB, which, depending on the adenyl nucleotide bound to it, can modulate the activity of the transporter. When AMP or ADP are bound to SbtB (Fig. 3), the T-loop is capable of interfacing with SbtA, causing a shift of the core domain to an inward facing conformation. When bound to SbtB, both cAMP and c-di-AMP protrude from the binding pocket and clash with SbtA, preventing the interaction. The binding of ATP to SbtB causes the T-loop to assume a conformation that sterically clashes with SbtA, preventing the formation of the SbtAB complex. With the fluctuating concentrations of the adenyl nucleotides depending on the environmental conditions and their competition for the binding pockets, SbtB finely modulates the activity of the bicarbonate transport of SbtA. (Fang *et al*., 2021; Förster *et al*., 2023; Liu *et al*., 2021; Selim *et al*., 2021) It achieves this by both preventing the uptake of bicarbonate when unnecessary, and by acting as a plug of SbtA to prevent the leakage of the reverse-flowing bicarbonate. (Förster *et al*., 2023; Haffner *et al*., 2023) Furthermore, the interaction between the two proteins adds a further layer of regulation to SbtB, given by the apyrase activity of the protein, which is 4 folds higher in the presence of SbtA. (Haffner *et al*., 2023)

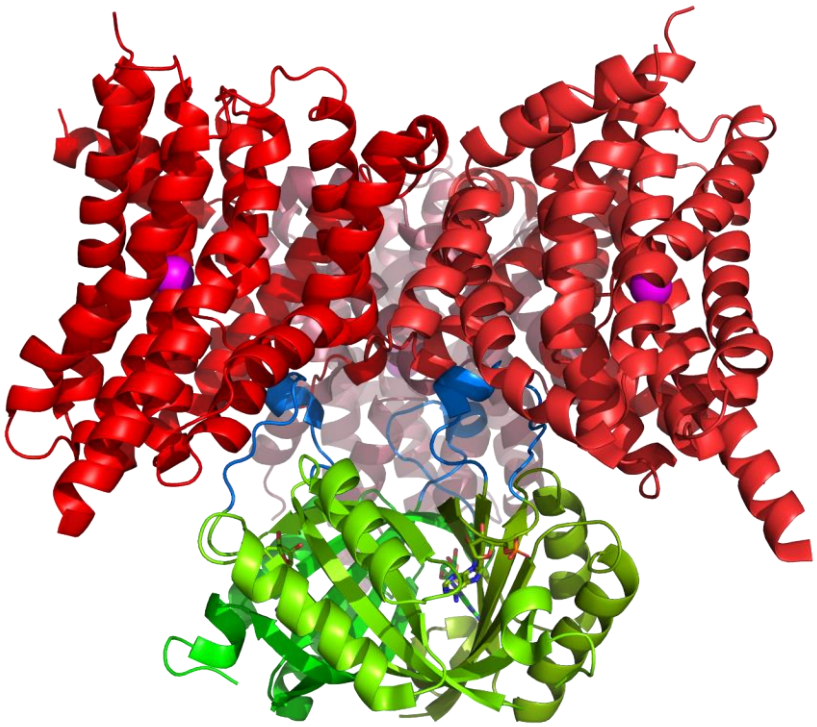

Figure 3: Tri-dimensional structure of the interaction of SbtB(+AMP)-SbtA. The three sub-units of SbtB (Green), bound to AMP, directly interact with the three subunits of SbtA (Red), mainly through the interaction of the structured T-loop (Blue), which is inserted in the cleft formed by SbtA. The Na^+ ions used for the transport activity are shown in magenta.

Goal of the dissertation

The aim of this work, performed in collaboration with the group led by Prof. Dr. Karl Forchhammer from the University of Tubingen, is to provide further insight into the regulatory properties of the PII-like protein SbtB in the cyanobacterium *Synechocystis* sp. 6803. Specifically, this investigation focuses on three main points, being the specific role of second messengers on SbtB regulation, the identification of more interaction partners and the involvement of SbtB in the acclimation to diurnal light conditions.

Capable of rapid fluctuations depending on the environmental conditions, second messengers transduce a large variety of signals. Possessing the ability to bind multiple adenyl nucleotide second messengers, the regulatory activity of SbtB is largely affected by their concentration. However, the current knowledge of the effect of the binding of each second messenger to SbtB is incomplete, and mainly regards the interaction with the transporter SbtA. The first investigation point is therefore to provide further details about the specific role of each second messenger on the regulation of SbtB and the CCM, especially during fluctuating C_i conditions.

As PII proteins possess large regulatory networks and the ability to directly interact with other proteins, as part of the superfamily, SbtB is likely capable of directly affecting the functionality of different proteins, although until recently only the transporter SbtA has been confirmed as an interaction partner. Accordingly, the second goal of this

investigation is the identification of more targets of SbtB, to attempt to provide insight into the existence and amplitude of its regulatory network.

Given cyanobacterial dependence on the light cycle, many components of its metabolism are subjected to diurnal regulation, including carbon fixation. As the likely most important regulatory component of the CCM, a system of vital importance for cyanobacteria, there is a strong possibility for SbtB to be involved in the physiological acclimation of cyanobacteria to changing light conditions. It is therefore the third goal of this investigation to determine the mechanism and degree of involvement of SbtB in the cyanobacterial acclimation to diurnal rhythm.

SbtB regulates diurnal glycogen metabolism through c-di-AMP

While SbtA remains the main interaction partner of SbtB, just like PII proteins, it is capable of interacting with multiple proteins to regulate carbon metabolism. In fact, co-immunoprecipitation and bacterial two-hybrid experiments revealed that the glycogen branching enzyme GlgB is a major target for SbtB in *Synechocystis*. (Selim *et al*., 2021) This enzyme is responsible for the formation of the α-1,6-glycosidic bond every 10 to 14 glucose units on a glycogen chain, forming branching side chains. The importance of this reaction relies in the significant reduction in the osmotic pressure caused by glycogen build-up. (Froese *et al*., 2015) In cyanobacteria, glycogen is particularly relevant during the diurnal rhythm. As these organisms rely on photosynthesis for energy acquisition, their metabolism is controlled by a circadian clock, experiencing constant shifts from anabolism during the day to catabolism during the night. During light phases, in fact, excess of the CO_2 fixed through the CBB cycle is used for the anabolic production of glycogen, for both energy storage and for the regeneration of CBB cycle intermediates. During dark phases, glycogen is catabolised, mainly through the oxidative pentose-pathway (OPP), for both energy production, through respiration, and all carbohydrate-requiring biosynthetic processes to maintain cell metabolism during the night. (Makowka *et al*., 2020; Wan *et al*., 2017) The circadian clock that regulates the constant metabolic changes from anabolism to catabolism during the diurnal rhythm is a complex system which is still poorly understood. The circadian clock involves the perception of different signals, especially the redox state and energy levels of the cells, to produce a large signalling cascade for the regulation of metabolism at both protein and genome level. This signalling cascade strongly involves the use of second messengers, of which c-di-AMP is of particular relevance. (Rubin *et al*., 2018; Welkie *et al*., 2018)

In cyanobacteria, c-di-AMP is produced by the membrane associated di-adenylate cyclase DacA. The synthesis of c-di-AMP is strictly related to the light cycle cyanobacteria undergo, as in *Synechocystis*, c-di-AMP concentrations increase during light phases and decrease during the dark, while the opposite happens in *S. elongatus*. While the reason behind the difference is yet not known, c-di-AMP plays a vital role in both model organisms under a diurnal rhythm, as when absent from the cells, in Δ*dacA* mutants, the growth rate of the cyanobacteria is significantly lowered. (Rubin *et al*., 2018; Selim *et al*., 2021) The importance of c-di-AMP during the diurnal rhythm is

strictly correlated to SbtB and glycogen metabolism. In fact, not only does SbtB have a high affinity for c-di-AMP, but it is the protein with the highest affinity for c-di-AMP in *Synechocystis*. The binding of the second messenger in the binding pocket causes the T-loop to assume a conformation unlike any of the other second messengers that bind SbtB. The relevance of the formation of the SbtB-c-di-AMP complex relies in the interaction between SbtB and GlgB, which increases up to 20 fold compared to SbtB alone. Mediating the interaction between SbtB and GlgB, c-di-AMP plays a large role in the synthesis of glycogen under diurnal rhythm, as seen in *Synechocystis* mutant strains Δ*dacA*, Δ*sbtB* and Δ*glgB*, which show similar significantly reduced levels of glycogen, which likely explains the impact on survivability in the absence of c-di-AMP in the cells during diurnal conditions. (Selim *et al.*, 2021) While c-di-AMP is important for the regulation of glycogen metabolism, it does not directly influence the uptake of C_i. The measurement of the *in vivo* bicarbonate-dependent photosynthetic activity of *Synechocystis* strains WT and Δ*dacA*, acclimated to either high-C_i (HC) or LC conditions, revealed in fact no significant difference in affinity to bicarbonate between the two strains (Fig. 4). The experiment, however, highlighted a net decrease in the maximum photosynthetic rate in the Δ*dacA* mutant under LC conditions, suggesting a decreased CBB cycle activity at saturating C_i conditions. (Mantovani *et al.*, 2022; Selim *et al.*, 2021)

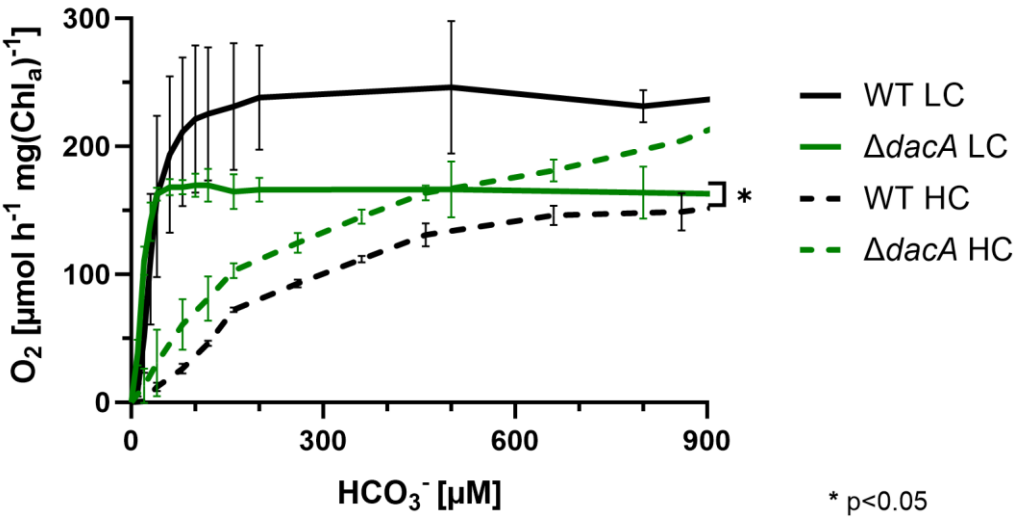

Figure 4: Bicarbonate-dependent photosynthetic activity characterization of Δ*dacA *mutant. Oxygen evolution measurement of *in vivo* bicarbonate uptake of *Synechocystis* strains WT (Black) and Δ*dacA* (Green), acclimated to either HC (Solid lines) or LC (Dashed lines) conditions. *p<0.05 (Selim *et al.*, 2021)

SbtB, cAMP and c-di-AMP are involved in regulation of gene expression and CCM activity in a CO_2-dependent manner

PII proteins, despite their size, possess vast and complex regulatory properties of the nitrogen metabolism, even extending to the regulation of gene transcription by affecting transcription factors, such as the nitrogen regulator II, NtrB and the regulator

of nitrogen assimilation, NtcA. (P. Jiang & Ninfa, 1999; Labella *et al*., 2020) Though not many have yet been identified, as part of the PII superfamily, SbtB is capable of interacting with multiple partners to regulate different components of the CCM and of the carbon metabolism. The regulatory mechanism is mediated by the interaction with the adenyl nucleotides the protein is able to bind, and of particular interest are cAMP and c-di-AMP. As ATP, ADP, and ADP mainly represent a signal for the energy state of the cell, c-di-AMP and more importantly cAMP are more directly related to carbon metabolism. c-di-AMP is in fact involved in the regulation of glycogen metabolism, while in the case of cAMP, the main adenylate cyclase in *Synechocystis*, Cya1, is activated by the binding of CO_2 and thereby represents the currently only known sensing protein for the C_i levels of the cell. (Cann *et al*., 2003; Hammer *et al*., 2006; Hardie, 2011)

The relevance of SbtB, cAMP and c-di-AMP in *Synechocystis* during changing C_i conditions extends also to gene regulation. In fact, Δ*sbtB*, Δ*cya1*, and Δ*dacA* *Synechocystis* mutants, lacking SbtB, the main adenylate cyclase and the only di-adenylate cyclase, respectively, when compared to WT, show a high impact on gene expression when shifting from HC to LC conditions. Their general importance is directly visible when observing the number of genes which are significantly up- or down-regulated in the three mutants upon changing C_i conditions on a global scale. (Fig. 5) At constant HC conditions, in fact, both mutants Δ*cya1* and Δ*dacA* affect the regulation of a large number of genes, while the absence of SbtB does not impact gene expression as much as the second messengers. Upon changing C_i conditions, however, the situation is reversed, as the lack of SbtB causes the expression of a much larger number of genes to become deregulated when compared to the two second messengers. Compared to SbtB, the two second messengers are much less directly involved in the regulation of gene expression under C_i fluctuations, with the lack of c-di-AMP causing a more significant deregulation compared to cAMP. (Mantovani *et al*., 2022)

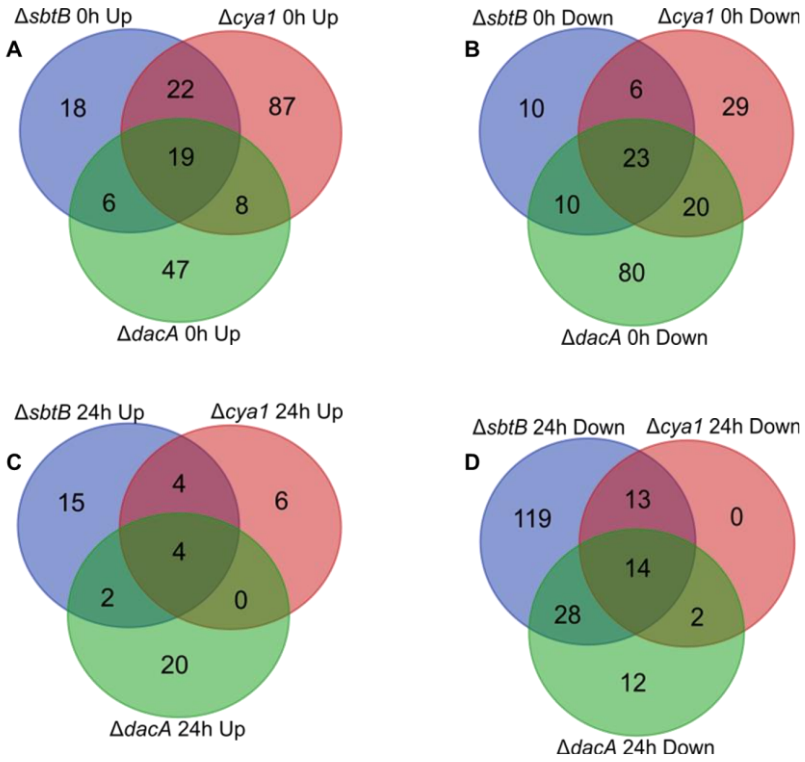

***Figure 5: Venn diagrams showing global CO_2-regulated gene expression changes in mutants Δ*sbtB*, Δ*cya1*, and Δ*dacA* compared to wild type in* Synechocystis. **A** – Significantly up-regulated gene expression at HC conditions; **B** – Significantly down-regulated gene expression at HC conditions; **C –** Significantly up-regulated gene expression 24 h after LC shift; **D –** Significantly down-regulated gene expression 24 h after LC shift. Only protein-coding genes were considered. (Mantovani *et al*., 2022)

cAMP

In *Synechocystis*, cAMP exercises an important regulatory function on the CCM through the action of the main cAMP receptor protein (CRP), the transcription factor SyCRP1. When missing, in fact, under LC conditions, the expression of multiple CCM components is affected, causing the downregulation of carboxysomes and the upregulation of bicarbonate transporters. (Bantu *et al*., 2022) The knock-out of *cya1*, however, while it causes the total cAMP concentration to be reduced to around 4% of its initial concentration, (Terauchi & Ohmori, 1999) does not lead to significant changes in gene expression of CCM components, outside of a slightly reduced expression of the *sbtAB* operon under HC conditions (Fig. 6A-B). In fact, among the many genes whose expression is affected by the changes in cAMP concentration during shifting carbon conditions, few to none are obviously related to carbon metabolism. Likely, this is due to the great significance of cAMP in cell physiology and its involvement in a large number of regulatory mechanisms. In fact, the reduced concentration of cAMP causes a wider gene expression de-regulation under constant HC conditions than after shift in C_i conditions. Possibly, the difference in the effect the knock-out of *cya1* and SyCRP1 have on cyanobacterial CCM expression is due to SyCRP, possessing a high affinity for cAMP, still maintaining its functionality despite the lower cAMP concentration. (Bantu *et al*., 2022; Mantovani *et al*., 2022, 2023)

While cAMP is seemingly important for the SbtB-mediated regulation of the CCM, given the high affinity the protein has for the cyclic nucleotide, it does not appear to directly affect its activity under constant C_i conditions, as both the bicarbonate affinity and CBB cycle activity observed for the Δ*cya1* mutant when measuring the *in vivo* bicarbonate-dependent oxygen evolution remain unaffected, both under HC and LC conditions (Fig. 6C). (Mantovani *et al*., 2022) This is in contrast to the knock-out of SyCRP1, which, due to the downregulation of carboxysomes, causes a significant decrease in the maximum carbon fixation rates under LC conditions, leading to a net decrease in growth rate for the mutant. Likely, cAMP represents the main signal for high C_i availability among cyanobacteria, but its importance in the modulation of the activity of SbtB relies mostly in conditions of fluctuating C_i concentrations, though this remains unclear. (Bantu *et al*., 2022; Mantovani *et al*., 2022; Selim *et al*., 2018)

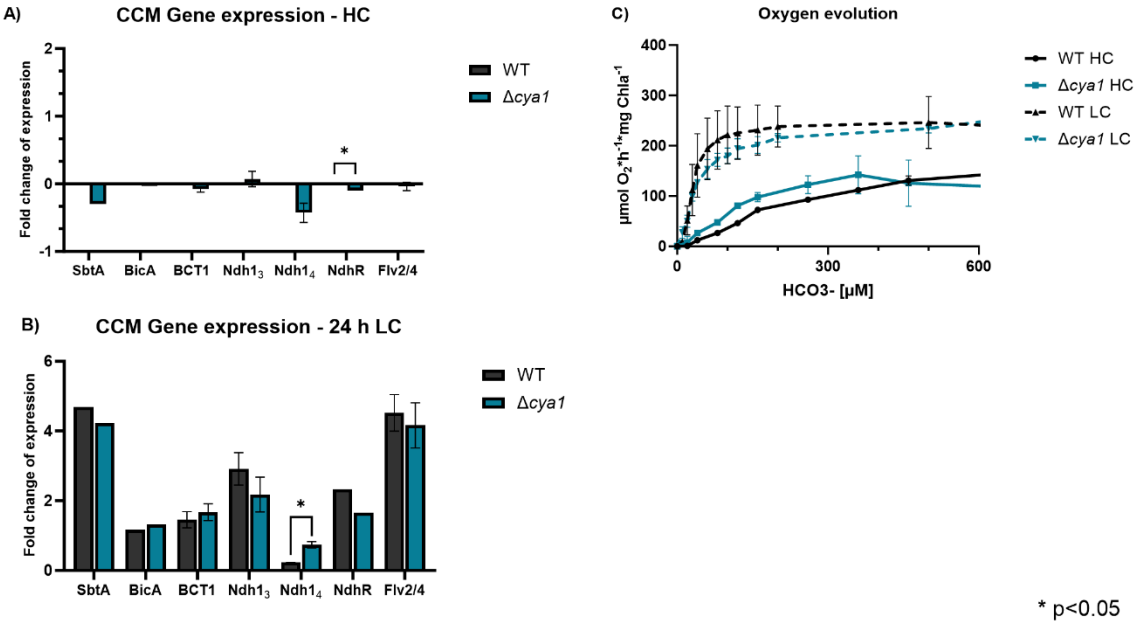

Figure 6: Impact of Δ*cya1 *mutation on gene expression of main CCM components and oxygen evolution of* in vivo *cultures. Fold changes in gene expression of main CCM components at HC (**A**) or 24 h after shift to LC (**B**) of *Synechocystis* strains WT (Black) and Δ*cya1* (Blue). HC expression of WT was set to 0. The CCM components include bicarbonate transporters SbtA, BicA and BCT1, the constitutive Ndh4 or the LC-induced Ndh3 complex, and the flavoprotein (Flv) 2,4-encoding operon *sll0217*,*0218*,*0219*. (**C**) Bicarbonate-dependent oxygen evolution of *Synechocystis* strains WT and Δ*cya1* adapted to either HC or LC conditions. *p<0.05 (Mantovani *et al*., 2022)

c-di-AMP

Compared to cAMP, c-di-AMP, plays a more direct role in the regulation of gene expression of both CCM related and C_i-regulated genes. This can be easily observed in the Δ*dacA* mutants in *Synechocystis*. In fact, as DacA is the only di-adenylate-cyclase present in *Synechocystis*, its knock-out causes the complete absence of c-di-AMP from the cells. (Mantovani *et al*., 2022; Selim *et al*., 2021) Under HC conditions, this leads to a significant increase in the expression of all three bicarbonate transporters and one component of the CO_2 hydration system, NDH1$_3$, while the expression of the second, the constitutive NDH1$_4$, is reduced (Fig. 7A). Furthermore, the absence of c-di-AMP causes numerous C_i-regulated genes to be differently

expressed, especially under HC conditions. One such example is the operon coding for flavoproteins 2 and 4, which provide photoprotection for the photosynthetic complex. The operon is normally strongly induced under LC conditions, but the lack of c-di-AMP causes its expression to be upregulated under HC conditions. (Allahverdiyeva *et al*., 2015; Mantovani *et al*., 2022) Upon shifting C_i conditions, however, the role of c-di-AMP on CCM-related and C_i-regulated genes is reduced. In fact, the number of genes the lack of c-di-AMP causes to be differently regulated is greatly inferior after the shifting to LC compared to constant HC-conditions. The main effect on components of the CCM is the down-regulation of the two bicarbonate transporters SbtA and BicA, and of $1NDH1_3$. (Fig. 7B) (Mantovani *et al*., 2022) The effect the lack of c-di-AMP has on the expression of CCM components, however, is not reflected on the activity of the CCM *in vivo* in *Synechocystis* (Fig. 4, Fig. 7C), where only a slight increase in bicarbonate affinity under HC conditions and reduced CBB activity under LC can be observed. Likely, c-di-AMP is most significant not during changing C_i conditions, but in the regulation of carbon metabolism during diurnal rhythm, such as the influence on the synthesis of glycogen. (Mantovani *et al*., 2022; Selim *et al*., 2021)

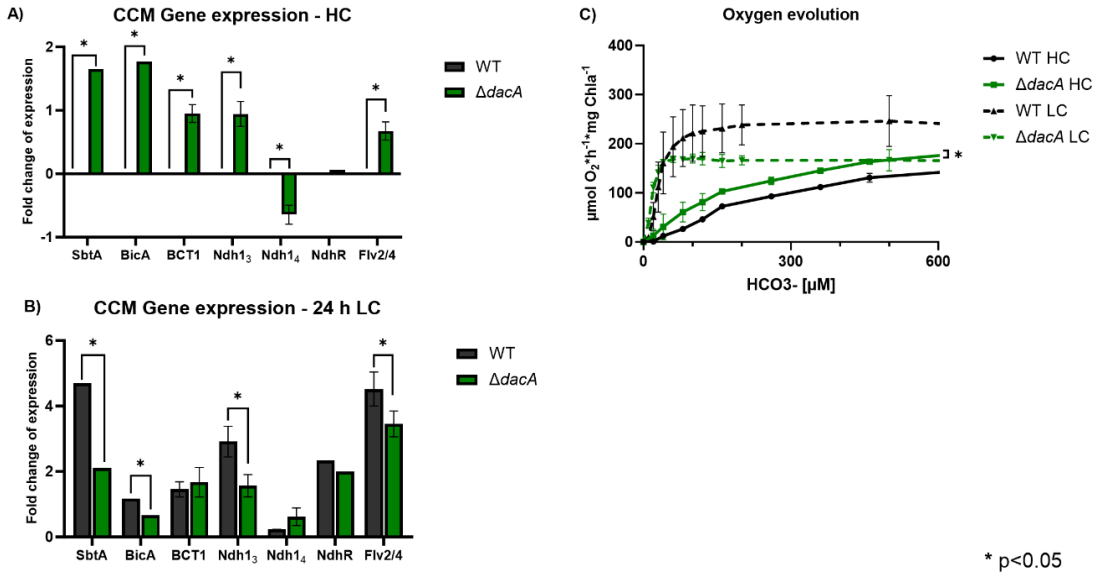

Figure 7: Impact of ΔdacA mutation on gene expression of main CCM components and oxygen evolution of in vivo cultures. Fold changes in gene expression of main CCM components at HC (**A**) or 24 h after shift to LC (**B**) of *Synechocystis* strains WT (Black) and Δ*dacA* (Green). HC expression of WT was set to 0. The CCM components include bicarbonate transporters SbtA, BicA and BCT1, the constitutive Ndh4 or the LC-induced Ndh3 complex, and the flavoprotein (Flv) 2,4-encoding operon *sll0217*,*0218*,*0219*. (**C**) Bicarbonate-dependent oxygen evolution of *Synechocystis* strains WT and Δ*dacA* adapted to either HC or LC conditions. *p<0.05 (Mantovani *et al*., 2022)

SbtB

Compared to cAMP and c-di-AMP individually, SbtB-mediated regulation of cell metabolism and gene expression under changing C_i conditions is much higher. The lack of SbtB in *Synechocystis*, in fact, causes significant changes in the expression of many genes when shifting from HC to LC conditions. These include not only components of the CCM, but also a large number of genes that are normally regulated

by C_i conditions and are under the regulation of the known C_i acquisition transcription regulator NdhR and other unknown regulators. (Klähn *et al*., 2015; Mantovani *et al*., 2022)

Under constant HC conditions, the absence of SbtB does not impact the expression of components of the CCM significantly (Fig. 8 A), only causing a slight up-regulation of the two bicarbonate transporters BCT1 and BicA, and the downregulation of the transporter SbtA and the CO_2 hydration system component $Ndh1_3$. However, numerous genes are significantly up- or down- regulated in the Δ*sbtB* mutant under HC conditions, among which many show a similar or opposite expression patter in WT only after the shift to LC conditions. Among the upregulated genes are the ATP synthase operon *sll1321-1327* and AtpΘ, the inhibitor of ATP hydrolysis, correlating with a significantly higher ATP concentration in the Δ*sbtB* mutant under HC conditions. (Klähn *et al*., 2015; Mantovani *et al*., 2022; Song *et al*., 2022)

Upon shifting to LC conditions, the knock-out of *sbtB* has an even greater effect on the regulation of gene expression. Among the components of the CCM, both SbtA and $Ndh1_3$ are significantly downregulated (Fig. 8 B). While not many genes are upregulated, however, the Δ*sbtB* mutation causes the downregulation of a large number of genes, many of which regulated by C_i regimes, including the regulator NdhR and other genes normally induced under LC conditions such as the operon coding for the flavoproteins Flv2/4. (Mantovani *et al*., 2022)

The numerous C_i-regulated genes which are significantly less induced after shifting to LC conditions when SbtB is missing show how this mutation causes the cells to adapt to a LC-like state when under HC conditions. This is further highlighted by the C_i-uptake affinity under HC and LC conditions (Fig. 8 C), where, in WT *Synechocystis*, cells have a much higher affinity when adapted to LC than HC conditions, as in a state of low C_i, the CCM is induced and bicarbonate can be taken up more quickly. When SbtB is knocked-out, however, the cells, both when acclimated to either HC or LC conditions, have an affinity to bicarbonate which is between the HC- and LC- states of WT *Synechocystis*. (Mantovani *et al*., 2022; Selim *et al*., 2018) Furthermore, the levels of 2PG, the product of the oxygenation reaction of RuBisCO, normally low under HC and spiking upon shift to LC, do not increase as rapidly after shifting cells from HC to LC conditions in the Δ*sbtB* when compared to WT, showing the mutant can more easily acclimate to the shift to low C_i concentration (Fig. 8 D). (Mantovani *et al*., 2022; Orf *et al*., 2016) More than constant C_i conditions, which are not a true representation of the environment cyanobacteria grow in, SbtB is much more relevant for the acclimation of cells to changing C_i regimes than the single second messengers. In fact, when SbtB is missing in *Synechocystis*, the cells become much more sensitive to fluctuating C_i conditions, greatly impacting their survivability. (Selim *et al*., 2018)

Outside of C_i related genes, the regulatory role of SbtB extends also to the photosynthetic apparatus of *Synechocystis*. When shifting Δ*sbtB* cells from HC to LC conditions, multiple genes coding for components essential for photosynthesis, including PSI, PSII and phycobilisomes, become downregulated, while some genes are already downregulated under HC conditions. This is visible in a Δ*sbtB* mutant by pigmentation, displaying a lower chlorophyll content and a reduced growth speed,

further affected by a high light sensibility, especially under LC conditions. (Mantovani *et al*., 2022; Selim *et al*., 2018)

While until now only the glycogen branching enzyme GlgB and the bicarbonate transporter SbtA have been identified as direct targets for SbtB regulation, the significant physiological effects the knock-out of SbtB causes to cyanobacteria shows that, like canonical PII proteins, SbtB possess a widespread regulatory network, even though many components still need to be identified. (Forchhammer *et al*., 2022; Mantovani *et al*., 2023)

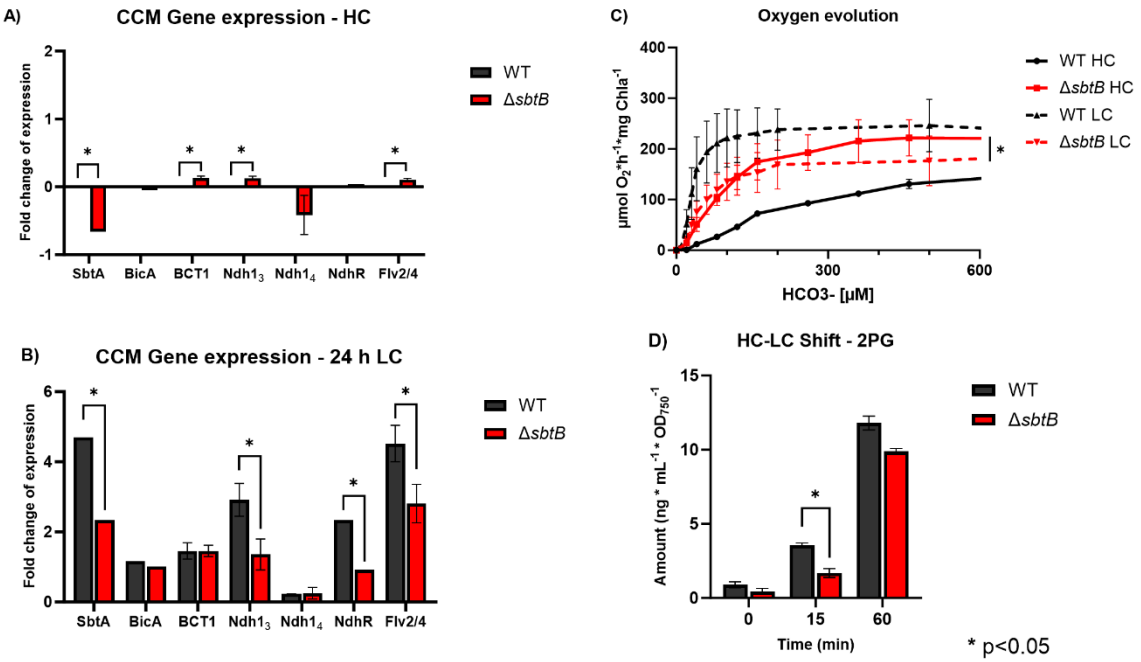

Figure 8: Impact of ⊿*sbtB *mutation on gene expression of main CCM components and oxygen evolution of* in vivo *cultures. Fold changes in gene expression of main CCM components at HC (**A**) or 24 h after shift to LC (**B**) of *Synechocystis* strains WT (Black) and Δ*cya1* (Red). HC expression of WT was set to 0. The CCM components include bicarbonate transporters SbtA, BicA and BCT1, the constitutive Ndh4 or the LC-induced Ndh3 complex, and the flavoprotein (Flv) 2,4-encoding operon *sll0217*,*0218*,*0219*. (**C**) Bicarbonate-dependent oxygen evolution of *Synechocystis* strains WT and Δ*sbtB* adapted to either HC or LC conditions. (**D**) Concentrations of 2-phosphoglycolate (2PG) at HC (0 min) and 15 and 60 min after shift to LC. *p<0.05 (Mantovani *et al*., 2022)

Although SbtB appears more relevant for cyanobacteria during changing C_i conditions than cAMP or c-di-AMP, the knock-out of the enzymes responsible for the synthesis of the two second messengers only gives an insight into their roles in the physiology of cyanobacteria. Such an experiment, in fact, does not provide information regarding how the SbtB-mediated regulation is affected by the binding of the two adenyl nucleotides. For this purpose, site-specific SbtB mutants with the inability to bind specific second messengers can provide a more detailed insight into their role in the regulation of SbtB and its modulation of the rest of the CCM.

The interaction of SbtB with SbtA regulates bicarbonate uptake and prevents leakage

While SbtB regulates multiple C_i-related components of the metabolism of cyanobacteria, its main role is the modulation of the activity of the bicarbonate transporter SbtA. In fact, not only are they expressed in the same operon, but they present a similarly trimeric structure, allowing a monomer-monomer interaction. The most relevant structural components of SbtB that allow the interaction, outside of the T-loop, are the α1-β1 and the B loops. Between the three, however, only the T-loop is involved in the modulation of the transport activity, as the other two loops only serve the purpose of increasing the affinity of SbtB to SbtA through van der Waals interaction. In fact, in a SbtB-ΔT-loop *Synechocystis* mutant strain where the T-loop is removed, SbtB is still capable of interfacing with SbtA, albeit with a reduced affinity. (Fang *et al*., 2021; Haffner *et al*., 2023; Liu *et al*., 2021)

Of particular relevance for the modulating activity of the T-loop are the residues R43 and R46, coordinating with the β- and γ- phosphates of ATP and ADP, and K40, situated close to the metal ion coordinating the β- and γ- phosphates. These residues are highly conserved among cyanobacterial SbtBs, as they are not only important for the binding affinity of SbtB to ATP and ADP, but also for the apyrase activity the protein possesses for the two adenyl nucleotides. In fact, in *Synechocystis* SbtB mutant strains where these residues were replaced by alanine, both the binding affinity and the phosphate release rate were heavily reduced. On the other hand, the three residues are not relevant for the interaction with AMP and cAMP, as the mutations do not affect the affinity of SbtB for the two. (Haffner *et al*., 2023; Selim *et al*., 2023)

Among the three residues of the T-loop, R46 is of particular significance, as it is not only relevant for stabilizing the SbtB-ATP interaction, but also the SbtB-SbtA association. In fact, when the R-loop of SbtB is reduced and the T-loop adopts the ATP-protecting conformation, when ATP is bound to SbtB, R46 coordinates with N59, to potentially prevent the hydrolysis of ATP, while when ADP is bound to SbtB, R46 coordinates with the β- phosphate instead. However, when the R-loop is oxidised and the apyrase activity of SbtB is present, R46 coordinates with the γ- phosphate and becomes relevant for the hydrolysis of ATP. As the binding of this nucleotide to SbtB causes the structuring of the T-loop and the dissociation of the SbtB-SbtA complex, the replacement of the R46 with alanine, in the SbtB-R46A mutation, promotes the association of SbtB to SbtA. (Selim *et al*., 2023) The significance of this residue in the modulation of the activity of SbtB is seen in the changes in the CCM activity the R46A mutation causes. When measuring the oxygen evolution of the mutant strain compared to WT, adapted to either HC or LC conditions, in fact, the SbtB-R46A mutation causes the cells to become unable to change their bicarbonate affinity in response to changing C_i conditions, displaying a high bicarbonate affinity under HC conditions, similarly to the Δ*sbtB* mutation (Fig. 9 A-B). Contrary to the knock-out of SbtB, however, the R46A mutation does not affect the general activity of the CBB cycle, as SbtB possesses more regulatory properties that those mediated by ATP. (Haffner *et al*., 2023; Mantovani *et al*., 2022)

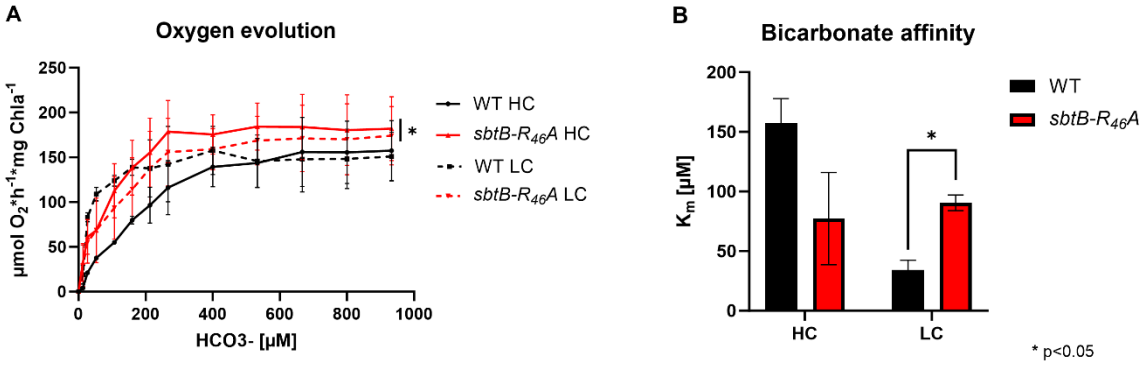

Fig. 9: CCM activity characterization of SbtB-R46A mutant. (A) Bicarbonate-dependent photosynthetic activity of *Synechocystis* WT (Black) and SbtB-R46A (Red) mutant cells acclimated to either HC (Continuous line) or LC (Dashed line) conditions. (B) Bicarbonate affinity represented by the K_m (HCO_3^-) values of WT and SbtB-R46A mutant under either HC or LC conditions. *p<0.05 (Haffner *et al*., 2023)

The regulatory roles of SbtB and its T-loop on the transport activity of SbtA are still under debate. In fact, when SbtA and SbtB are co-expressed in the heterologous host *E. coli*, SbtB inhibits the transport activity of SbtB. Similarly, structural data of the SbtA:SbtB complex indicate that the T-loop of SbtB, when free to interact with SbtA, when AMP or ADP are bound to SbtB, apparently blocks the transporter in the inward facing configuration, preventing bicarbonate uptake. (Du *et al*., 2014; Fang *et al*., 2021; Liu *et al*., 2021) These results, however, greatly contrast with the large amount of evidence of the lower growth rate of the Δ*sbtB* mutant, the induction of the *sbtAB* operon and the formation of the SbtA:SbtB complex under low C_i supply, when bicarbonate transport is needed the most. (Mantovani *et al*., 2022; Selim *et al*., 2018)

Further investigation showed that the main regulatory property of SbtB on SbtA is not the simple inhibition of bicarbonate uptake, but to act as a modulator for different SbtA activity modes including a function as a plug to prevent the backflowing leakage of bicarbonate from the cells. In fact, the family of Na^+ symporters SbtA belongs to is capable of a reverse activity, potentially leaking Na^+ and the transported substrate. Cyanobacteria spend a considerable amount of energy not only to maintain the Na^+ gradient necessary for it to act as a driving force for transport, but also for the activity of the CCM, as it allows the intracellular bicarbonate concentration to be 100-1000 times higher than in the environment. (Hagemann *et al*., 2021; Sauer *et al*., 2022) As such, the function of SbtB as a plug allows cyanobacteria to save a considerable amount of energy by preventing bicarbonate leakage when transport is inactive, such as in the darkness, when the CBB cycle is not active. As a result, if SbtB is knocked-out, *Synechocystis* experiences a two-fold increase in leaked bicarbonate only 5 minutes after shifting cells from light to darkness (Fig. 10). (Haffner *et al*., 2023; Hagemann *et al*., 2021)

ATP also plays a large role in the regulation of the plug function of SbtB. As the binding of ATP to Sbtb causes the dissolution of the SbtA:SbtB complex, thereby preventing the plug function of SbtB, the SbtB-R46A mutant, unable to bind ATP, has a strongly reduced bicarbonate leakage (Fig. 10). This correlates with the ATP and higher AMP concentrations measured in LC grown *Synechocystis* cells compared to HC, as in low

C_i-regimes, the CCM needs to be active and the leakage of bicarbonate prevented. (Haffner *et al*., 2023; Selim *et al*., 2018, 2023)

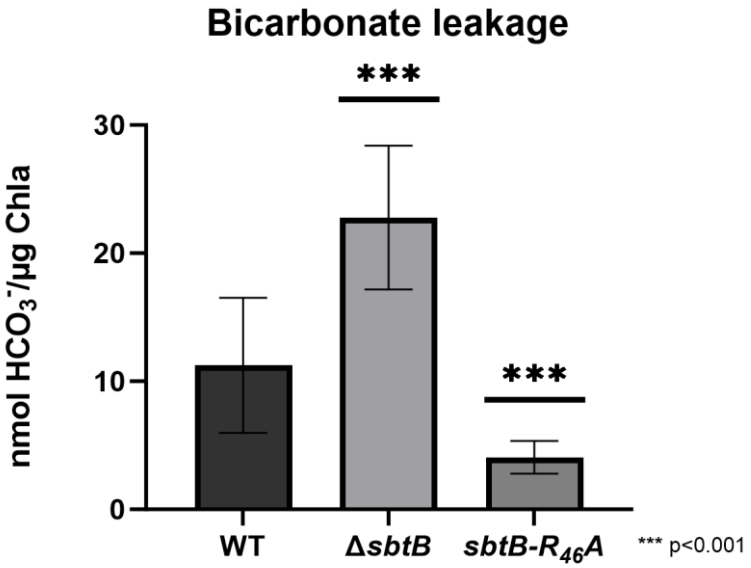

Fig. 10: Bicarbonate leakage measurement. Levels of leaked ^{14}C-labelled bicarbonate from *Synechocystis* WT, Δ*sbtB* and SbtB-R46A cells. ***p<0.001 (Haffner *et al*., 2023)

Insight into the mechanical regulation SbtB exercises on SbtA was revealed by structural analyses comparing the SbtA:SbtB and SbtA:SbtB-ΔT-loop, in the presence and absence of AMP. The structure of SbtA when alone or when bound to SbtB-ΔT-loop is in an occluded conformation, with HCO_3^- trapped in the transporter and both the intra- and extra- cellular binding sites inaccessible. In the SbtA:SbtB-AMP complex, however, the core shifts against the immobile gate domain of SbtA to an inward-open conformation. In this conformation the intracellular binding site of HCO_3^- is open, but partially blocked by the T-loop, which is structured and inserted in SbtA. The formation of the SbtA:SbtB complex without AMP, however, still causes the shift of the core domain of SbtA to an inward-open conformation, but the T-loop of SbtB is disordered. A simulation of a tunnel from the HCO_3^- binding site showed how bicarbonate movement is still possible in the SbtA:SbtB and not in the SbtA:SbtB-ΔT-loop complex, indicating that the binding of AMP could prevent the leakage of bicarbonate by partially blocking the intracellular binding site. (Fang *et al*., 2021; Haffner *et al*., 2023; Liu *et al*., 2021)

Ultimately, the regulation of the activity of SbtA by SbtB is strongly dependent on the adenyl nucleotide bound to SbtB. While the main significance of the formation of the SbtA:SbtB complex appears to be the inhibition of the bicarbonate leakage, SbtB also retains a transport inhibition function. In fact, an experiment with membrane vesicles containing either SbtA only or both SbtA and SbtB, incubated with AMP, showed that the presence of SbtB does not affect the activity of SbtA. (Haffner *et al*., 2023) The uptake inhibition, on the other hand, appears more relevant in the diurnal cycle, to prevent the energetically unfavourable uptake of bicarbonate. Indeed, in *Synechococcus elongatus*, the bicarbonate uptake is switched off in the dark independently on the presence of SbtB, but SbtA-mediated uptake in the initial

adaptation of the cells from darkness to low light is strongly reduced in the presence of SbtB. (Förster *et al*., 2023) The role of SbtB in the modulation of CCM activity under diurnal light regimes is further seen in *Synechocystis* as well, where the different light conditions cause significant and SbtB-dependent changes in the bicarbonate transport activity. (Oren *et al*., 2021)

Interestingly, the novel plug function of SbtB is not unique to this protein but appears to be common among canonical PII proteins. In fact, similarly to SbtB, PII was previously reported to act as an inhibitor of the ammonia transporter AmtB, even under low intracellular ammonia conditions. However, after the finding about the plug function of SbtB, an investigation of PII functionality in *Synechocystis* revealed that, just like SbtB, PII can act as a plug to prevent backflow of ammonia through AmtB. (Conroy *et al*., 2007; Forchhammer *et al*., 2022; Haffner *et al*., 2023)

The R-loop is a redox sensor that affects diurnal SbtB functionality

As photosynthesis is the only energy source for most cyanobacteria, they are highly dependent on light and developed mechanisms to adapt to its changes in order to most effectively utilize the available light. They achieve this through a large variety of sensor proteins, capable of detecting light intensity at different wavelengths. These exercise their regulatory function either through protein-protein interactions or through signalling cascades often mediated by second messengers such as c-di-AMP and c-di-GMP. As such, changes in light intensity and quality affect many aspects of their physiology, starting from gene expression to metabolism and even motility. (Enomoto *et al*., 2023; Ho *et al*., 2017)

One of the most common mechanisms cyanobacteria have to respond to changes in light conditions is through redox-sensing proteins. The final product of the photosynthetic electron transfer chain is reduced ferredoxin (Fdx), used to produce $NADPH_2$, which is released in the cytoplasm, causing it to be reducing in the light and oxidising in the dark. (McFarlane *et al*., 2019) Both the reduced Fdx and $NADPH_2$ are used in cyanobacteria for the redox-dependent regulation of protein activity with two different systems. The first is the ferredoxin-thioredoxin reductase (FTR) protein, which uses the reduced Fdx to reduce the thiol groups of thioredoxin (Trx), breaking the disulphide bridge between them. (Schürmann & Buchanan, 2008) The second system is the $NADPH_2$-dependent thioredoxin reductase (NTR), which catalyses the reduction of Trx through the oxidation of $NADPH_2$. (Shahpiri *et al*., 2008) The reduced Trx, obtained through either of the two systems, regulates the activity of proteins by opening the disulphide bond, reducing their target and thereby increasing or decreasing their activity. Through this mechanism, the functional role of disulphide bonds lies beyond structural stabilization, but extends to redox-regulation of proteins. While the light-dependent is not the only type of redox regulation in nature, it is the most common in photoautotrophs such as cyanobacteria, experiencing large changes in the redox state during the diurnal rhythm. This type of regulation is common among many proteins of cyanobacteria involved in key metabolic processes, such as

gluconeogenesis and the CBB cycle. (Bechtel & Weerapana, 2017; McFarlane *et al*., 2019; Schürmann & Buchanan, 2008)

Another example of a protein which is subjected to redox-regulation is SbtB. In fact, roughly 50% of all cyanobacterial SbtBs possess the C-terminal R-loop, which possesses a conserved C_{105}GPxGC_{110} motif capable of forming a disulphide bridge under oxidizing conditions. (Selim *et al*., 2018, 2023) Similar motifs of C-terminal redox-regulated extensions appear among several enzymes of the CBB cycle, indicating a role of such redox-sensitive hairpins in the regulation of carbon metabolism in photoautotrophic organisms. (Gurrieri *et al*., 2021) Like many of the redox-regulated disulphide bonds in cyanobacteria, the R-loop is regulated by the main Trx in cyanobacteria, TrxA, which is among the proteins with the highest binding affinity for SbtB and is capable of efficiently reducing the disulphide bridge. (Selim *et al*., 2023; Mantovani *et al*., 2023b) Just like other Trx-regulated proteins, the R-loop of SbtB responds to changes in light intensity and in *Synechocystis*, which possesses an SbtB protein with an R-loop, mutations of SbtB greatly impact the regulation of the CCM and C metabolism under changing light conditions. In fact, the knock-out of SbtB and the mutations SbtB-C_{105}A-C_{110}A, with two cysteines replaced with alanine to simulate a permanently reduced R-loop, and SbtB-Δ104, with a truncated R-loop, all cause a significant reduction in the photosynthetic oxygen production and glycogen synthesis in a 12 h day, 12 h night diurnal rhythm under LC conditions. This results in a strongly reduced growth speed for both the Δ*sbtB* and R-loop mutants, which is not the case under constant light conditions, in which only the knock-out of *sbtB* causes a growth defect, as the protein exercises regulation not mediated by the redox-state (Fig. 11 A-B) In fact, under HC conditions, when the activity of the CCM is not required as much, among the three mutations, only Δ*sbtB* causes a defect in both glycogen synthesis and growth (Fig. 11 C-D). (Selim *et al*., 2021, 2023; Mantovani *et al*., 2023b) Furthermore, the redox-sensing ability of the R-loop is not limited to the adaptation to a diurnal rhythm, but also extends to short-term fluctuations in redox-state, as all three SbtB mutations cause *Synechocystis* the inability to adjust its growth to light intensity fluctuations (Fig. 11 E). (Mantovani *et al*., 2023b)

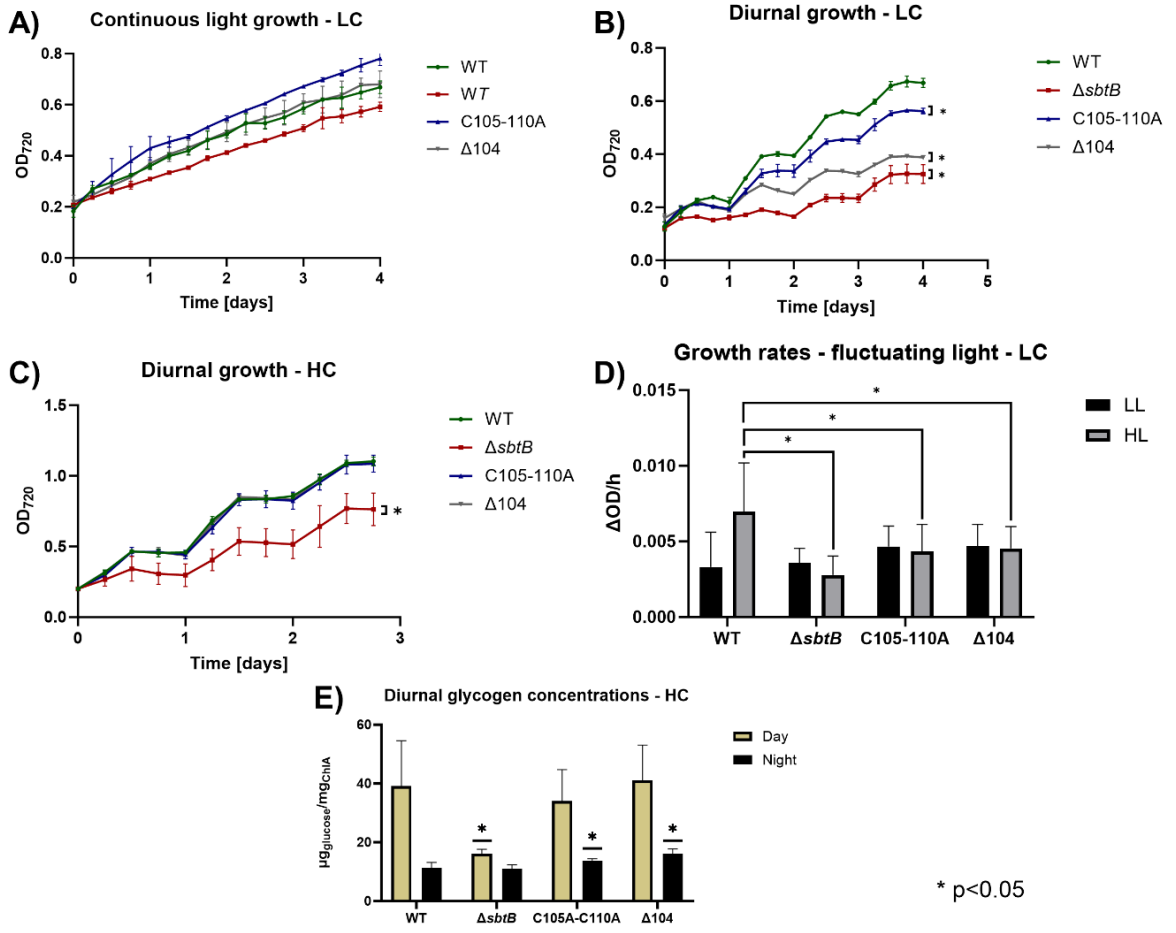

Figure 11: Phenotypic characterization of SbtB R-loop as a redox sensor for changing light conditions. Growth of *Synechocystis* WT strain and mutants Δ*sbtB*, Δ*sbtB*::SbtB-C_{105}A-C_{110}A, Δ*sbtB*::SbtB-Δ104. **A)** Growth under continuous light in LC conditions. **B)** Growth under 12 h light, 12 h darkness regime under HC conditions. **C)** Growth in 12 h light, 12 h darkness diurnal rhythm under LC conditions. **D)** Growth rates (ΔOD_{720}/h) under 6 cycles of fluctuating light conditions (LL: 3 h 100 µmol photons m^{-2} s^{-1}, HL: 3 h 500 µmol photons m^{-2} s^{-1}) at LC. **E)** Glycogen concentration in the middle of the light and dark phases after 3 days adaptation to diurnal rhythm at HC conditions. *p<0.05 (Mantovani *et al*., 2023b)

The main influence the R-loop has on the regulation of SbtB is the modulation of the adenyl nucleotides binding affinity and apyrase activity. Not only does the reduction of the R-loop cause the apyrase activity to be severely reduced, but the ability of the different second messengers to bind SbtB changes. Normally, native *Synechocystis* SbtB binds cAMP and c-di-AMP with the highest affinity, followed by ADP, ATP and AMP. However, if the R-loop is reduced, as simulated in the SbtB-C_{105}A-C_{110}A and SbtB-C_{105}S-C_{110}S mutants, the protein binds ATP with the highest affinity, the binding of cAMP is reduced and SbtB is almost completely unable to bind ADP and AMP, while the apyrase activity decreases substantially. (Selim *et al*., 2023; Mantovani *et al*., 2023b) When the R-loop is truncated, however, the ability of SbtB to bind ADP and AMP is restored, but with a lower affinity than ATP (Table 1), while the apyrase activity

disappears completely. Interestingly, the nucleotide binding affinity the *Synechocystis* truncated R-loop SbtB variant displays is very similar to that of those SbtB proteins that do not naturally possess the R-loop, such as C*yanobium* sp. PCC7001. (Kaczmarski *et al*., 2019; Selim *et al*., 2023; Mantovani *et al*., 2023b)

***Table 1**: Affinity of SbtB variants with exchanged cysteine residues (C_{105}A-C_{110}A, C_{105}S-C_{110}S) or truncated R-loop (Δ109, Δ104) to ATP, ADP, AMP and cAMP, expressed as dissociation constants (K_d) in (μM). UND: undetermined.* (Mantovani *et al*., 2023b)

	***SbtB* WT (oxidized)**		***SbtB*-C105A-C110A**		***SbtB*-C105S-C110S**		***SbtB*-Δ109**		***SbtB*-Δ104**	
	Binding	**K_d (μM)**	**Binding**	**K_d (μM)**	**Binding**	**K_d (μM)**	**binding**	**K_d (μM)**	**Binding**	**K_d (μM)**
ATP	Binding	62.5 ± 16.6	Binding	29.8 ± 14.1	Binding	47.6 ± 21.3	Binding	32.5 ± 17.9	Binding	35.0 ±7.1
ADP	Binding	55.8 ± 7.7	very weak Binding	UND	very weak Binding	UND	very weak Binding	UND	Binding	79.2 ±55.1
AMP	Binding	87.4 ± 3.7	very weak Binding	UND	very weak Binding	UND	very weak Binding	UND	Binding	78.2 ±6.0
cAMP	Binding	30.3 ± 5.0	Binding	106 ± 42.4	Binding	52.8 ± 34.7	Binding	70.2 ± 28.9	Binding	68.1 ±10.1

The great changes in nucleotide binding affinity by the SbtB and R-loop mutants is reflected in the CCM activity of *Synechocystis*, as when cells acclimated to either HC or LC conditions, the SbtB-C_{105}A-C_{110}A mutation causes a Δ*sbtB*-like phenotype, with HC-adapted cells showing a high increase in bicarbonate affinity. This is possibly due to the activity of SbtB as an AMP-mediated inhibitor of bicarbonate uptake, which, due to the inability to bind AMP, would be absent in the reduced state of *Synechocystis* SbtB. However, when the R-loop is truncated and SbtB is again capable of binding to ADP and AMP, the affinity to bicarbonate is restored to WT-like levels (Fig. 12). (Förster *et al*., 2023; Mantovani *et al*., 2023b)

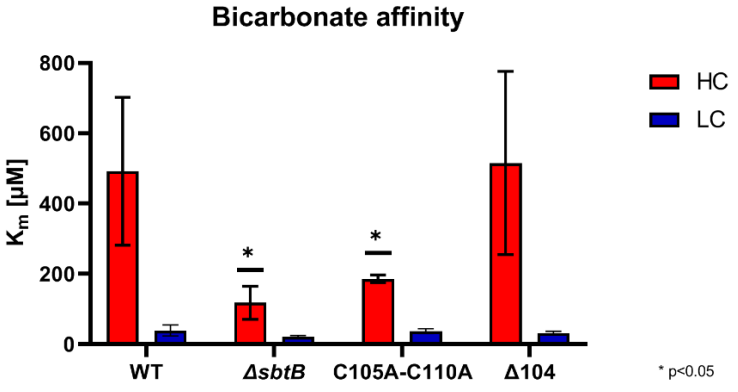

***Figure 12**: **Impact of the sbtB R-loop mutations on CCM activity**. In vivo* affinity to bicarbonate of *Synechocystis* strains WT, Δ*sbtB*, Δ*sbtB*::SbtB-C_{105}A-C_{110}A, Δ*sbtB*::SbtB-Δ104 adapted to HC (Red) or LC (Blue) conditions, expressed as average K_m values of μM bicarbonate of an oxygen evolution experiment. *p<0.05 (Mantovani *et al*., 2023b)

The changes in ligand affinity of the R-loop mutants, however, are not reflected on ability of SbtB to prevent leakage of bicarbonate (Fig. 13). As the reduced R-loop prevents ADP and AMP binding to SbtB, the ATP- and cAMP-bound states of the protein should increase, thereby reducing the formation of the SbtA:SbtB complex and increasing the leakage of bicarbonate from *Synechocystis*. However, this is not the case, and the $C_{105}A$-$C_{110}A$ mutation does not cause an increase in the bicarbonate leakage, contrary to how the truncation of the R-loop does, which causes an increase in the leakage by almost two-fold. This suggests that either the apyrase activity is more relevant for the function of SbtB as a plug, especially considering that the formation of the SbtA:SbtB complex normally causes a four-fold increase in the hydrolysis rate of ATP and ADP, or more unknown mechanics come into play in the interaction between SbtA and SbtB, which are influenced more by the truncation of the R-loop than its reduction. (Haffner *et al*., 2023; Mantovani *et al*., 2023b)

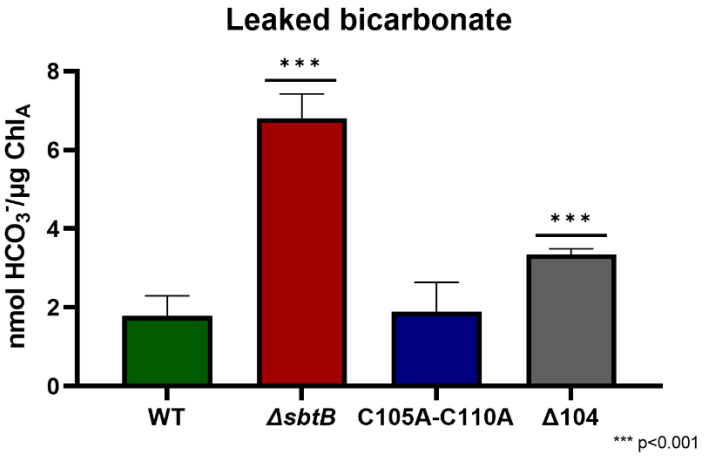

***Figure 13: effect of R-loop mutations on the plug function of SbtB in* Synechocystis.** Concentration of ^{14}C-labelled bicarbonate per amount of Chlorophyll A leaked from cells of WT, Δ*sbtB*, Δ*sbtB*::SbtB-$C_{105}A$-$C_{110}A$, Δ*sbtB*::SbtB-Δ104 strains after incubation for 5 min in the darkness. ***p<0.001 (Mantovani *et al*., 2023b)

While the modulation of the activity of SbtB by the R-loop is still not completely understood, its widespread presence among cyanobacteria highlights its significance. Especially, the evolutionary role of the R-loop is unknown, as among the 50% of cyanobacteria that possess the R-loop, any specific metabolic, environmental or morphological common factor is yet to be identified. Given the current knowledge, however, it appears that the significance of the R-loop relies in adding another layer of regulation to the protein, for a finer response to changing light conditions. (Selim *et al*., 2023; Mantovani *et al*., 2023b)

Conclusions

Research into the metabolism and physiology of cyanobacteria is important for the modern world. Not only do they substantially contribute to the global carbon cycle, but they hold relevance in a variety of fields, ranging from biotechnological uses to working as a model for research of plant plastids. The main current practical application of cyanobacteria resides in the food industry, for the production of food additives, both for animal feed and human consumption. The most used cyanobacteria in this field, *Arthrospira platensis*, commonly known as *Spirulina*, is in fact rich in nutrients and easily digestible, and is therefore consumed regularly in many countries in the world. Research is also being performed for the use of cyanobacteria in the fields of medicine, due to their abundance in novel bioactive compounds, fertilizers, bioremediation and energy production, for both biofuels and hydrogen production. (Abed *et al*., 2009; Żymańczyk-Duda *et al*., 2022) Due to the close relationship cyanobacteria have with plant plastid, these microorganisms are commonly used as models for research into shared processes, such as photosynthesis, carbon fixation and photorespiration. (Hohmann-Marriott & Blankenship, 2011; Orf *et al*., 2016)

Due to their role in the global carbon cycle and the large number of possible application of cyanobacteria, it is of particular relevance to investigate the CCM. For both plants and cyanobacteria, in most cases, the low CO_2 concentration is the factor limiting growth instead of light or nutrients. Since land plants experience a rate of oxygenation reaction of RuBisCO close to 30%, many approaches are being investigated in order to reduce the frequency of oxygenation, as it would provide a significant increase in growth yield, presenting a possible solution for the impending food crisis the world is going to experience in the not-so-distant future. (Hagemann *et al*., 2021; Price *et al*., 2013) The CCM evolved by cyanobacteria is the most efficient system among oxygenic phototrophs to reduce the oxygenation reaction rate and therefore the implementation of components of the CCM in plastids is one of the routes being investigated in order to increase crop yields. Starting from bicarbonate transporters, all the main components of the CCM could be implemented, ultimately establishing a functional CCM which could provide not only an up to 28% increase in carbon fixation rates, but also increase the water usage efficiency of leaves. Until now, the expression of carboxysomes in plant leaves has been successful, but due to the absence of all other components that make the CCM functional, no noticeable improvement in plant growth has been measured yet. (Long *et al*., 2018; Price *et al*., 2013) Gaining a better understanding of the CCM could therefore prove helpful not only for biotechnological applications of cyanobacteria, but plants as well. As such, being one of the main components and regulator of many of the aspects of the CCM, studying the function of SbtB is of particular interest. (Du *et al*., 2014; Price *et al*., 2013)

Part of the PII superfamily of regulators, SbtB possesses a large regulatory network, with multiple interaction partners and varied regulatory mechanics (Fig. 14). With the ability to bind only the adenyl nucleotides ATP, ADP, AMP, cAMP and c-di-AMP, its mode of action is highly affected by the energy state, carbon concentration and diurnal rhythm of the cell. When bound to ATP or cAMP, representing high energy and C_i states, the T-loop of the protein, the main structural component that allows protein-protein interactions, reduces the interaction of SbtB with its main target, the

bicarbonate transporter SbtA. Under high C_i regimes, as SbtA is mostly relevant under LC conditions, its modulation is not as necessary, and SbtB regulates other components of the CCM. Possibly through the interaction with cAMP, the main indicator for sufficient C_i levels, SbtB negatively affects gene expression of some components of the CCM and C_i-regulated genes, likely mediated through the transcription factor CRP1, though a direct interaction between the two has not been observed yet. When bound to AMP, a signal for low energy and limiting C_i levels, SbtB mainly interacts with SbtA, exercising two main functions. The first is as plug, to prevent bicarbonate to leak from the cell. Since the CCM is highly efficient and allows an intracellular concentration of HCO_3^- up to 1000 higher than the extracellular environment, and since the SbtA-mediated transport can work in reverse, SbtB prevents bicarbonate leakage allowing cyanobacteria to avert energy loss. As the intracellular C_i concentration undergo fluctuations, the second function of the interaction between SbtB and SbtA is to prevent bicarbonate uptake when not necessary. Furthermore, under LC conditions, SbtB mediates the up regulation of gene expression of the CCM and multiple C_i-regulated genes. The interaction with c-di-AMP, a daytime signal in a diurnal rhythm, allows SbtB to regulate glycogen synthesis through the interaction with the glycogen branching enzyme GlgB. Moreover, whether through the interaction with SbtB or other proteins, c-di-AMP affects the expression of the CCM, inducing it under HC conditions and repressing it under LC. Outside of the binding with c-di-AMP, SbtB also possesses a diurnal regulatory property thanks to the redox-sensitive C-terminal loop. This R-loop detects the redox state of the cell through a disulphide-bridge between two cysteines residues, oxidised during the night and reduced during the day by thioredoxin. The main function of the R-loop is to regulate the binding affinity of SbtB to the adenyl nucleotides and to trigger the ATP/ADPase activity of SbtB, causing ATP and ADP to be hydrolysed to AMP, increasing the rate of the SbtA:SbtB complex formation to prevent leakage of bicarbonate during the night.

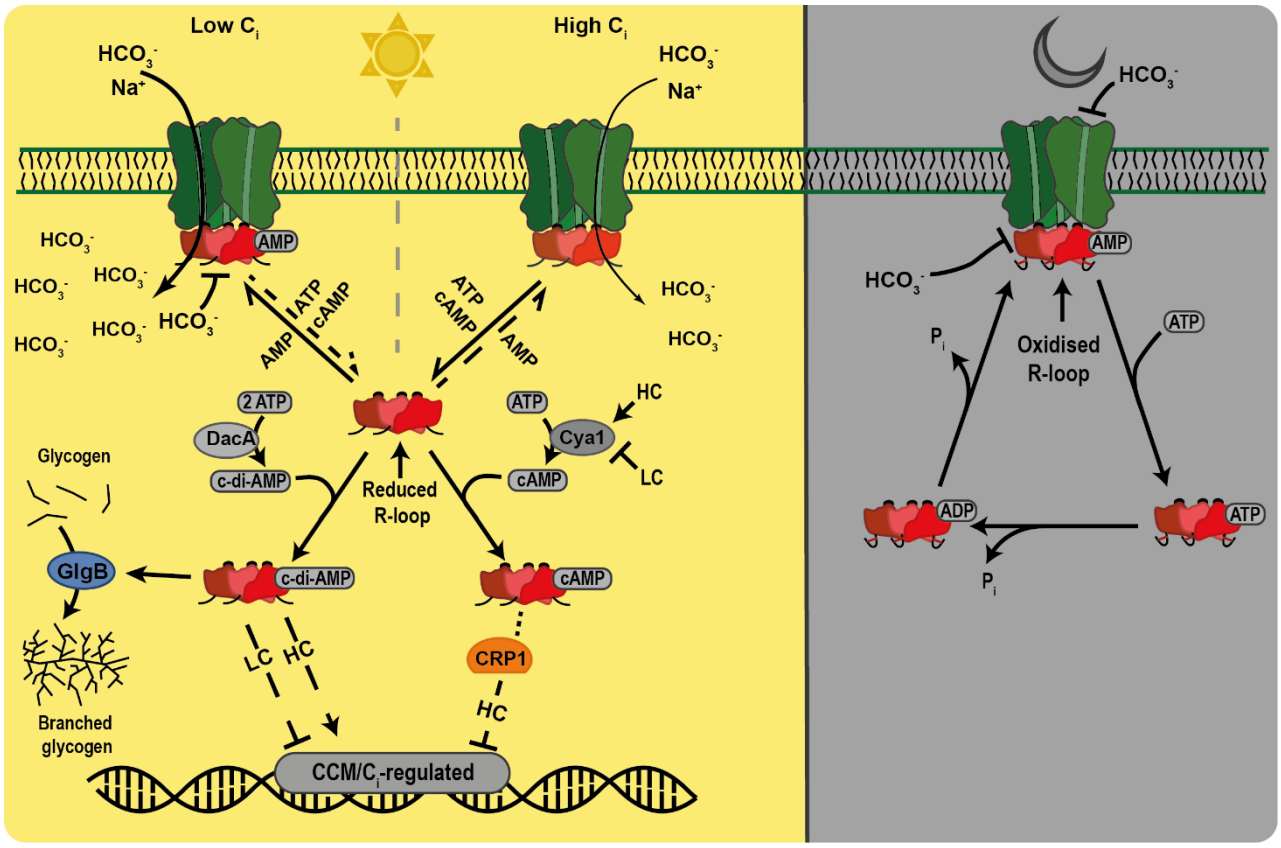

Figure 14: Model of regulatory network of SbtB in* Synechocystis sp. *PCC 6803. On the left, the regulation during the day is shown, both under low and high C_i regimes, with highlight on the interaction of SbtB and SbtA, the role of the adenyl nucleotides binding and the regulation of the glycogen branching enzyme GlgB and gene transcription of CCM components. On the right, the nocturnal regulation of SbtB is shown, showcasing its interaction with SbtA to prevent bicarbonate leakage.

Despite more than 20 years of research into PII proteins, new targets and regulatory mechanisms are still being discovered in recent years and as part of the superfamily, the regulatory network of SbtB appears to be equally vast. While much light has already been shed on the interaction of SbtB with its main partner, SbtA, details are still missing regarding the exact effect of each ligand has on the interaction. Furthermore, only GlgB has been confirmed as a target of SbtB regulation, while the other interaction partners, such as the mediator(s) for gene transcription regulators and other components of the CCM still need to be identified. (Forchhammer *et al*., 2022; Mantovani *et al*., 2023) Another matter that requires investigation is the potential role of protein phosphorylation of SbtB, as the protein possesses two sites capable of accepting a phosphate and the canonical PII is also subjected to phosphorylation to modulate its activity. (Forchhammer *et al*., 2022) More common among eukaryotes, even among prokaryotes protein phosphorylation is a versatile regulatory mechanism, capable of greatly impacting the activity of a protein, while still maintaining reversibility, allowing phosphates to be added and removed depending on specific cell signals, to finely modulate protein activity. Protein phosphorylation is achieved thanks to a concerted action between protein kinases, which catalyse the transfer of a phosphate

group from ATP to the target protein, and phosphatases, which remove the phosphate. (Kennelly, 2002) The involvement of protein phosphorylation for proper acclimation to HC/LC shifts has been shown involving two main protein kinases SpkB (Barske *et al*. 2023) and SpkC (Spät *et al*., 2021). In the case of SbtB, the protein is a candidate for regulation by phytochromes, photoreceptors with possess a kinase activity. As sensor for red/far-red light, which act as signals for dawn and dusk, respectively, the phosphorylation of SbtB could serve as additional regulation of the protein activity in response to the diurnal rhythm. (Oren *et al*., 2021; Shin *et al*., 2016)

Collectively, all the current knowledge about SbtB shows its importance and the value of the past and future research about the protein, promising to be a valuable target of investigation for more years to come.

References

Abed, R. M. M., Dobretsov, S., & Sudesh, K. (2009). Applications of cyanobacteria in biotechnology. J*ournal of Applied Microbiology*, 106(1), 1–12. https://doi.org/10.1111/j.1365-2672.2008.03918.x

Agostoni, M., Logan-Jackson, A. R., Heinz, E. R., Severin, G. B., Bruger, E. L., Waters, C. M., & Montgomery, B. L. (2018). Homeostasis of Second Messenger Cyclic-di-AMP Is Critical for Cyanobacterial Fitness and Acclimation to Abiotic Stress. *Frontiers in Microbiology*, 9, 1121. https://doi.org/10.3389/fmicb.2018.01121

Agostoni, M., & Montgomery, B. L. (2014). Survival Strategies in the Aquatic and Terrestrial World: The Impact of Second Messengers on Cyanobacterial Processes. *Life*, 4(4), 745–769. https://doi.org/10.3390/life4040745

Allahverdiyeva, Y., Isojärvi, J., Zhang, P., & Aro, E.-M. (2015). Cyanobacterial Oxygenic Photosynthesis is Protected by Flavodiiron Proteins. *Life*, 5(1), 716–743. https://doi.org/10.3390/life5010716

Badger, M. R., & Price, G. D. (2003). CO2 concentrating mechanisms in cyanobacteria: Molecular components, their diversity and evolution. *Journal of Experimental Botany*, 54(383), 609–622. https://doi.org/10.1093/jxb/erg076

Bantu, L., Chauhan, S., Srikumar, A., Hirakawa, Y., Suzuki, I., Hagemann, M., & Prakash, J. S. S. (2022). A membrane-bound cAMP receptor protein, SyCRP1 mediates inorganic carbon response in Synechocystis sp. PCC 6803. *Biochimica Et Biophysica Acta*. Gene Regulatory Mechanisms, 1865(3), 194803. https://doi.org/10.1016/j.bbagrm.2022.194803

Bechtel, T. J., & Weerapana, E. (2017). From structure to redox: The diverse functional roles of disulfides and implications in disease. *Proteomics*, 17(6), 10.1002/pmic.201600391. https://doi.org/10.1002/pmic.201600391

Berner, R. A. (2006). GEOCARBSULF: A combined model for Phanerozoic atmospheric O2 and CO2. *Geochimica et Cosmochimica Acta*, 70(23), 5653–5664. https://doi.org/10.1016/j.gca.2005.11.032

Bryant, D. A., & Frigaard, N.-U. (2006). Prokaryotic photosynthesis and phototrophy illuminated. *Trends in Microbiology*, 14(11), 488–496. https://doi.org/10.1016/j.tim.2006.09.001

Calteau, A., Fewer, D. P., Latifi, A., Coursin, T., Laurent, T., Jokela, J., Kerfeld, C. A., Sivonen, K., Piel, J., & Gugger, M. (2014). Phylum-wide comparative genomics unravel the diversity of secondary metabolism in Cyanobacteria. *BMC Genomics*, 15(1), 977. https://doi.org/10.1186/1471-2164-15-977

Cann, M. J., Hammer, A., Zhou, J., & Kanacher, T. (2003). A defined subset of adenylyl cyclases is regulated by bicarbonate ion. *The Journal of Biological Chemistry*, 278(37), 35033–35038. https://doi.org/10.1074/jbc.M303025200

Cohen, S. E., & Golden, S. S. (2015). Circadian Rhythms in Cyanobacteria. *Microbiology and Molecular Biology Reviews*, 79(4), 373–385. https://doi.org/10.1128/mmbr.00036-15

Conroy, M. J., Durand, A., Lupo, D., Li, X.-D., Bullough, P. A., Winkler, F. K., & Merrick, M. (2007). The crystal structure of the Escherichia coli AmtB-GlnK complex reveals how GlnK regulates the ammonia channel. *Proceedings of the National Academy of Sciences of the USA*, 104(4), 1213–1218. https://doi.org/10.1073/pnas.0610348104

DiMario, R. J., Machingura, M. C., Waldrop, G. L., & Moroney, J. V. (2018). The many types of carbonic anhydrases in photosynthetic organisms. *Plant Science: An International Journal of Experimental Plant Biology*, 268, 11–17. https://doi.org/10.1016/j.plantsci.2017.12.002

Du, J., Förster, B., Rourke, L., Howitt, S. M., & Price, G. D. (2014). Characterisation of cyanobacterial bicarbonate transporters in E. coli shows that SbtA homologs are functional in this heterologous expression system. *PloS One*, 9(12), e115905. https://doi.org/10.1371/journal.pone.0115905

Dvořák, P., Poulíčková, A., Hašler, P., Belli, M., Casamatta, D. A., & Papini, A. (2015). Species concepts and speciation factors in cyanobacteria, with connection to the problems of diversity and classification. *Biodiversity and Conservation*, 24(4), 739–757. https://doi.org/10.1007/s10531-015-0888-6

Eisenhut, M., Ruth, W., Haimovich, M., Bauwe, H., Kaplan, A., & Hagemann, M. (2008). The photorespiratory glycolate metabolism is essential for cyanobacteria and might have been conveyed endosymbiontically to plants. *Proceedings of the National Academy of Sciences of the USA*, 105(44), 17199–17204. https://doi.org/10.1073/pnas.0807043105

Enomoto, G., Wallner, T., & Wilde, A. (2023). Control of light-dependent behaviour in cyanobacteria by the second messenger cyclic di-GMP. *microLife*, 4, uqad019. https://doi.org/10.1093/femsml/uqad019

Fang, S., Huang, X., Zhang, X., Zhang, M., Hao, Y., Guo, H., Liu, L.-N., Yu, F., & Zhang, P. (2021). Molecular mechanism underlying transport and allosteric inhibition of bicarbonate transporter SbtA. *Proceedings of the National*

Academy of Sciences of the USA, 118(22), e2101632118. https://doi.org/10.1073/pnas.2101632118

Fokina, O., Chellamuthu, V.-R., Forchhammer, K., & Zeth, K. (2010). Mechanism of 2-oxoglutarate signaling by the Synechococcus elongatus PII signal transduction protein. *Proceedings of the National Academy of Sciences of the USA*, 107(46), 19760–19765. https://doi.org/10.1073/pnas.1007653107

Forchhammer, K., & Lüddecke, J. (2016). Sensory properties of the PII signalling protein family. *The FEBS Journal*, 283(3), 425–437. https://doi.org/10.1111/febs.13584

Forchhammer, K., & Selim, K. A. (2020). Carbon/nitrogen homeostasis control in cyanobacteria. *FEMS Microbiology Reviews*, 44(1), 33–53. https://doi.org/10.1093/femsre/fuz025

Forchhammer, K., Selim, K. A., & Huergo, L. F. (2022). New views on PII signaling: From nitrogen sensing to global metabolic control. *Trends in Microbiology*, 30(8), 722–735. https://doi.org/10.1016/j.tim.2021.12.014

Förster, B., Mukherjee, B., Rourke, L. M., Kaczmarski, J. A., Jackson, C. J., & Price, G. D. (2023). Adenylnucleotide-mediated binding of the PII-like protein SbtB contributes to controlling activity of the cyanobacterial bicarbonate transporter SbtA. *eLife*, 12. https://doi.org/10.7554/eLife.88488

Francko, D. A., & Wetzel, R. G. (1981). Dynamics of cellular and extracellular cAMP in Anabaena Flor-Aquae (Cyanophyta): Intrinsic culture variability and correlation with metabolic variables. *Journal of Phycology*, 17(2), 129–134. https://doi.org/10.1111/j.1529-8817.1981.tb00831.x

Froese, D. S., Michaeli, A., McCorvie, T. J., Krojer, T., Sasi, M., Melaev, E., Goldblum, A., Zatsepin, M., Lossos, A., Álvarez, R., Escribá, P. V., Minassian, B. A., von Delft, F., Kakhlon, O., & Yue, W. W. (2015). Structural basis of glycogen branching enzyme deficiency and pharmacologic rescue by rational peptide design. *Human Molecular Genetics*, 24(20), 5667–5676. https://doi.org/10.1093/hmg/ddv280

Görke, B., & Stülke, J. (2008). Carbon catabolite repression in bacteria: Many ways to make the most out of nutrients. *Nature Reviews. Microbiology*, 6(8), 613–624. https://doi.org/10.1038/nrmicro1932

Gurrieri, L., Fermani, S., Zaffagnini, M., Sparla, F., & Trost, P. (2021). Calvin-Benson cycle regulation is getting complex. *Trends in Plant Science*, 26(9), 898–912. https://doi.org/10.1016/j.tplants.2021.03.008

Haffner, M., Hou, W.-T., Mantovani, O., Walke, P. R., Hauf, K., Borisova, M., Hagemann, M., Zhou, C.-Z., Forchhammer, K., & Selim, K. A. (2023). PII signal transduction superfamily acts as a valve plug to control bicarbonate and ammonia homeostasis among different bacterial phyla (p. 2023.08.10.552651). *bioRxiv*. https://doi.org/10.1101/2023.08.10.552651

Hagemann, M., & Kaplan, A. (2020). Is the Structure of the CO2-Hydrating Complex I Compatible with the Cyanobacterial CO2-Concentrating Mechanism?. *Plant Physiology*, 183(2), 460–463. https://doi.org/10.1104/pp.20.00220

Hagemann, M., Kern, R., Maurino, V. G., Hanson, D. T., Weber, A. P. M., Sage, R. F., & Bauwe, H. (2016). Evolution of photorespiration from cyanobacteria to land plants, considering protein phylogenies and acquisition of carbon concentrating mechanisms. J*ournal of Experimental Botany*, 67(10), 2963–2976. https://doi.org/10.1093/jxb/erw063

Hagemann, M., Song, S., & Brouwer, E.-M. (2021). Inorganic Carbon Assimilation in Cyanobacteria: Mechanisms, Regulation, and Engineering. In Cyanobacteria Biotechnology (pp. 1–31). *John Wiley & Sons, Ltd*. https://doi.org/10.1002/9783527824908.ch1

Hammer, A., Hodgson, D. R. W., & Cann, M. J. (2006). Regulation of prokaryotic adenylyl cyclases by CO2. *Biochemical Journal*, 396(Pt 2), 215–218. https://doi.org/10.1042/BJ20060372

Hardie, D. G. (2011). AMP-activated protein kinase—An energy sensor that regulates all aspects of cell function. *Genes & Development*, 25(18), 1895–1908. https://doi.org/10.1101/gad.17420111

Ho, M.-Y., Soulier, N. T., Canniffe, D. P., Shen, G., & Bryant, D. A. (2017). Light regulation of pigment and photosystem biosynthesis in cyanobacteria. Current *Opinion in Plant Biology*, 37, 24–33. https://doi.org/10.1016/j.pbi.2017.03.006

Hohmann-Marriott, M. F., & Blankenship, R. E. (2011). Evolution of photosynthesis. *Annual Review of Plant Biology*, 62, 515–548. https://doi.org/10.1146/annurev-arplant-042110-103811

Hu, Y., Zhang, X., Shi, Y., Zhou, Y., Zhang, W., Su, X.-D., Xia, B., Zhao, J., & Jin, C. (2011). Structures of Anabaena calcium-binding protein CcbP: Insights into Ca2+ signaling during heterocyst differentiation. *The Journal of Biological Chemistry*, 286(14), 12381–12388. https://doi.org/10.1074/jbc.M110.201186

Jiang, P., & Ninfa, A. J. (1999). Regulation of autophosphorylation of Escherichia coli nitrogen regulator II by the PII signal transduction protein. *Journal of Bacteriology*, 181(6), 1906–1911. https://doi.org/10.1128/JB.181.6.1906-1911.1999

Jiang, Y.-L., Wang, X.-P., Sun, H., Han, S.-J., Li, W.-F., Cui, N., Lin, G.-M., Zhang, J.-Y., Cheng, W., Cao, D.-D., Zhang, Z.-Y., Zhang, C.-C., Chen, Y., & Zhou, C.-Z. (2018). Coordinating carbon and nitrogen metabolic signaling through the cyanobacterial global repressor NdhR. *Proceedings of the National Academy of Sciences* of the USA, 115(2), 403–408. https://doi.org/10.1073/pnas.1716062115

Kaczmarski, J. A., Hong, N.-S., Mukherjee, B., Wey, L. T., Rourke, L., Förster, B., Peat, T. S., Price, G. D., & Jackson, C. J. (2019). Structural Basis for the Allosteric Regulation of the SbtA Bicarbonate Transporter by the PII-like

Protein, SbtB, from Cyanobium sp. PCC7001. *Biochemistry*, 58(50), 5030–5039. https://doi.org/10.1021/acs.biochem.9b00880

Kaplan, A., & Reinhold, L. (1999). CO2 concentrating mechanism in photosynthetic microorganisms. A*nnual Review of Plant Physiology and Plant Molecular Biology*, 50, 539–570. https://doi.org/10.1146/annurev.arplant.50.1.539

Kennelly, P. J. (2002). Protein kinases and protein phosphatases in prokaryotes: A genomic perspective. *FEMS Microbiology Letters*, 206(1), 1–8. https://doi.org/10.1111/j.1574-6968.2002.tb10978.x

Klähn, S., Orf, I., Schwarz, D., Matthiessen, J. K. F., Kopka, J., Hess, W. R., & Hagemann, M. (2015). Integrated Transcriptomic and Metabolomic Characterization of the Low-Carbon Response Using an ndhR Mutant of Synechocystis sp. PCC 6803. *Plant Physiology*, 169(3), 1540–1556. https://doi.org/10.1104/pp.114.254045

Kupriyanova, E. V., Sinetova, M. A., Cho, S. M., Park, Y.-I., Los, D. A., & Pronina, N. A. (2013). CO2-concentrating mechanism in cyanobacterial photosynthesis: Organization, physiological role, and evolutionary origin. *Photosynthesis Research*, 117(1–3), 133–146. https://doi.org/10.1007/s11120-013-9860-z

Labella, J. I., Cantos, R., Salinas, P., Espinosa, J., & Contreras, A. (2020). Distinctive Features of PipX, a Unique Signaling Protein of Cyanobacteria. *Life*, 10(6), 79. https://doi.org/10.3390/life10060079

Liu, X.-Y., Hou, W.-T., Wang, L., Li, B., Chen, Y., Chen, Y., Jiang, Y.-L., & Zhou, C.-Z. (2021). Structures of cyanobacterial bicarbonate transporter SbtA and its complex with PII-like SbtB. *Cell Discovery*, 7(1), Article 1. https://doi.org/10.1038/s41421-021-00287-w

Long, B. M., Hee, W. Y., Sharwood, R. E., Rae, B. D., Kaines, S., Lim, Y.-L., Nguyen, N. D., Massey, B., Bala, S., von Caemmerer, S., Badger, M. R., & Price, G. D. (2018). Carboxysome encapsulation of the CO2-fixing enzyme Rubisco in tobacco chloroplasts. *Nature Communications*, 9, 3570. https://doi.org/10.1038/s41467-018-06044-0

Lyons, T. W., Reinhard, C. T., & Planavsky, N. J. (2014). The rise of oxygen in Earth's early ocean and atmosphere. *Nature*, 506(7488), 307–315. https://doi.org/10.1038/nature13068

Makowka, A., Nichelmann, L., Schulze, D., Spengler, K., Wittmann, C., Forchhammer, K., & Gutekunst, K. (2020). Glycolytic Shunts Replenish the Calvin-Benson-Bassham Cycle as Anaplerotic Reactions in Cyanobacteria. *Molecular Plant*, 13(3), 471–482. https://doi.org/10.1016/j.molp.2020.02.002

Mandal, M., & Breaker, R. R. (2004). Gene regulation by riboswitches. *Nature Reviews Molecular Cell Biology*, 5(6), Article 6. https://doi.org/10.1038/nrm1403

Mantovani, O., Haffner, M., Selim, K. A., Hagemann, M., & Forchhammer, K. (2023). Roles of second messengers in the regulation of cyanobacterial

physiology: The carbon-concentrating mechanism and beyond. *microLife*, 4, uqad008. https://doi.org/10.1093/femsml/uqad008

Mantovani O., Haffner M., Walke P., Elshereef A.A., Wagner B., Petras D., Forchhammer K., Selim K.A., Hagemann M. (2023)b. The redox-sensitive R-loop of the carbon control protein SbtB contributes to the regulation of the cyanobacterial CCM. *ResearchGate* DOI: 10.21203/rs.3.rs-3292191/v1

Mantovani, O., Reimann, V., Haffner, M., Herrmann, F. P., Selim, K. A., Forchhammer, K., Hess, W. R., & Hagemann, M. (2022). The impact of the cyanobacterial carbon-regulator protein SbtB and of the second messengers cAMP and c-di-AMP on CO2-dependent gene expression. *New Phytologist*, 234(5), 1801–1816. https://doi.org/10.1111/nph.18094

Mareš, J., Strunecký, O., Bučinská, L., & Wiedermannová, J. (2019). Evolutionary Patterns of Thylakoid Architecture in Cyanobacteria. *Frontiers in Microbiology*, 10. https://www.frontiersin.org/articles/10.3389/fmicb.2019.00277

McFarlane, C. R., Shah, N. R., Kabasakal, B. V., Echeverria, B., Cotton, C. A. R., Bubeck, D., & Murray, J. W. (2019). Structural basis of light-induced redox regulation in the Calvin-Benson cycle in cyanobacteria. Proceedings of the *National Academy of Sciences of the USA*, 116(42), 20984–20990. https://doi.org/10.1073/pnas.1906722116

Mehdizadeh Allaf, M., & Peerhossaini, H. (2022). Cyanobacteria: Model Microorganisms and Beyond. *Microorganisms*, 10(4), 696. https://doi.org/10.3390/microorganisms10040696

Melnicki, M. R., Sutter, M., & Kerfeld, C. A. (2021). Evolutionary relationships among shell proteins of carboxysomes and metabolosomes. *Current Opinion in Microbiology*, 63, 1–9. https://doi.org/10.1016/j.mib.2021.05.011

Monchamp, M.-E., Spaak, P., & Pomati, F. (2019). Long Term Diversity and Distribution of Non-photosynthetic Cyanobacteria in Peri-Alpine Lakes. *Frontiers in Microbiology*, 9. https://www.frontiersin.org/articles/10.3389/fmicb.2018.03344

Newton, A. C., Bootman, M. D., & Scott, J. D. (2016). Second Messengers. *Cold Spring Harbor Perspectives in Biology*, 8(8), a005926. https://doi.org/10.1101/cshperspect.a005926

Nishimura, T., Takahashi, Y., Yamaguchi, O., Suzuki, H., Maeda, S.-I., & Omata, T. (2008). Mechanism of low CO2-induced activation of the cmp bicarbonate transporter operon by a LysR family protein in the cyanobacterium Synechococcus elongatus strain PCC 7942. *Molecular Microbiology*, 68(1), 98–109. https://doi.org/10.1111/j.1365-2958.2008.06137.x

Nitschmann, W. H., & Peschek, G. A. (1986). Oxidative phosphorylation and energy buffering in cyanobacteria. *Journal of Bacteriology*, *168*(3), 1205–1211.

Omata, T., Price, G. D., Badger, M. R., Okamura, M., Gohta, S., & Ogawa, T. (1999). Identification of an ATP-binding cassette transporter involved in bicarbonate uptake in the cyanobacterium Synechococcus sp. Strain PCC 7942.

Proceedings of the National Academy of Sciences of the USA, *96*(23), 13571–13576. https://doi.org/10.1073/pnas.96.23.13571

Oren, N., Timm, S., Frank, M., Mantovani, O., Murik, O., & Hagemann, M. (2021). Red/far-red light signals regulate the activity of the carbon-concentrating mechanism in cyanobacteria. *Science Advances*, *7*(34), eabg0435. https://doi.org/10.1126/sciadv.abg0435

Orf, I., Timm, S., Bauwe, H., Fernie, A. R., Hagemann, M., Kopka, J., & Nikoloski, Z. (2016). Can cyanobacteria serve as a model of plant photorespiration? - A comparative meta-analysis of metabolite profiles. *Journal of Experimental Botany*, *67*(10), 2941–2952. https://doi.org/10.1093/jxb/erw068

Peng, X., Zhang, Y., Bai, G., Zhou, X., & Wu, H. (2016). Cyclic di-AMP mediates biofilm formation. *Molecular Microbiology*, *99*(5), 945–959. https://doi.org/10.1111/mmi.13277

Price, G. D., Pengelly, J. J. L., Forster, B., Du, J., Whitney, S. M., von Caemmerer, S., Badger, M. R., Howitt, S. M., & Evans, J. R. (2013). The cyanobacterial CCM as a source of genes for improving photosynthetic CO2 fixation in crop species. *Journal of Experimental Botany*, *64*(3), 753–768. https://doi.org/10.1093/jxb/ers257

Price, G. D., Woodger, F. J., Badger, M. R., Howitt, S. M., & Tucker, L. (2004). Identification of a SulP-type bicarbonate transporter in marine cyanobacteria. *Proceedings of the National Academy of Sciences of the USA*, *101*(52), 18228–18233. https://doi.org/10.1073/pnas.0405211101

Rae, B. D., Long, B. M., Badger, M. R., & Price, G. D. (2013). Functions, Compositions, and Evolution of the Two Types of Carboxysomes: Polyhedral Microcompartments That Facilitate CO2 Fixation in Cyanobacteria and Some Proteobacteria. *Microbiology and Molecular Biology Reviews : MMBR*, *77*(3), 357–379. https://doi.org/10.1128/MMBR.00061-12

Raven, J. A., Beardall, J., & Sánchez-Baracaldo, P. (2017). The possible evolution and future of CO2-concentrating mechanisms. *Journal of Experimental Botany*, *68*(14), 3701–3716. https://doi.org/10.1093/jxb/erx110

Rubin, B. E., Huynh, T. N., Welkie, D. G., Diamond, S., Simkovsky, R., Pierce, E. C., Taton, A., Lowe, L. C., Lee, J. J., Rifkin, S. A., Woodward, J. J., & Golden, S. S. (2018). High-throughput interaction screens illuminate the role of c-di-AMP in cyanobacterial nighttime survival. *PLoS Genetics*, *14*(4), e1007301. https://doi.org/10.1371/journal.pgen.1007301

Sauer, D. B., Marden, J. J., Sudar, J. C., Song, J., Mulligan, C., & Wang, D.-N. (2022). Structural basis of ion – substrate coupling in the Na+-dependent dicarboxylate transporter VcINDY. *Nature Communications*, *13*. https://doi.org/10.1038/s41467-022-30406-4

Schuergers, N., & Wilde, A. (2015). Appendages of the Cyanobacterial Cell. *Life*, *5*(1), 700–715. https://doi.org/10.3390/life5010700

Schürmann, P., & Buchanan, B. B. (2008). The ferredoxin/thioredoxin system of oxygenic photosynthesis. *Antioxidants & Redox Signaling*, *10*(7), 1235–1274. https://doi.org/10.1089/ars.2007.1931

Selim, K. A., Haase, F., Hartmann, M. D., Hagemann, M., & Forchhammer, K. (2018). PII-like signaling protein SbtB links cAMP sensing with cyanobacterial inorganic carbon response. *Proceedings of the National Academy of Sciences of the USA*, *115*(21), E4861–E4869. https://doi.org/10.1073/pnas.1803790115

Selim, K. A., Haffner, M., Burkhardt, M., Mantovani, O., Neumann, N., Albrecht, R., Seifert, R., Krüger, L., Stülke, J., Hartmann, M. D., Hagemann, M., & Forchhammer, K. (2021). Diurnal metabolic control in cyanobacteria requires perception of second messenger signaling molecule c-di-AMP by the carbon control protein SbtB. *Science Advances*, *7*(50), eabk0568. https://doi.org/10.1126/sciadv.abk0568

Selim, K. A., Haffner, M., Mantovani, O., Albrecht, R., Zhu, H., Hagemann, M., Forchhammer, K., & Hartmann, M. D. (2023). Carbon signaling protein SbtB possesses atypical redox-regulated apyrase activity to facilitate regulation of bicarbonate transporter SbtA. *Proceedings of the National Academy of Sciences of the USA*, *120*(8), e2205882120. https://doi.org/10.1073/pnas.2205882120

Shahpiri, A., Svensson, B., & Finnie, C. (2008). The NADPH-Dependent Thioredoxin Reductase/Thioredoxin System in Germinating Barley Seeds: Gene Expression, Protein Profiles, and Interactions between Isoforms of Thioredoxin h and Thioredoxin Reductase. *Plant Physiology*, *146*(2), 789–799. https://doi.org/10.1104/pp.107.113639

Sharkey, T. D. (1988). Estimating the rate of photorespiration in leaves. *Physiologia Plantarum*, *73*(1), 147–152. https://doi.org/10.1111/j.1399-3054.1988.tb09205.x

Shibata, M., Katoh, H., Sonoda, M., Ohkawa, H., Shimoyama, M., Fukuzawa, H., Kaplan, A., & Ogawa, T. (2002). Genes essential to sodium-dependent bicarbonate transport in cyanobacteria: Function and phylogenetic analysis. *The Journal of Biological Chemistry*, *277*(21), 18658–18664. https://doi.org/10.1074/jbc.M112468200

Shibata, M., Ohkawa, H., Kaneko, T., Fukuzawa, H., Tabata, S., Kaplan, A., & Ogawa, T. (2001). Distinct constitutive and low-CO2-induced CO2 uptake systems in cyanobacteria: Genes involved and their phylogenetic relationship with homologous genes in other organisms. *Proceedings of the National Academy of Sciences of the USA*, *98*(20), 11789–11794. https://doi.org/10.1073/pnas.191258298

Shin, A.-Y., Han, Y.-J., Baek, A., Ahn, T., Kim, S. Y., Nguyen, T. S., Son, M., Lee, K. W., Shen, Y., Song, P.-S., & Kim, J.-I. (2016). Evidence that phytochrome functions as a protein kinase in plant light signalling. *Nature Communications*, *7*(1), Article 1. https://doi.org/10.1038/ncomms11545

Song, K., Baumgartner, D., Hagemann, M., Muro-Pastor, A. M., Maaß, S., Becher, D., & Hess, W. R. (2022). AtpΘ is an inhibitor of F0F1 ATP synthase to arrest ATP hydrolysis during low-energy conditions in cyanobacteria. *Current Biology: CB*, *32*(1), 136-148.e5. https://doi.org/10.1016/j.cub.2021.10.051

Sukenik, A., Zohary, T., & Padisák, J. (2009). Cyanoprokaryota and Other Prokaryotic Algae. In G. E. Likens (Ed.), *Encyclopedia of Inland Waters* (pp. 138–148). Academic Press. https://doi.org/10.1016/B978-012370626-3.00133-2

Tchernov, D., Helman, Y., Keren, N., Luz, B., Ohad, I., Reinhold, L., Ogawa, T., & Kaplan, A. (2001). Passive entry of CO2 and its energy-dependent intracellular conversion to HCO3- in cyanobacteria are driven by a photosystem I-generated deltamuH+. *The Journal of Biological Chemistry*, *276*(26), 23450–23455. https://doi.org/10.1074/jbc.M101973200

Terauchi, K., & Ohmori, M. (1999). An adenylate cyclase, Cya1, regulates cell motility in the cyanobacterium Synechocystis sp. PCC 6803. *Plant & Cell Physiology*, *40*(2), 248–251. https://doi.org/10.1093/oxfordjournals.pcp.a029534

von Rozycki, T., Schultzel, M. A., & Saier, M. H. (2004). Sequence analyses of cyanobacterial bicarbonate transporters and their homologues. *Journal of Molecular Microbiology and Biotechnology*, *7*(3), 102–108. https://doi.org/10.1159/000078653

Wallner, T., Pedroza, L., Voigt, K., Kaever, V., & Wilde, A. (2020). The cyanobacterial phytochrome 2 regulates the expression of motility-related genes through the second messenger cyclic di-GMP. *Photochemical & Photobiological Sciences*, *19*(5), 631–643. https://doi.org/10.1039/c9pp00489k

Wan, N., DeLorenzo, D. M., He, L., You, L., Immethun, C. M., Wang, G., Baidoo, E. E. K., Hollinshead, W., Keasling, J. D., Moon, T. S., & Tang, Y. J. (2017). Cyanobacterial carbon metabolism: Fluxome plasticity and oxygen dependence. *Biotechnology and Bioengineering*, *114*(7), 1593–1602. https://doi.org/10.1002/bit.26287

Welkie, D. G., Rubin, B. E., Chang, Y.-G., Diamond, S., Rifkin, S. A., LiWang, A., & Golden, S. S. (2018). Genome-wide fitness assessment during diurnal growth reveals an expanded role of the cyanobacterial circadian clock protein KaiA. *Proceedings of the National Academy of Sciences of the USA*, *115*(30), E7174–E7183. https://doi.org/10.1073/pnas.1802940115

Xu, Y., Carr, P. D., Clancy, P., Garcia-Dominguez, M., Forchhammer, K., Florencio, F., Vasudevan, S. G., Tandeau de Marsac, N., & Ollis, D. L. (2003). The structures of the PII proteins from the cyanobacteria Synechococcus sp. PCC 7942 and Synechocystis sp. PCC 6803. *Acta Crystallographica. Section D, Biological Crystallography*, *59*(Pt 12), 2183–2190. https://doi.org/10.1107/s0907444903019589

Yoshimura, H., Hisabori, T., Yanagisawa, S., & Ohmori, M. (2000). Identification and characterization of a novel cAMP receptor protein in the cyanobacterium

Synechocystis sp. PCC 6803. *The Journal of Biological Chemistry*, *275*(9), 6241–6245. https://doi.org/10.1074/jbc.275.9.6241

Young, J. D., Shastri, A. A., Stephanopoulos, G., & Morgan, J. A. (2011). Mapping photoautotrophic metabolism with isotopically nonstationary (13)C flux analysis. *Metabolic Engineering*, *13*(6), 656–665. https://doi.org/10.1016/j.ymben.2011.08.002

Żymańczyk-Duda, E., Samson, S. O., Brzezińska-Rodak, M., & Klimek-Ochab, M. (2022). Versatile Applications of Cyanobacteria in Biotechnology. *Microorganisms*, *10*(12), Article 12. https://doi.org/10.3390/microorganisms10122318

Publications

The impact of the cyanobacterial carbon-regulator protein SbtB and of the second messengers cAMP and c-di-AMP on CO_2-dependent gene expression.

Mantovani O, Reimann V, Haffner M, Herrmann FP, Selim KA, Forchhammer K, Hess WR, Hagemann M 2022**.** *New Phytologist* 234:1801-1816. doi: 10.1111/nph.18094.

New Phytologist

Research

The impact of the cyanobacterial carbon-regulator protein SbtB and of the second messengers cAMP and c-di-AMP on CO_2-dependent gene expression

Oliver Mantovani[1], Viktoria Reimann[2], Michael Haffner[3], Felix Philipp Herrmann[1], Khaled A. Selim[3], Karl Forchhammer[3], Wolfgang R. Hess[2] and Martin Hagemann[1,4]

[1]Department of Plant Physiology, Institute of Biosciences, University of Rostock, Rostock D-18059, Germany; [2]Genetics and Experimental Bioinformatics, Faculty of Biology, University of Freiburg, Freiburg D-79104, Germany; [3]Department of Organismic Interactions, Interfaculty Institute of Microbiology and Infection Medicine Tübingen, University of Tübingen, Tübingen D-72076, Germany; [4]Department Life, Light and Matter, Interdisciplinary Faculty, University of Rostock, Rostock D-18059, Germany

Author for correspondence:
Martin Hagemann
Email: martin.hagemann@uni-rostock.de

Received: *26 November 2021*
Accepted: *2 March 2022*

New Phytologist (2022)
doi: 10.1111/nph.18094

Key words: c-di-AMP, inorganic carbon acclimation, photosynthesis, PII-like, signaling, transcriptomics.

Summary

- The amount of inorganic carbon (C_i) fluctuates in aquatic environments. Cyanobacteria evolved a C_i-concentrating mechanism (CCM) that is regulated at different levels. The regulator SbtB binds to the second messengers cAMP or c-di-AMP and is involved in acclimation to low C_i (LC) in *Synechocystis* sp. PCC 6803. Here, we investigated the role of SbtB and of associated second messengers at different C_i conditions.
- The transcriptome of wild-type (WT) *Synechocystis* and the Δ*sbtB* mutant were compared with Δ*cya1*, a mutant defective in cAMP production, and Δ*dacA*, a mutant defective in generating c-di-AMP.
- A defined subset of LC-regulated genes in the WT was already changed in Δ*sbtB* under high C_i (HC) conditions. This response of Δ*sbtB* correlated with a diminished induction of many CCM-associated genes after LC shift in this mutant. The Δ*cya1* mutant showed less deviation from WT, whereas Δ*dacA* induced CCM-associated genes under HC. Metabolome analysis also revealed differences between the strains, whereby Δ*sbtB* showed slower accumulation of 2-phosphoglycolate and Δ*dacA* differences among amino acids compared to WT.
- Collectively, these results indicate that SbtB regulates a subset of LC acclimation genes while c-di-AMP and especially cAMP appear to have a lesser impact on gene expression under different C_i availabilities.

Introduction

Cyanobacteria are the only prokaryotic oxygenic phototrophs that can convert inorganic carbon (C_i), either in the form of CO_2 or HCO_3^-, into organic carbon compounds using the energy of sunlight. The concentrations of C_i available in the Earth's atmosphere have declined over geological timescales to the present day 0.04% CO_2. However, concentrations of available C_i fluctuate rapidly in aquatic environments, in response to different temperatures and pH values. Cyanobacteria have evolved an efficient C_i-concentrating mechanism (CCM) as an adaptation to changing and, often, suboptimal C_i levels. The CCM increases the CO_2 concentration in the vicinity of ribulose 1,5-bisphosphate carboxylase/oxygenase (RubisCO) (Raven *et al.*, 2017). RubisCO is a rather slow enzyme and can also consume O_2 during its oxygenase reaction (Tcherkez *et al.*, 2006), which leads to the production of the byproduct 2-phosphoglycolate (2PG). The 2PG exerts an inhibitory effect on Calvin–Benson–Bassham cycle (CBBC) enzymes (Flügel *et al.*, 2017), and therefore needs to be detoxified and the carbon skeleton salvaged in the photorespiratory pathway (Hagemann *et al.*, 2016). The CCM largely suppresses photorespiration and permits cyanobacteria to efficiently fix CO_2 under low C_i (LC) conditions. It employs different C_i uptake systems, namely the LC-induced bicarbonate transporters BCT1 and sodium-dependent bicarbonate transporter A (SbtA), or the constitutive BicA. Furthermore, the LC-induced NDH1-3 and constitutive NDH1-4 complexes convert cellular CO_2 to HCO_3^-. Collectively, these C_i uptake systems accumulate high cellular amounts of HCO_3^-, which then diffuses into the carboxysome, a protein-coated bacterial micro-compartment harboring carbonic anhydrase and RubisCO (reviewed by Rae *et al.*, 2013; Hagemann *et al.*, 2021).

The CCM in cyanobacteria is regulated according to the external C_i concentrations. The expression of genes encoding C_i uptake systems is induced under LC conditions, whereas genes encoding carboxysome proteins or enzymes of the CBBC and photorespiration are less regulated at the transcriptional level and may be subject to posttranscriptional regulation (Jablonsky *et al.*,

2016; Spät *et al.*, 2021). In cyanobacteria, three transcription factors, namely NdhR, CmpR, and CyAbrB2 regulate different sets of genes in response to changing C_i conditions (reviewed in Hagemann *et al.*, 2021). NdhR and CmpR alter their DNA affinity by binding of low-molecular-mass effector molecules. NdhR senses high C_i (HC) or LC conditions by binding of 2-oxoglutarate or 2PG, respectively, which results in the activation or inactivation of its repressor activity (Daley *et al.*, 2012; Jiang *et al.*, 2018). The DNA-binding capacity of the activator of CmpR increases by 2PG or ribulose 1,5-bisphosphate interaction under LC conditions (Nishimura *et al.*, 2008).

Recently, the protein SbtB was identified as a regulator of C_i acclimation in *Synechocystis* sp. PCC 6803 (*Synechocystis* hereafter). In cyanobacteria, SbtB is often encoded in an operon together with SbtA, one of the LC-induced HCO_3^- transporters (Selim *et al.*, 2018). With its characteristic trimeric ferredoxin-like fold, SbtB is considered as a new member of the PII superfamily. The canonical cyanobacterial PII protein GlnB is a multifunctional signal processing protein that plays a wide range of regulatory roles by interacting with enzymes, transporters, and transcription factors, especially during nitrogen acclimation (Forchhammer & Selim, 2020). In many bacteria, PII homologs interact with transporters to fine-tune their activities. A similar function is suspected for the SbtB–SbtA couple. The co-expression of SbtB and SbtA in *Escherichia coli* revealed that SbtB may exhibit a direct inhibitory effect on SbtA-mediated HCO_3^- transport activity (Du *et al.*, 2014), which was recently supported by the identification of structural interactions (Fang *et al.*, 2021; Liu *et al.*, 2021). *Synechocystis* cells harboring *sbtB* mutations were shown to have impaired C_i acclimation, pointing to a broader regulatory function of this PII-like protein (Selim *et al.*, 2018). Like other PII proteins, SbtB can bind different effector molecules, which modulate its flexible T-loop, a structure that is important for mediating interactions with potential binding partners. However, unlike PII, SbtB binds not only to ATP, ADP, or AMP, but also to the second messengers cAMP (Selim *et al.*, 2018) and c-di-AMP (Selim *et al.*, 2021). The second messenger cAMP has previously been proposed to act as a C_i-sensing signal, since the activity of the cAMP-producing soluble adenylate cyclase is modulated by different C_i concentrations (Cann *et al.*, 2003; Hammer *et al.*, 2006). In cyanobacteria, cAMP has additional functions, such as the control of cell motility (Terauchi & Ohmori, 1999). The other second messenger, c-di-AMP, has been previously linked to potassium homeostasis and osmoregulation (Agostoni *et al.*, 2018; Stülke & Krüger, 2020). In cyanobacteria, c-di-AMP is also involved in growth regulation under light : dark conditions (Rubin *et al.*, 2018), as it controls glycogen metabolism during diurnal cycles via SbtB (Selim *et al.*, 2021).

Despite the earlier findings and the fact that homologs of SbtB are widely conserved among cyanobacteria, many aspects of its functionality remain unknown. In the present study, we set out to investigate the broader impact of SbtB on C_i acclimation in *Synechocystis*, other than as a regulator of the SbtA-mediated HCO_3^- transport activity. In order to check for signaling overlap between SbtB and its cAMP or c-di-AMP interaction, we compared the transcriptome, metabolome, and photosynthetic activity of Δ*sbtB* under different C_i conditions to *Synechocystis* (1) wild-type (WT), (2) the Δ*cya1* mutant (defective in the main adenylate cyclase required for cAMP synthesis), and (3) the Δ*dacA* mutant (defective in the diadenylate cyclase required for c-di-AMP production). We found that SbtB affects a subset of LC-induced gene expression, while c-di-AMP and especially cAMP are more important under HC than LC conditions.

Materials and Methods

Strains and cultivation

The cyanobacterium *Synechocystis* sp. PCC 6803 sub-strain Tübingen was used as WT strain for the generation of mutants. The cyanobacteria were grown in buffered BG11 media (Rippka *et al.*, 1979) at 30°C under constant light (130 µmol photons m^{-2} s^{-1}). The media for HC and LC cultures were buffered with TES–KOH until a pH of 8 and 7, respectively. HC cultures were bubbled with CO_2-enriched air (5%, v/v), while LC cultures with ambient air (0.04% CO_2).

The generation of the Δ*sbtB* (Δ*slr1513*) and Δ*dacA* (Δ*sll0505*) mutants has been previously described (Selim *et al.*, 2018, 2021). The Δ*cya1* (Δ*slr1991*) knockout mutant was generated by deletion of *slr1991*. Briefly, in the *slr1991* ORF of *Synechocystis* a synthetic gBlock DNA-fragment (IDT, Redwood City, CA, USA), which encodes an erythromycin-resistance cassette, was inserted between the upstream and downstream regions of *slr1991* (0.5 kb each) and cloned into the pUC19 vector cut with *Bam*HI, using Gibson assembly. All knockout mutants were selected on BG11 plates supplemented with proper antibiotics followed by PCR verification.

Sampling of cells during the HC to LC shift

The transcriptome and metabolome were analyzed during a HC to LC shift. Cultures were pre-acclimated to HC conditions for 3 d with daily transfer into fresh BG11 pH 8.0 at optical density measured at 750 nm (OD_{750}) *c.* 1. On the day of the shift, the cultures were re-started in HC conditions at an OD_{750} of 1–1.2. After cultivation for 2 h under HC conditions, 10 ml of the HC cultures were collected by filtration through 2.5 cm glass fiber filters (Macherey-Nagel, Düren, Germany). Afterwards, the cells were diluted to an OD_{750} of 0.8–1 and shifted to LC conditions. Following the shift, the cultures were sampled by filtration at 15 min and 1 h for the metabolome analysis and at 3 h and 24 h for the transcriptome analysis. The cells on the filters were quickly frozen in liquid nitrogen and stored at −80°C until the extraction.

RNA extraction, qPCR, and Northern blotting

RNA extraction was performed as previously described (Hein *et al.*, 2013). RNA quality was verified by performing a DNA contamination assay and by running 4 µg of each sample on a denaturating RNA gel. For the measurement of individual RNA concentrations by qPCR, 1 µg of RNA was reverse transcribed

with 1 µl reverse transcriptase (NEB, Ipswich, MA, USA) in a mixture containing 1 µl Random Hexamer Primer (NEB), 4 µl 5× reaction buffer, 1 µl RNase inhibitor, 2 µl of dNTPs (10 mM), and nuclease-free water (total volume 20 µl). The reverse transcription was performed by incubating the reaction mixture for 5 min at 25°C, then 60 min at 42°C, and finally 5 min at 70°C. The expression levels of selected genes were then measured using a LightCycler v.1.5 (Roche, Basel, Switzerland), with the capillaries, reaction mixes, and SYBR1 green DNA stain all purchased from Roche. The complementary DNA (cDNA) concentrations were normalized according to the ΔC_T levels of the housekeeping gene *rnpB*.

RNA extraction and subsequent Northern-hybridization was performed as described (Jesser *et al.*, 2019) with the following changes: 50 ml *Synechocystis* cultures were harvested by centrifugation. Pellets were then resuspended in 1 ml PGTX and incubated for 15 min at 65°C. Next, 10 µg total RNA was separated on a 10% PAA 8.3 M urea gel. The riboswitch-specific probe template was generated by PCR, using the OneTaq DNA polymerase (NEB) and the following primers: ncr1680_fwd, caata gataacagtaacaagtc; ncr1680_T7_rev, **taatacgactcactatagggg**aaagt caaaacatcgttaaac (bold, T7 promoter sequence).

Microarray

Total RNA was DNase-treated using TURBO DNase (ThermoFisher Scientific, Waltham, MA, USA). Next, 2 µg of DNase-treated RNA were labeled with Cy3 using the ULS Fluorescent Labeling Kit for Agilent arrays (Kreatech, Amsterdam, the Netherlands). A high-resolution microarray manufactured by Agilent Technologies, Santa Clara, CA, USA (design ID 075764, format 8 × 60k, slide layout = IS-62976-8-V2) was used. Then, 600 ng of labeled RNA were used for hybridization for 17 h at 65°C, per array. Each condition was analyzed in two biological replicates. Raw data were processed with R software. The thresholds for the analysis were set as being significant at $|\log_2$ fold change (FC)$| \geq 1.00$ and a P-value ≤ 0.05. All details relating to the processing and statistical evaluation of the data can be found in Klotz *et al.* (2016). The full datasets are accessible in the GEO database with the following accession numbers: GSE185294 (*Synechocystis* WT and Δ*sbtB* mutant), GSE185296 (*Synechocystis* WT and Δ*cya1* mutant), and GSE185297 (*Synechocystis* WT and Δ*dacA* mutant).

Metabolome analysis

Low molecular mass compounds were extracted from cells with ethanol (80%, HPLC grade; Roth, Dautphetal-Buchenau, Germany) at 65°C for 2 h. The metabolites were analyzed by liquid chromatography tandem mass spectrometry (LC–MS/MS) system LCMS-8050 (Shimadzu, Kyoto, Japan) as described by Reinholdt *et al.* (2019). Briefly, 1 µg of carnitine was added per sample as an internal standard. The dry extracts were dissolved in 200 µl MS-grade water and filtered through 0.2 µm filters (Omnifix®-F, Braun, Germany). The cleared supernatants were separated on a pentafluorophenylpropyl column (Supelco Discovery HS FS, 3 µm, 150 mm × 2.1 mm). Sample aliquots were continuously injected into the MS/MS part and ionized via electrospray ionization. The compounds were identified and quantified using the multiple reaction monitoring values given in the LC–MS/MS method package and the LabSolutions software package (Shimadzu). The metabolite peaks were normalized to the signal intensity of the internal standard carnitine and quantified using authentic substances as standards in the same LC–MS/MS run.

The intracellular ATP levels were determined as described in Doello *et al.* (2021) using the ATP Bioluminescence Assay Kit CLS II (Roche). ATP was extracted from the *Synechocystis* WT and Δ*sbtB* mutant strains, which were grown at HC and constant illumination of 50 µE at an OD_{750} of 0.5. ATP levels were calculated based on an ATP standard curve and were normalized to an OD_{750} of 1.0.

Pigments were quantified by *in vivo* absorption measurements according to Sigalat & Kouchkovsky (1975). More details are given in the Supporting Information Methods S1.

Results

Global evaluation of gene expression

The gene expression of *Synechocystis* WT was compared to that of the mutants *ΔsbtB*, *Δcya1*, and *ΔdacA* either after a 3-d acclimation to HC conditions or after 3 h or 24 h shifts to LC, using a DNA microarray covering all protein-coding genes as well as non-coding RNAs. The global comparison via principal component analysis showed that the HC-grown cell samples all had a gene expression profile that differed from the LC-shifted samples (Fig. S1). Among the HC-samples, the gene expression patterns of the mutants Δ*cya1* and Δ*sbtB* were more similar to each other than to WT or Δ*dacA*. A similar trend was observed for the gene expression pattern after a 3 h shift to LC. In contrast, 24 h after the shift to LC, the gene expression pattern of mutant Δ*sbtB* was markedly different from both *Synechocystis* WT and the Δ*cya1* and Δ*dacA* mutants (Fig. S1). Thus, these data indicate that the mutation of target genes had a global impact on the gene expression under HC as well as LC conditions.

The expression of a gene was regarded as upregulated or downregulated if the $\log_2$ FC was higher or lower than 1 or −1, respectively, with a P-value < 0.05. Focusing on the protein-coding genes, we found that the largest number of genes were expressed at higher levels in HC-acclimated Δ*cya1* (136 genes) and Δ*dacA* (80 genes) mutants, compared to WT. Meanwhile, the highest number of downregulated genes was detected in the Δ*sbtB* (174 genes) mutant 24 h after the shift to LC. Relatively few genes showed similar patterns of upregulation or downregulation in two or all three mutants (Fig. 1; Venn diagrams for the 3 h time point are shown in Fig. S2). Therefore, in the next sections, we will discuss mutant-specific alterations in gene expression compared to WT.

Gene expression analysis – comparison of Δ*sbtB* and WT

We observed that the mutation of *sbtB* altered the expression of a defined set of protein-coding genes when the cyanobacteria were

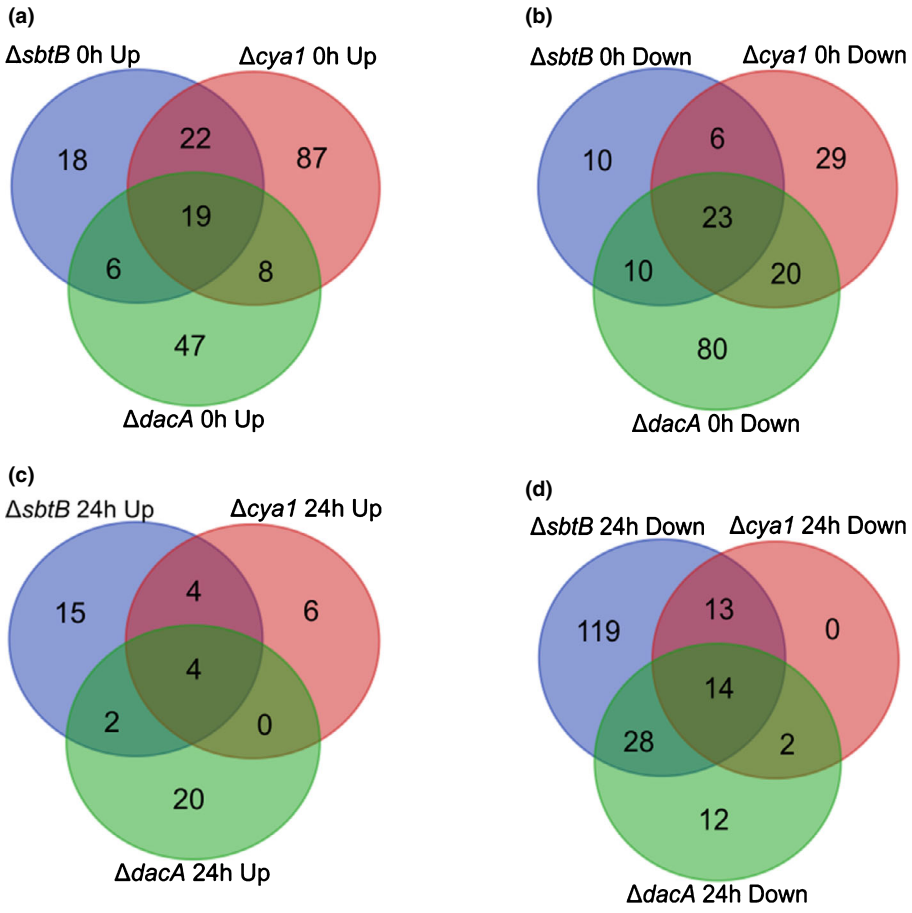

Fig. 1 Venn diagrams showing the overlap of CO_2-regulated gene expression changes in mutants Δ*sbtB*, Δ*cya1*, and Δ*dacA* compared to wild-type of *Synechocystis* sp. PCC 6803. (a) Comparison of upregulated gene expression at high CO_2 (5%, high inorganic carbon (HC)) conditions; (b) comparison of downregulated gene expression at HC conditions; (c) comparison of upregulated gene expression 24 h after shift to low CO_2 (0.04%, low inorganic carbon (LC)); (d) Comparison of downregulated gene expression 24 h after LC shift. Here, only protein-coding genes were considered. (Venn diagrams of changes after 3 h LC are displayed in Supporting Information Fig. S2).

grown under HC conditions. The transcription levels of 65 genes were significantly elevated in mutant Δ*sbtB*, compared to WT. Interestingly, 10 of the 65 upregulated genes in the Δ*sbtB* mutant were upregulated in WT cells only after a shift to LC conditions. This group includes the genes encoding the glutamine synthetase inactivation factors IF7 and IF17 (that are involved in the downregulation of N-assimilation (Brandenburg & Klähn, 2020)) and the PII-interacting regulator of arginine synthesis (PirA) (Bolay *et al.*, 2021). Furthermore, six of the 65 upregulated genes in the Δ*sbtB* mutant became downregulated in WT cells post LC shift (Fig. 1; Table 1). Hence, the Δ*sbtB*-specific differentially expressed genes comprise a substantial number of genes previously reported to be regulated by different C_i conditions in *Synechocystis* (Klähn *et al.*, 2015) and indicate a similarity to a state of pre-acclimation to LC conditions in HC-grown mutant cells.

Under HC-conditions, CCM-associated genes did not undergo significant changes in expression in the Δ*sbtB* mutant compared to WT. The gene *slr0897*, encoding the endoglucanase SsGlc (Tamoi *et al.*, 2007), underwent the highest level upregulation under HC in the Δ*sbtB* mutant compared to WT. Some other protein-coding genes associated with carbon metabolism, such as the glucose transporter GlcP, malate dehydrogenase, and fructose-bisphosphate aldolase, were also more highly expressed in HC-grown Δ*sbtB* cells (Table 1). Furthermore, the ATP synthase operon *sll1321-1327* was higher expressed (Table S1), consistent with an upregulated *atpT* gene, encoding AtpΘ, the inhibitor of ATP hydrolysis (back reaction) of the ATP synthase complex (Song *et al.*, 2022). The higher ATP synthase expression correlated with a significantly higher ATP accumulation in Δ*sbtB* (504.9 ± 8.7 nmol ml^{-1} $OD_{750}{}^{-1}$) compared to WT (350.6 ± 36.7 nmol ml^{-1} $OD_{750}{}^{-1}$), under HC conditions. These expression changes also indicate that the absence of SbtB has a more general negative impact on the cell, because several of the upregulated genes encode proteins involved in the general stress response of *Synechocystis* such as Hsp17, GroES, DnaK2, and OCP. Finally, two genes that are regulated via cAMP (Yoshimura *et al.*, 2002) were among the upregulated genes seen when Δ*sbtB* cells were grown at HC, namely *slr1667* and *slr1928*, which encode CccS and PilA5, respectively (Table 1).

In addition, 49 genes were significantly underexpressed in Δ*sbtB* cells compared to WT at HC. Remarkably, 19 of these genes were downregulated in WT cells only after the shift to LC conditions, and only two of these genes were upregulated in WT cells post LC shift (Fig. 1; Table 2). The highest decrease was observed for the genes *slr0750* and *slr0749* that respectively encode the ChlN and ChlL subunits of the light-independent protochlorophyllide reductase. The lower expression of genes associated with chlorophyll biosynthesis also applies to the proteins HemL, ChlP, HemA, and ChlB in Δ*sbtB* at HC compared to WT (Table 2). However, the spectral analysis did not reveal a notably lower chlorophyll content in Δ*sbtB* compared to WT at HC (Fig. S3). In *Synechocystis*, most chlorophyll is bound to

Table 1 Protein-coding genes that were significantly upregulated in cells of mutant Δ*sbtB* in comparison to wild-type (WT) of *Synechocystis* sp. PCC 6803 grown under high CO_2 (high inorganic carbon (HC) time point 0 h) conditions.

Locus	Gene	Annotation	sbtB/0-WT/0	sbtB/3-WT/3	sbtB/24-WT/24	sbtB/3-sbtB/0	sbtB/24-sbtB/0	sbtB/24-sbtB/3	WT/24-WT/0	WT/24-WT/3	WT/3-WT/0
slr0897	*slr0897*	Probable endoglucanase SsglC	**2.87**	**2.84**	**2.02**	0.06	−0.71	−0.76	0.15	0.06	0.09
slr1667	*cccS*	Cell surface protein CccS (target gene of SyCRP1)	**2.40**	0.16	0.01	**−2.57**	**−2.26**	0.31	0.14	0.47	−0.33
sll1515	*gifB*	Glutamine synthetase inactivating factor IF17	**2.29**	0.77	−0.30	0.41	−0.11	−0.52	**2.47**	0.54	**1.93**
sll0573	*arcC*	Carbamate kinase	**2.18**	0.09	−0.04	**−3.01**	**−2.55**	0.45	−0.33	0.59	−0.92
sll1514	*hsp17*	16.6 kDa small heat shock protein, chaperone	**2.05**	**1.36**	0.53	−0.86	−0.96	−0.10	0.56	0.73	−0.17
ssl1911	*gifA*	Glutamine synthetase inactivating factor IF7	**1.96**	0.27	**−1.35**	**2.74**	**1.17**	**−1.57**	**4.49**	0.06	**4.43**
slr1739	*psb28*	Photosystem II 13 kDa protein homolog	**1.78**	0.46	−0.09	**−1.38**	**−1.82**	−0.44	0.06	0.11	−0.06
ssr2153	*ssr2153*	Unknown protein	**1.73**	0.29	−0.07	**−1.00**	0.10	**1.09**	**1.90**	**1.46**	0.45
slr1232	*slr1232*	Unknown protein	**1.71**	0.07	−0.10	**−2.71**	**−2.38**	0.32	−0.58	0.49	**−1.07**
ssr0692	*pirA*	PII-interacting regulator of arginine synthesis PirA	**1.64**	−0.12	**−1.68**	0.14	**−1.14**	**−1.28**	**2.19**	0.28	**1.91**
norf1	*atpT*	ATP synthase inhibitory factor	**1,63**	−0.21	**−1.42**	**−3.73**	**−3.63**	0.09	−0.59	**1.30**	**−1.88**
slr1851	*slr1851*	Hypothetical protein with PPR domain	**1.62**	0.29	0.15	**−1.82**	**−1.48**	0.34	−0.01	0.49	−0.50
sll0170	*dnaK2*	DnaK2, heat shock protein 70, chaperone	**1.57**	0.06	−0.82	**−1.99**	**−1.76**	0.23	0.64	**1.11**	−0.47
sll0771	*glcP*	Glucose transport protein	**1.51**	**1.24**	**1.40**	−0.90	−0.59	0.30	−0.49	0.14	−0.63
slr0587	*slr0587*	Unknown protein	**1.49**	−0.17	−0.57	**−2.70**	**−2.26**	0.44	−0.20	0.85	**−1.05**
slr2075	*groES*	10 kD chaperonin	**1.42**	−0.31	−0.61	**−2.29**	**−1.98**	0.32	0.05	0.62	−0.57
sll0522	*ndhE*	NADH dehydrogenase subunit 4l	**1.40**	0.30	**−1.24**	0.41	−0.92	**−1.34**	**1.71**	0.20	**1.51**
sll1655	*birA*	Similar to biotin (acetyl-CoA-carboxylase) ligase	**1.32**	0.18	0.16	**−3.00**	**−2.86**	0.14	**−1.69**	0.16	**−1.85**
slr1928	*pilA5*	Type 4 pilin-like protein	**1.26**	−0.62	**−1.32**	**−1.94**	**−2.74**	−0.80	−0.16	−0.10	−0.06
sll1852	*ndkR*	Nucleoside diphosphate kinase	**1.26**	−0.56	0.26	−0.49	−0.77	−0.27	0.23	**−1.09**	**1.32**
sll0891	*citH*	Malate dehydrogenase	**1.25**	−0.07	−0.16	**−1.40**	**−1.49**	−0.08	−0.08	0.01	−0.09
slr0193	*rbp3*	RNA-binding protein	**1.24**	−0.19	−0.10	−0.70	**−1.00**	−0.31	0.34	−0.40	0.74
sll0856	*rpoE*	RNA polymerase group 3 sigma-E factor	**1.24**	0.04	0.09	−0.82	**−1.02**	−0.19	0.14	−0.24	0.38
ssr1038	*ssr1038*	Unknown protein	**1.24**	0.02	**−1.15**	**1.11**	0.57	−0.54	**2.95**	0.63	**2.33**
sll1323	*atpG*	ATP synthase subunit b′ of CF(0)	**1.22**	−0.50	−0.30	**−1.78**	**−2.00**	−0.22	−0.48	−0.42	−0.06
sll1806	*rplN*	50S ribosomal protein L14	**1.20**	−0.87	−0.14	**−2.94**	**−2.61**	0.33	**−1.27**	−0.40	−0.87
sll0253	*sll0253*	DUF6335 protein	**1.17**	−0.17	−0.43	**−2.70**	**−2.65**	0.05	**−1.04**	0.31	**−1.36**
ssl3436	*rpmC*	50S ribosomal protein L29	**1.15**	−0.83	−0.17	**−2.57**	**−2.10**	0.47	−0.78	−0.19	−0.59
sll1807	*rplX*	50S ribosomal protein L24	**1.12**	**−1.07**	−0.30	**−3.40**	**−2.75**	0.65	**−1.33**	−0.12	**−1.21**
slr1704	*slr1704*	Hypothetical protein	**1.11**	0.13	0.52	−0.77	0.53	**1.29**	**1.12**	0.90	0.21
sll0772	*sll0772*	Probable major outer membrane porin	**1.07**	0.39	0.61	−0.89	−0.65	0.24	−0.19	0.02	−0.21
ssl1690	*ndhO*	NDH1 complex small subunit	**1.06**	0.11	−0.33	−0.91	**−1.53**	−0.61	−0.14	−0.18	0.04
sll1803	*rplV*	50S ribosomal protein L22	**1.06**	−0.97	−0.33	**−2.80**	**−2.26**	0.53	−0.87	−0.11	−0.76
sll0018	*cbbA*	Fructose-bisphosphate aldolase, class II	**1.06**	−0.43	−0.58	0.15	−0.17	−0.32	**1.47**	−0.17	**1.64**
sll1324	*atpF*	ATP synthase B chain (subunit I) of CF(0)	**1.05**	−0.25	0.43	**−1.23**	−0.94	0.29	−0.32	−0.39	0.07
sll1325	*atpD*	ATP synthase delta chain of CF(1)	**1.03**	−0.36	0.02	**−1.44**	**−1.56**	−0.12	−0.55	−0.50	−0.06
slr1963	*ocp*	Water-soluble carotenoid protein	**1.01**	−0.27	−0.52	**−1.64**	**−1.81**	−0.17	−0.28	0.08	−0.36
ssl3437	*rpsQ*	30S ribosomal protein S17	**1.00**	**−1.02**	−0.41	**−2.81**	**−2.39**	0.42	−0.98	−0.18	−0.80

A gene was regarded as induced or repressed if the $\log_2$ fold change was higher or lower than 1 or −1 ($P < 0.05$, in bold). Mostly genes are shown that are functionally annotated. Genes for hypothetical or unknown proteins are included if they showed inorganic carbon-dependent regulation (upregulated genes marked in light yellow, downregulated genes marked in dark-yellow) in WT cells after shifts for 3 h or 24 h into low CO_2 conditions.

photosystem 1 (PSI). Accordingly, the genes encoding several of the PSI subunits (namely PsaF, PsaJ, PsaK1, and PsaC) were also found at lower messenger RNA (mRNA) levels in mutant Δ*sbtB* at HC (Table 2). Furthermore, many genes encoding proteins involved in nitrogen uptake, assimilation, and metabolism were downregulated in Δ*sbtB* cells under HC, while the expression of

Table 2 Protein-coding genes that are significantly downregulated in cells of mutant Δ*sbtB* in comparison to wild-type (WT) of *Synechocystis* sp. PCC 6803 grown under high CO_2 (high inorganic carbon (HC) time point 0 h) conditions.

Locus	Gene	Annotation	sbtB/0-WT/0	sbtB/3-WT/3	sbtB/24-WT/24	sbtB/3-sbtB/0	sbtB/24-sbtB/0	sbtB/24-sbtB/3	WT/24-WT/0	WT/24-WT/3	WT/3-WT/0
slr0750	*chlN*	Light-independent protochlorophyllide reductase ChlN	**−2.17**	−0.11	0.08	**−1.21**	**−1.00**	0.21	**−3.26**	0.02	**−3.28**
slr0749	*chlL*	Light-independent protochlorophyllide reductase ChlL	**−2.16**	−0.22	−0.12	**−1.57**	**−1.69**	−0.11	**−3.73**	−0.21	**−3.51**
sll0819	*psaF*	Photosystem I reaction center subunit III	**−2.07**	−1.23	**−2.52**	0.59	−0.75	**−1.34**	−0.30	−0.05	−0.25
sll1830	*sll1830*	Unknown protein	**−2.00**	−0.31	**−1.02**	0.35	−0.18	−0.53	**−1.17**	0.17	**−1.34**
sml0008	*psaJ*	Photosystem I subunit IX	**−1.81**	−1.21	**−2.53**	0.53	**−1.08**	**−1.60**	−0.35	−0.27	−0.08
sll1398	*psb13*	Photosystem II reaction center 13 kDa protein	**−1.68**	−0.43	**−1.33**	**1.10**	0.15	−0.95	−0.21	−0.05	−0.16
slr0288	*glnN*	Glutamate–ammonia ligase	**−1.62**	−0.61	−0.38	**−1.92**	**−1.24**	0.68	**−2.48**	0.45	**−2.94**
slr1984	*rps1b*	30S ribosomal protein S1 homolog	**−1.59**	−0.32	−0.71	**1.15**	0.64	−0.51	−0.24	−0.12	−0.12
ssr2831	*psaE*	Photosystem I subunit IV	**−1.58**	−0.74	−0.78	0.88	0.61	−0.27	−0.19	−0.23	0.04
sll0017	*hemL*	Glutamate-1-semialdehyde aminomutase	**−1.47**	0.00	−0.09	**1.29**	**1.05**	−0.24	−0.32	−0.15	−0.17
slr2057	*apqZ*	Water channel protein	**−1.45**	−0.87	**−1.58**	0.92	−0.70	**−1.62**	−0.57	−0.91	0.34
sll0680	*pstS*	Phosphate-binding periplasmic protein	**−1.42**	0.35	−0.04	0.39	0.02	−0.37	**−1.36**	0.02	**−1.38**
ssr0390	*psaK1*	Photosystem I reaction center subunit X	**−1.39**	−0.61	**−2.05**	0.15	−1.05	**−1.20**	−0.39	0.24	−0.63
sll1244	*rplI*	50S ribosomal protein L9	**−1.36**	−0.45	0.26	0.42	0.83	0.41	−0.80	−0.30	−0.49
sll1091	*chlP*	Geranylgeranyl hydrogenase	**−1.36**	−0.78	**−1.40**	0.71	0.08	−0.63	0.12	−0.01	0.14
ssl0563	*psaC*	Photosystem I subunit VII	**−1.22**	−0.86	**−2.91**	0.05	**−1.86**	**−1.91**	−0.17	0.15	−0.31
slr0447	*amiC*	ABC-type urea transport substrate-binding protein	**−1.20**	−0.81	−0.72	**−1.77**	**−1.69**	0.08	**−2.18**	−0.01	**−2.16**
sll1172	*thrC*	Threonine synthase	**−1.19**	−0.56	−0.50	0.66	0.42	−0.24	−0.28	−0.30	0.02
slr0077	*csd*	Cysteine desulfurase	**−1.17**	−0.13	−0.33	−0.10	0.14	0.24	−0.70	0.44	**−1.14**
sll1471	*cpcL*	Phycobilisome rod-core linker polypeptide	**−1.16**	−0.35	−0.64	0.03	−0.71	−0.74	**−1.23**	−0.45	−0.78
sll1899	*ctaB*	Cytochrome *c* oxidase folding protein	**−1.15**	−0.01	−0.18	0.84	0.59	−0.25	−0.38	−0.08	−0.30
sll0450	*norB*	Cytochrome *b* subunit of nitric oxide reductase	**−1.14**	−0.02	**−1.90**	**−1.03**	**−1.10**	−0.07	−0.34	**1.80**	**−2.15**
slr0150	*petF*	Ferredoxin, PetF-like protein	**−1.12**	−0.88	**−1.27**	**−2.26**	**−2.42**	−0.15	**−2.27**	0.23	**−2.50**
sll1536	*moeB*	Molybdopterin biosynthesis MoeB protein	**−1.09**	−0.15	−0.51	0.79	0.56	−0.23	−0.01	0.14	−0.15
slr0151	*slr0151*	Unknown protein	**−1.09**	−0.36	−0.54	**−1.08**	**−1.13**	−0.05	**−1.68**	0.12	**−1.80**
ssr1600	*ssr1600*	Similar to anti-sigma f factor antagonist	**−1.08**	−0.71	**−1.11**	0.25	−0.47	−0.72	−0.44	−0.32	−0.13
sll1638	*sll1638*	Hypothetical protein	**−1.08**	−0.97	**−1.15**	−0.83	**−1.99**	**−1.16**	**−1.92**	−0.98	−0.94
slr1622	*ppa*	Soluble inorganic pyrophosphatase	**−1.07**	−0.75	−0.84	0.64	−0.37	**−1.01**	−0.60	−0.92	0.32
sll0517	*rbpA*	Putative RNA binding protein	**−1.07**	0.46	0.13	−0.06	−0.15	−0.09	**−1.35**	0.24	**−1.59**
sll0661	*ycf35*	Hypothetical protein YCF35	**−1.07**	−0.04	**−1.49**	**2.80**	**1.63**	**−1.17**	**2.05**	0.28	**1.78**
slr1171	*gpx1*	Glutathione peroxidase-like NADPH peroxidase	**−1.06**	0.33	−0.04	**1.61**	0.67	−0.94	−0.35	−0.57	0.22
slr0585	*argG*	Argininosuccinate synthetase	**−1.05**	−0.42	−0.64	−0.45	**−1.05**	−0.59	**−1.46**	−0.37	**−1.09**
slr0623	*trxA*	Thioredoxin	**−1.05**	−0.06	**−1.40**	−0.63	**−1.73**	**−1.10**	**−1.38**	0.24	**−1.62**
sll1196	*pfkA1*	Phosphofructokinase	**−1.03**	−0.41	−0.44	**−2.03**	**−2.13**	−0.10	**−2.71**	−0.07	**−2.65**
sml0002	*psbX*	Photosystem II PsbX protein	**−1.03**	**−1.11**	**−1.80**	−0.46	**−1.32**	−0.86	−0.54	−0.17	−0.37
slr0149	*apcD*	Allophycocyanin gamma subunit ApcD	**−1.02**	−0.83	**−1.37**	**−2.40**	**−2.65**	−0.25	**−2.29**	0.30	**−2.59**
slr0213	*guaA*	GMP synthetase	**−1.01**	−0.33	−0.21	0.61	0.58	−0.03	−0.22	−0.15	−0.08
slr1239	*pntA*	Pyridine nucleotide transhydrogenase alpha subunit	**−1.01**	0.29	−0.38	−0.36	−0.65	−0.29	**−1.29**	0.38	**−1.66**
slr1808	*hemA*	Transfer RNA-Gln reductase	**−1.01**	−0.62	**−1.08**	0.19	−0.42	−0.61	−0.35	−0.16	−0.20
slr2094	*glpX*	Fructose-1,6-/sedoheptulose-1,7-bisphosphatase	**−1.00**	**−1.19**	**−1.14**	−0.13	−0.48	−0.35	−0.34	−0.40	0.06
slr0772	*chlB*	Light-independent protochlorophyllide reductase ChlB	**−1.00**	−0.56	**−1.01**	**−2.21**	**−2.30**	−0.09	**−2.29**	0.36	**−2.65**

A gene was regarded as induced or repressed if the $\log_2$ fold change was higher or lower than 1 or −1 ($P < 0.05$, in bold). Only genes are shown that are functionally annotated or showed inorganic carbon-dependent regulation (downregulated genes marked in light yellow, upregulated genes marked in dark-yellow) in WT cells after shifts for 3 h or 24 h into low CO_2 conditions.

these genes was typically only reduced in WT cells after a shift to LC conditions. It has been shown that reduced C_i availability also lowers the accumulation of many amino acids in *Synechocystis* (Orf *et al.*, 2016b). The group of genes involved in nitrogen metabolism comprise the nitrogen-starvation specific glutamine synthetase GlnN, which helps to assimilate ammonia during nitrogen-limiting conditions (García-Domínguez *et al.*, 1997). Moreover, genes encoding proteins involved in the uptake of urea (e.g. AmiC) and ammonia (e.g. AMT1; $\log_2$ FC −0.97, slightly below significance threshold), or in amino acid metabolism (e.g. ThrC, Csd, and ArgG) were among the downregulated genes in Δ*sbtB* (Table 2). Only two genes, encoding the proteins Pfk1 and GlpX, which are involved in sugar metabolism, were also underexpressed in the Δ*sbtB* mutant at HC.

The comparison of gene expression changes 3 h and 24 h after the LC shift revealed that only 16 and 25 genes, respectively, showed significantly higher expression in Δ*sbtB* compared to WT. Among them, the expression of *slr0897*, which encodes the probable endoglucanase GlcP, as well as Hsp17, remained elevated under HC. Messenger RNAs of the two high light-inducible proteins HliC and HliA were present at higher levels, indicating that LC-shifted mutant cells experienced light or oxidative stress. All of the CCM-associated genes and most others known to be induced in *Synechocystis* WT cells following the shift to LC, were also upregulated in the Δ*sbtB* mutant. However, the LC-mediated upregulation of genes belonging to the NdhR regulon (such as the *sbtA*- and *ndh3*-encoding operon) and the strongly LC-induced operon for flavoproteins Flv2/4 was much weaker in Δ*sbtB* than in WT cells (Fig. 2; diagrams for the changes after 3 h LC are displayed in Fig. S4), which is consistent with the assumption that HC-grown Δ*sbtB* cells are partially pre-acclimated to LC conditions. Meanwhile, the extent of LC stimulation was not changed regarding the expression of genes associated with the CmpR-activated BCT1 system and the constitutively expressed *bicA* or *ndh4* operon.

In contrast to the relatively few genes that were upregulated in Δ*sbtB* after the shift to LC, the mRNAs of 41 and 174 genes were less abundant in the mutant compared to WT cells 3 h and 24 h, respectively, after the transition to LC conditions. Among them were 17 genes encoding photosynthesis-associated proteins,

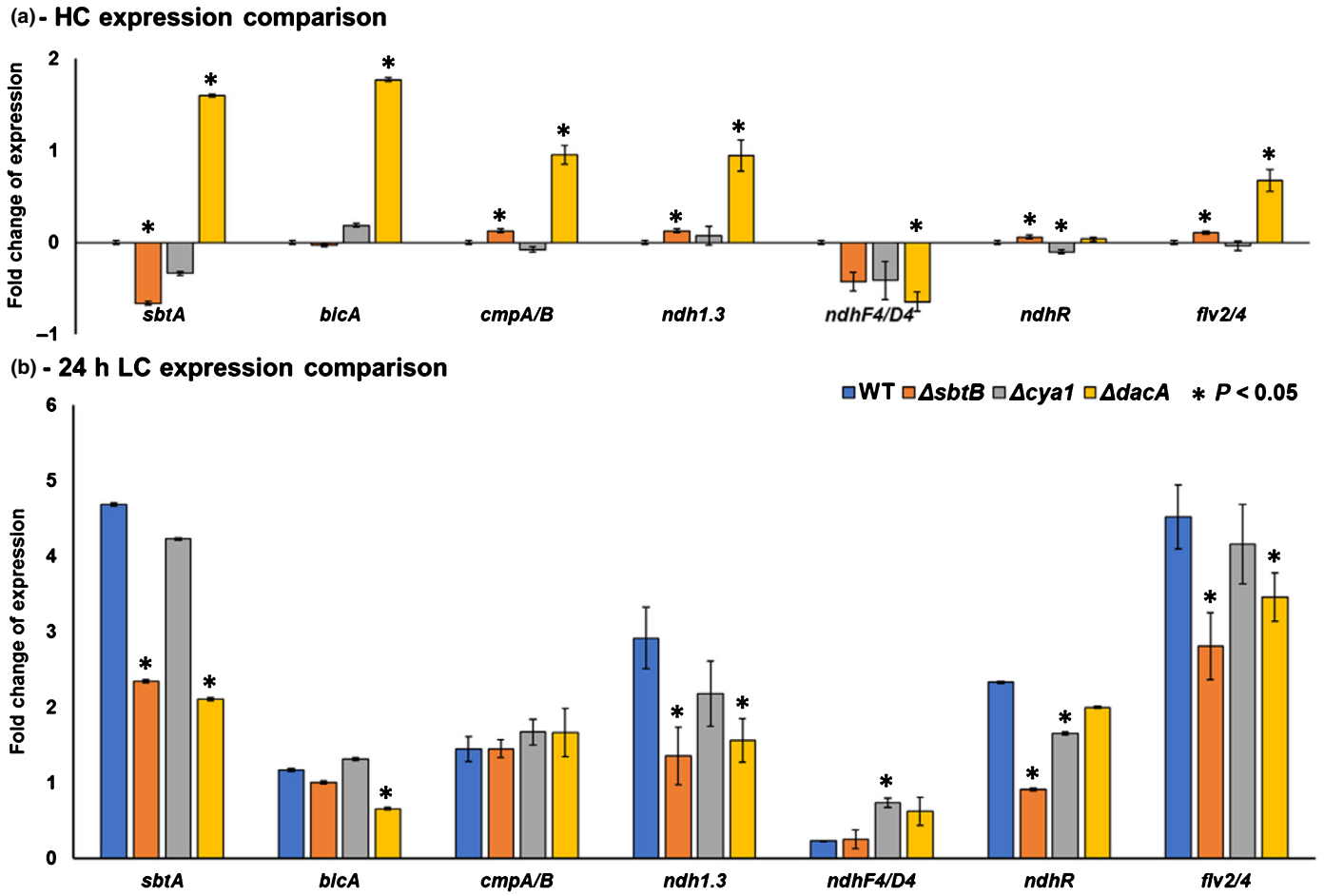

Fig. 2 Comparison of the expression of selected inorganic carbon (C_i)-regulated genes in *Synechocystis* sp. PCC 6803. The relative expression of genes (fold changes of expression at (a) high CO_2 (5%, high C_i (HC)) conditions, or (b) 24 h after shift to low CO_2 (0.04%, low C_i (LC)) relative to HC; HC expression of wild-type (WT) was set to 0 encoding proteins of the carbon-concentrating mechanism (CCM) such as the bicarbonate transporters SbtA, BicA and BCT1 (*cmpA/B*), the constitutive Ndh4 (*ndhF4/D4*) or the LC-induced Ndh3 (*sll1732,1733,1734,1735*) complex, and the flavoprotein (Flv) 2/4-encoding operon *sll0217,0218,0219* are shown. Mean values and standard deviations are displayed. Significantly changed expression compared to WT is indicated by an asterisk (Student's *t*-test, $P < 0.05$).

including those that were already underexpressed at HC (Table 2). The lower expression of the PS1 and PS2 subunits, as well as phycobilisomes, is consistent with the slower growth and photosynthetic activity of Δ*sbtB* cells under this condition (Selim *et al.*, 2018). The overall pigmentation of Δ*sbtB* cells was also clearly diminished following the shift to LC conditions (Fig. S3). Regarding LC acclimation, it is interesting to note that the 35 genes that were significantly upregulated in WT cells after the LC shift were significantly underexpressed in Δ*sbtB* after 24 h in LC. In addition to many genes encoding proteins of unknown function, this group includes many CCM-associated genes such as *sbtA*, the operon encoding the NDH1-3 complex, the *ndhA* operon (*sll0519-22*), the *flv2/4* operon (*sll0217-19*) (Fig. 2), and the gene for NdhR. The lower expression of these genes may reflect the already pre-acclimated state of Δ*sbtB* towards LC. However, the lower expression of genes encoding proteins involved in C_i uptake in the Δ*sbtB* mutant is also in line with the lower induction of the CCM in mutant compared to WT cells (see later). In addition to NdhR, other regulatory proteins such as LexA, Rre15, SigF, SigG, and SigE were found at lower mRNA levels, which possibly contributes to the large negative impact of the *sbtB* deletion on gene expression.

Collectively, these results clearly indicate that the absence of the carbon regulator SbtB had a marked impact on the expression of a defined subset of genes that belong to the C_i-regulated stimulon in *Synechocystis* WT cells. The partial induction or repression of C_i-regulated genes in Δ*sbtB* cells at HC is consistent with the reported higher photosynthetic C_i-affinity of HC-grown Δ*sbtB* mutant, compared to WT (Selim *et al.*, 2018; see later).

To confirm some of the gene expression changes observed in the microarray experiments, quantitative reverse transcription polymerase chain reaction (qRT-PCR) assays were performed. We found that the expression of *sbtA* was slightly lowered in HC-grown cells and became induced to a lesser extent in mutant Δ*sbtB* cells after the shift to LC. A similar picture appeared for the *cmpB* gene of the bicarbonate transporter BCT1. Moreover, the upregulation of *gifA* under HC conditions was once again observed, whereas the *nrtB* gene, encoding a subunit of the nitrate transporter, was not downregulated under LC conditions in Δ*sbtB* mutant as it was in the WT (Fig. S5).

Gene expression analysis – comparison Δ*dacA* and WT

The Δ*dacA* mutant underwent many more changes in gene expression compared to WT under HC conditions, rather than after the shift to LC (Table S2). Eighty significantly upregulated and 133 significantly downregulated genes were detected in the Δ*dacA* mutant, when cultivated under HC. Meanwhile, only 30 and 26 or 25 and 56 genes were overexpressed or underexpressed following a 3 h or 24 h shift to LC, respectively, in the Δ*dacA* mutant (Fig. 1). Interestingly, 20 of the genes that were overexpressed in Δ*dacA* under HC were induced in WT cells only under LC conditions. This group includes the genes *sbtAB*, the entire *cmp* operon, and the genes of the LC-induced *ndhF3/ndhD3/cupA/cupB* operon, which all encode proteins involved in the CCM-associated increase of C_i uptake in LC-grown WT cells. However, the higher expression of several genes encoding C_i uptake systems only slightly improved the C_i affinity of photosynthesis in HC-cultivated Δ*dacA* cells (see later). Furthermore, similarly to Δ*sbtB*, the genes for the GS-inactivating proteins IF7 and IF17, as well as the PII-dependent regulator PirA, were also expressed at higher levels in Δ*dacA* at HC, and only became elevated in the WT under LC conditions. Finally, a distinct group of genes were more highly expressed in Δ*dacA* under both, HC and LC conditions (Table 3). This group includes the *cmp* operon, *sll0556* (encoding the Na^+/H^+ antiporter NhaS6), *hliB*, *hliC* (encoding two small chlorophyll-binding proteins), and *slr0753* (encoding a putative transport protein (Kobayashi *et al.*, 2006)). The only c-di-AMP-dependent riboswitch in *Synechocystis* was predicted to lie upstream of *slr0753* (Nelson *et al.*, 2013). Similarly to *slr0753*, the riboswitch-corresponding RNA (5′UTR of *slr0753*) was upregulated in the microarray of Δ*dacA*, irrespective of the C_i supply (Table 3). Subsequent analysis by Northern-hybridization revealed the presence of riboswitch RNA, a short transcript detectable under all C_i conditions in WT, but not in Δ*dacA*, where instead larger transcripts had accumulated (Fig. 3). This result provides evidence that the missing di-adenylate cyclase activity and thus missing c-di-AMP production (Selim *et al.*, 2021) resulted in the expected post-transcriptional upregulation of *slr0753* via the altered riboswitch configuration.

Among the 133 genes found at lower mRNA levels in Δ*dacA* at HC, 52 were underexpressed in WT cells switched for 3 h or 24 h to LC conditions. This observation for Δ*dacA* is similar to the global change in gene expression previously observed in mutant Δ*sbtB* cells. In both the Δ*dacA* and Δ*sbtB* mutants, many genes encoding proteins involved in photosynthesis or nitrogen metabolism were already downregulated under HC conditions, not solely after the shift to LC as for the WT (Table 2). Among the genes encoding proteins involved in nitrogen metabolism, the uptake systems for ammonia, nitrate, and urea, as well as the nitrogen sensory protein PII and many enzymes involved in nitrogen assimilation (e.g. nitrite reductase NirA or the glutamine synthetases GlnA and GlnN) or arginine metabolism (e.g. Na-acetylglutamate kinase ArgB or argininosuccinate synthetase ArgG), were found. Many of the photosynthesis-associated genes remained underexpressed under all C_i conditions in Δ*dacA* compared to WT (Table 3). However, of the nitrogen-associated genes, only those encoding ammonia permease and nitrite reductase were consistently downregulated in the Δ*dacA* mutant. Furthermore, genes encoding the phycobilisome subunits were constantly underexpressed in this mutant (Table 3), which corresponds to the relatively lower content of these pigments in Δ*dacA* cells (Table 4; Fig. S3). In addition, *pfk* and *pgk*, two genes that encode proteins involved in C metabolism, were permanently downregulated in the Δ*dacA* mutant.

Gene expression analysis – comparison Δ*cya1* and WT

In the Δ*cya1* mutant, the main *Synechocystis* adenylate cyclase is knocked-out, which has been reported to reduce the cAMP level to *c.* 4% of that of the WT (Terauchi & Ohmori, 1999). The mRNA levels of 136 genes appeared elevated in the Δ*cya1*

Table 3 Genes showing inorganic carbon-independent upregulation or downregulation in mutant Δ*dacA* compared to wild-type (WT) of *Synechocystis* sp. PCC 6803.

Locus	Gene	Description	dacA/0 – WT/0	dacA/3 – WT/3	dacA/24 – WT/24
slr0753	*slr0753*	Probable transport protein	**1.23**	**2.30**	**2.15**
5′UTR slr0753	–	c-di-AMP riboswitch RF00379	0.63	**2.23**	**2.14**
sll1951	*hlyA*	Surface layer protein	**1.69**	**2.16**	**1.76**
ssr2595	*hliB*	High light-inducible protein HliB. CAB/ELIP/HLIP family	0.93	**2.09**	**1.85**
ssl1633	*hliC*	High light-inducible protein HliC. CAB/ELIP/HLIP family	**1.25**	**1.60**	**2.30**
sll1862	*sll1862*	Unknown protein	**0.96**	**1.78**	**3.06**
sll1863	*sll1863*	Unknown protein	**1.25**	**1.63**	**3.15**
slr0040	*cmpA*	Bicarbonate transport system. Substrate-binding	0.85	**1.78**	**1.21**
slr0041	*cmpB*	Bicarbonate transport system. Permease	**1.05**	**1.41**	**1.07**
slr0042	*slr0042*	Probable porin. Major outer membrane protein	**1.81**	**1.75**	**1.60**
slr0043	*cmpC*	Bicarbonate transport system. ATP-binding	0.98	**1.70**	**1.24**
slr0044	*cmpD*	Bicarbonate transport system. ATP-binding	**1.77**	**1.69**	**1.23**
sll1483	*sll1483*	Fasciclin domain-containing protein	**1.17**	**1.42**	**1.41**
sll0556	*nhaS6*	Na^+/H^+ antiporter	**1.36**	**1.24**	**1.52**
slr0789	*slr0789*	HPP family protein	**1.00**	**1.07**	0.92
ssl0563	*psaC*	Photosystem I subunit VII	**−1.06**	**−1.06**	**−1.52**
slr2057	*apqZ*	Water channel protein	**−1.29**	**−1.07**	**−1.15**
slr2067	*apcA*	Allophycocyanin alpha subunit	**−1.41**	**−1.07**	**−1.60**
sll0629	*psaK2*	Alternative photosystem I reaction center subunit X	**−1.05**	**−1.09**	−0.48
slr1986	*apcB*	Allophycocyanin beta subunit	**−1.73**	**−1.10**	**−1.63**
slr0737	*psaD*	Photosystem I subunit II	−0.98	**−1.12**	**−1.83**
sll1577	*cpcB*	Phycocyanin beta subunit	**−1.32**	**−1.12**	**−1.56**
ssr0390	*psaK*	Photosystem I reaction center subunit X	**−1.48**	**−1.13**	**−1.80**
sll0427	*psbO*	Photosystem II manganese-stabilizing polypeptide	**−1.15**	**−1.20**	**−1.04**
sll1575	*spkA*	Part of serine/threonine protein kinase SpkA	**−1.13**	**−1.20**	**−1.36**
slr0447	*amiC*	ABC-type urea transport system, substrate-binding	**−2.20**	**−1.26**	−0.89
sll1196	*pfk*	Phosphofructokinase	**−2.25**	**−1.27**	**−1.30**
sll0108	*amt1*	Ammonium/methylammonium permease	**−3.53**	**−1.34**	−0.73
slr0898	*nirA*	Ferredoxin–nitrite reductase	**−2.68**	**−1.52**	**−1.20**
ssr2831	*psaE*	Photosystem I subunit IV	**−2.04**	**−1.77**	**−1.60**
slr0394	*pgk*	Phosphoglycerate kinase	−0.83	**−1.79**	**−1.76**
sll1471	*cpcG*	Phycobilisome rod-core linker polypeptide	**−2.21**	**−2.08**	**−1.74**

A gene was regarded as induced or repressed if the $\log_2$ fold change was higher or lower than 1 or −1 ($P < 0.05$, in bold). Time point 0 represents high CO_2 (high inorganic carbon (HC)), air supplemented with 5% CO_2, 3 or 24 – shift for 3 h or 24 h towards low CO_2 (low inorganic carbon (LC)) of ambient air, 0.04% CO_2. Details for the c-di-AMP riboswitch can be found in the RFAM database (https://rfam.xfam.org/) under the accession no. RF00379. Boxed genes are expressed in an operon.

mutant under HC conditions, compared to WT (Fig. 1). Remarkably, 40 of these genes encode different *Synechocystis* genome-specific transposases (Table S3). Hence, the lowered amount of cAMP is likely to directly or indirectly activate transposase expression, which may subsequently impact on *Synechocystis* genome stability. Only five of the 96 remaining overexpressed genes in HC-grown Δ*cya1* cells were induced in WT under LC. Furthermore, 78 genes were downregulated in Δ*cya1* under HC, compared to WT. This list includes 25 genes that were less strongly expressed in WT cells under LC conditions. Hence, the overlap with the C_i stimulon is much higher among the downregulated than among the upregulated genes in Δ*cya1*, as was previously observed for Δ*sbtB*. In both cases, many genes encoding proteins involved in nitrogen assimilation were already underexpressed at HC.

Most of the assayed genes showed similar LC stimulation in Δ*cya1* as in WT (Fig. 2). Only 17 and 14 genes were more highly expressed at 3 h and 24 h, respectively, after the LC shift in Δ*cya1*. Several of these genes are situated on the *Synechocystis* plasmid pSYSM and encode proteins involved in the biosynthesis of extracellular sulfated polysaccharides (Maeda *et al.*, 2021). Similarly, only nine genes were less strongly induced in Δ*cya1* cells placed under LC for 3 h, including the *sbtAB* operon, however, this difference disappeared after 24 h at LC (Fig. 2). Among the 29 genes expressed at a lower level in Δ*cya1* after 24 h at LC, several encode regulatory factors such as the repressor LexA or the sigma factor SigE.

The combined impact of different mutations on gene expression

There was only a small overlap in the differentially expressed genes among the three mutants compared to WT (Fig. 1). The number of these shared genes was even smaller in cells shifted for 24 h to LC than in HC-grown cultures (18 vs 42). Furthermore, the majority of these genes encode hypothetical or unknown

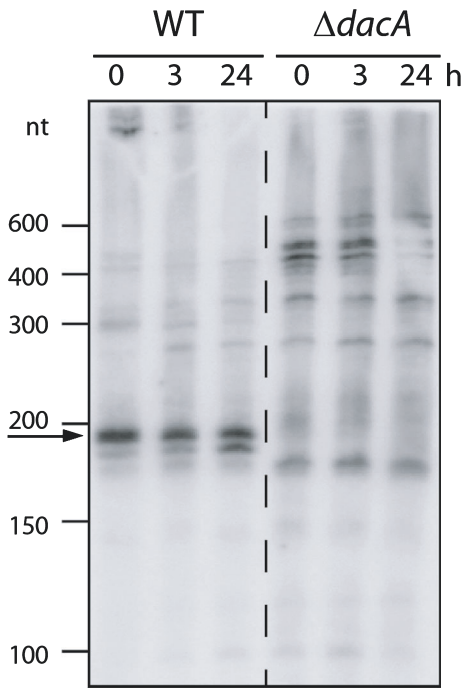

Fig. 3 Verification of the c-di-AMP riboswitch response *in vivo*. The c-di-AMP-dependent riboswitch upstream of *slr0753* in *Synechocystis* sp. PCC 6803 exists as a discrete transcript (marked by an arrow) less than 200 nt in size in wild-type (WT) cells, while longer transcript forms were detectable in RNA extracted from the mutant Δ*dacA*. The different inorganic carbon concentrations (5% CO_2 at 0 h, shift to ambient CO_2 of 0.04% for 3 h and 24 h) had no effect on the presence of the riboswitch RNA in WT. RiboRuler High Range RNA Ladder was used as molecular mass standard.

proteins (Tables S4, S5). Only a few of the annotated genes can be linked to C_i-mediated expression changes. Among the genes that were more highly expressed under HC conditions, were those encoding the fructose-bisphosphate aldolase (CbbA), the glutamine synthetase-inactivating factor IF17, and carbamate kinase (Table S4). Moreover, the Ccs protein, which is probably involved in cell surface synthesis, was commonly activated in all three mutants and was shown to be regulated by the cAMP-dependent transcription factor SyCRP (Yoshimura *et al.*, 2002). Among the annotated genes that were downregulated in all three mutants compared to WT after the shift to LC, were genes encoding PSI subunits and proteins involved in nitrogen metabolism (e.g. ammonia permease, GlnN, and a phycobilisome linker protein). In LC-shifted cells, a putative diguanylate cyclase (Slr1539) and a high light-induced protein (HliA) were higher expressed, whereas several genes associated with energy metabolism or iron regulation were commonly downregulated. Interestingly, the *cph1* gene, encoding the cyanobacterial phytochrome 1 that is involved in the diurnal activation/inactivation of bicarbonate uptake (Oren *et al.*, 2021) also belonged to the list of commonly downregulated genes (Table S5).

Pigmentation

Since some of the differentially expressed genes we detected encoded proteins implicated in chlorophyll synthesis, photosystems, or phycobilisomes (especially in the Δ*sbtB* and Δ*dacA* mutants), the pigmentation of the mutant and WT *Synechocystis* cells was compared when grown for up to 3 d under HC or LC. The visible light absorption spectra were measured for each strain (Fig. S3). No major differences appeared when comparing the spectra of WT and Δ*cya1*. The mutants Δ*sbtB* and Δ*dacA* showed diminished absorption at 625 nm, associated with reduced phycobilisome levels under HC conditions. Under LC conditions, the mutant Δ*sbtB* had the lowest overall pigmentation level, with phycobilisomes but also chlorophyll absorption peaks, whereas pigmentation of mutant Δ*dacA* was more WT-like under LC conditions.

The observations were verified by quantitative pigment estimations per biomass of multiple HC- and LC-acclimated cultures (Table 4). Similar pigment relations can be assumed per cell, because the cell diameter of all strains did not significantly differ (Fig. S6). In addition to the changes in chlorophyll and phycocyanin contents, we found that the Δ*sbtB* and Δ*dacA* mutants had a higher carotenoid content, especially under LC conditions, which is often a sign of light-stressed cyanobacteria and is consistent with the enhanced expression of genes encoding high-light-stress proteins in these strains.

Photosynthetic affinity for bicarbonate

Previously, we showed that the mutation of *sbtB* changed the photosynthetic C_i affinity (Selim *et al.*, 2018). To investigate whether the inability to synthesize cAMP or c-di-AMP, the two second messengers implicated in SbtB-mediated signaling, had similar effects, we measured the bicarbonate-dependent photosynthetic activities in all the experimental strains (Fig. S7). These data were used to calculate the V_{max} of photosynthesis as well as whole cell affinity K_m for bicarbonate (Fig. 4). Consistent with our previous data (Selim *et al.*, 2018), the bicarbonate affinity of mutant Δ*sbtB* was significantly higher under HC conditions, while it was significantly lower in LC-grown cells. Hence, HC-acclimated Δ*sbtB* cells are somehow locked in an LC state, an

Table 4 Pigmentation of the different strains of *Synechocystis* sp. PCC 6803 after cultivation at high CO_2 (5%, high inorganic carbon (HC)) or low CO_2 (0.04%, low inorganic carbon (LC)) conditions for 3 d.

	WT HC	SbtB HC	Cya1 HC	DacA HC	WT LC	SbtB LC	Cya1 LC	DacA LC
Chlorophyll *a*	3.75	3.32	4.23	3.92	4.03	3.03	4.15	3.90
Phycocyanin	1.83	1.34	1.86	1.09	1.89	1.39	1.63	1.24
Carotenoids	3.34	6.08	4.29	4.01	4.42	5.85	4.81	5.58

Pigment values were calculated from *in vivo* absorption measurements per optical density at 750 nm as proxy for biomass (μmol l^{-1} OD_{750}^{-1}).

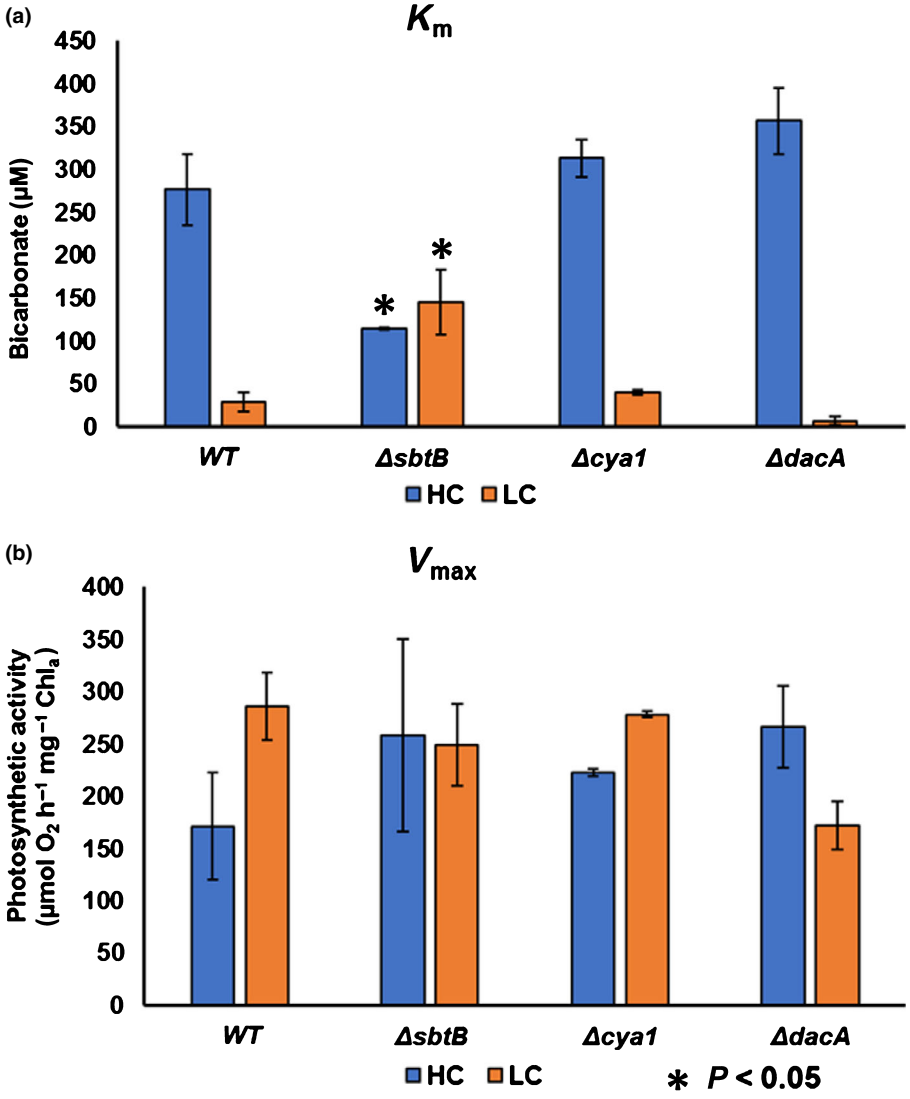

Fig. 4 Characterization of the photosynthesis in all strains of *Synechocystis* sp. PCC 6803 after long-term acclimation to 5% (high inorganic carbon (HC)) or 0.04% (low inorganic carbon (LC)) CO_2 conditions. The CO_2-affinities (K_m) and maximal photosynthetic rates (V_{max}) were calculated from bicarbonate-dependent photosynthetic activity measurements of the wild-type (WT) and the mutants Δ*sbtB*, Δ*cya1* and Δ*dacA* cultivated for 4–6 d at HC or LC conditions. (a) The K_m values. (b) The V_{max} values ($n = 3$). Mean values and standard deviations are displayed. Significantly changed expression compared to WT is indicated by an asterisk (Student's *t*-test, $P < 0.05$).

observation supported by the gene expression pattern. Meanwhile, the shift into LC conditions did not further improve C_i affinity. In contrast to the K_m values, the photosynthetic V_{max} values were similar to those of WT under both growth conditions. The cAMP-defective mutant Δ*cya1* did not show any significant alterations in the bicarbonate-dependent photosynthetic activity, compared to WT (Fig. 4), which surprisingly seems to indicate that cAMP binding is not an important trigger for C_i acclimation in *Synechocystis*. However, the bicarbonate-dependent photosynthesis of Δ*dacA* cells underwent changes compared to WT, which were different to the changes experienced by the Δ*sbtB* mutant. Compared to WT, the Δ*dacA* mutant had a slightly lower C_i affinity under HC and a higher C_i affinity under LC conditions. Moreover, the photosynthetic V_{max} was lower in this mutant under LC conditions, compared to WT (Fig. 4).

Changes in the mutant metabolome

Distinct changes in gene expression were detected, including the genes encoding enzymes involved in primary nitrogen and carbon metabolism, which likely lead to changes in the metabolic response to different C_i conditions. A targeted metabolome survey was used to investigate metabolic changes (Table S6) experienced by the cells of all experimental strains that were shifted from HC to LC for only 15 or 60 min, because second messengers are known to respond rapidly to environmental fluctuations. Glutamate and glutamine are the immediate products of the GS/GOGAT cycle for ammonia assimilation. Consistent with the reduced expression of genes for nitrogen uptake and metabolism, the pool of glutamate was lowered in the mutants Δ*sbtB* and Δ*dacA*, while it was less diminished in the mutant Δ*cya1*, compared to WT. When all strains were shifted to LC, the glutamate pool declined further, with the fastest decline being observed in Δ*dacA* after only 15 min (Fig. 5). Glutamine levels were lowest in Δ*sbtB* cells and remained so after the shift to LC. In all other strains, the glutamine amount transiently increased, and particularly high levels were measured in Δ*dacA* after 15 min at LC. However, 60 min after the shift to LC conditions, the glutamine levels for all three mutants fell back to those seen in HC conditions,

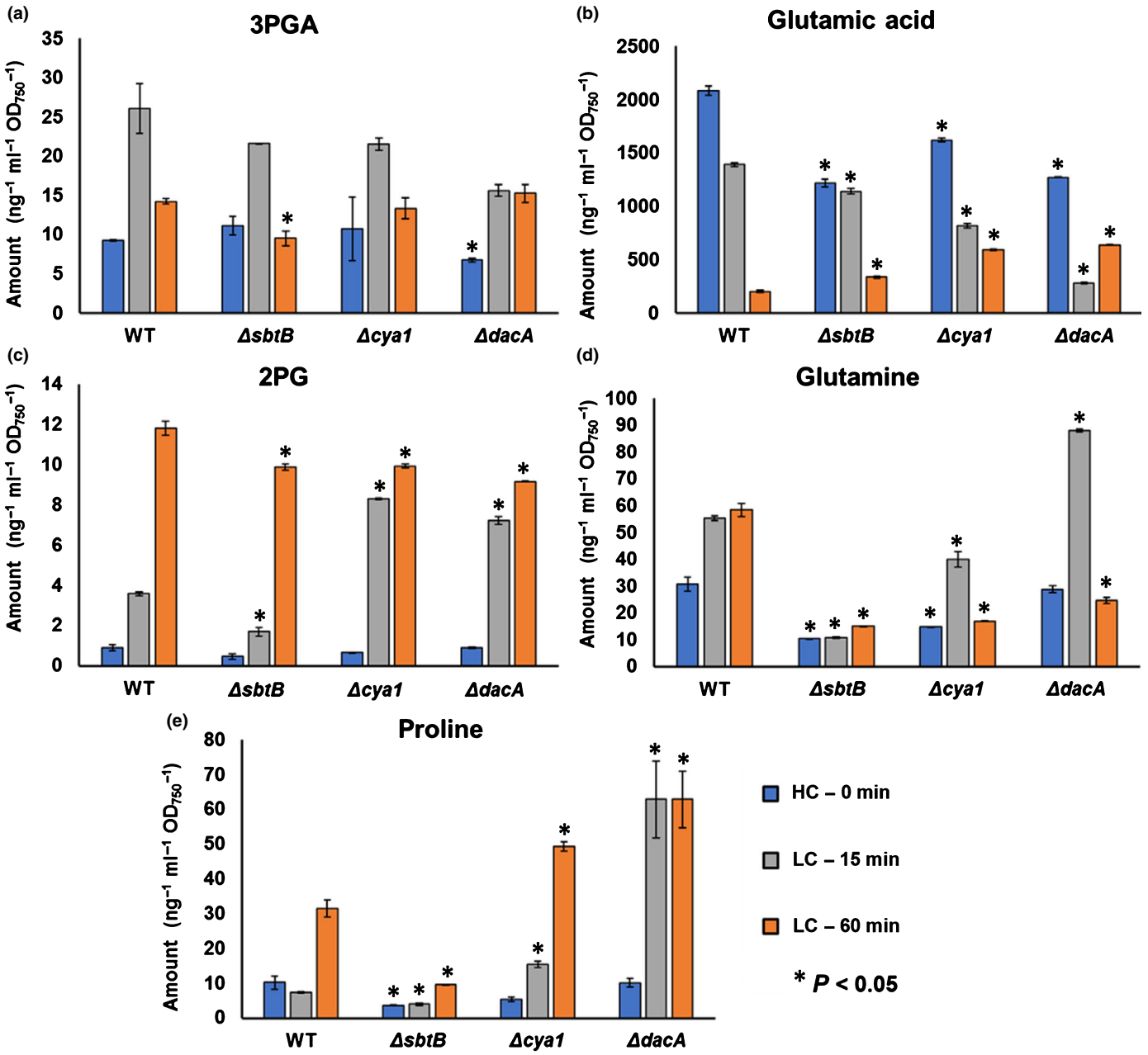

Fig. 5 Changes in the amounts of selected metabolites in the *Synechocystis* sp. PCC 6803 wild-type (WT) and the mutants Δ*sbtB*, Δ*cya1* and Δ*dacA*. Concentrations of (a) 3-phosphoglycerate (3PGA),(b) glutamic acid, (c) 2-phosphoglycolate (2PG), (d) glutamine and (e) proline are displayed when cells acclimated to high CO_2 (5%, high inorganic carbon (HC), time 0) were shifted for 15 or 60 min to low CO_2 (0.04%, low inorganic carbon (LC)) conditions. Mean values and standard deviations are displayed. Significantly changed expression compared to WT is indicated by an asterisk (Student's *t*-test, $P < 0.05$).

while remaining high in WT cells (Fig. 5). Proline is a compound that often accumulates in conditions of stress. An elevated proline pool was found in WT cells and the mutants Δ*cya1* and Δ*dacA* 60 min after the LC shift, while in the mutant Δ*sbtB* it increased only slightly. Since proline can be synthesized from glutamate, it is possible that the particularly high and rapid proline accumulation in Δ*dacA* cells may correlate with the fast glutamate decline in the LC-shifted cells of this mutant (Fig. 5). In addition to key amino acids, we were able to quantify 3-phosphoglycerate (3PGA), the stable product of the RubisCO carboxylation reaction, and 2PG, the product of the RubisCO oxygenation reaction. As expected, the 2PG levels rose immediately after the shift from HC to LC conditions. Here, it was obvious that this increase was delayed in Δ*sbtB*, which showed some signs of LC pre-acclimation not only in terms of gene expression but also in its improved bicarbonate affinity under HC conditions. The 3PGA amounts were mostly not altered between the different strains; 3PGA levels increased slightly immediately after the shift to LC conditions and returned to their initial concentration after 60 min.

Discussion

Gene expression, photosynthesis, and the metabolome were compared in four *Synechocystis* strains under different C_i conditions. The Δ*sbtB* mutant exhibited distinct changes in gene expression, compared to WT *Synechocystis* (Fig. 1). Many of these differentially expressed genes were previously reported as being C_i-regulated in the *Synechocystis* WT (Klähn *et al.*, 2015), especially the genes that were downregulated at HC in Δ*sbtB* and only at LC in WT. This large impact of SbtB depletion on C_i-regulated gene expression correlates with the major changes to photosynthetic C_i affinity (Fig. 4), which also suppresses the strong increase in 2PG levels immediately after WT cells are exposed to LC (Fig. 5). These results clearly imply that the absence of SbtB induces an LC pre-acclimated state in the Δ*sbtB* mutant and supports the notion that this carbon-regulating protein has a broader impact on C_i acclimation than merely regulating the SbtA bicarbonate uptake activity (Fig. 6). Like other proteins of the PII family, SbtB has no DNA-binding domain. It has been shown that structural changes in the T-loop of the canonical cyanobacterial PII protein, GlnB, permits interaction with several target proteins (Forchhammer & Selim, 2020). Among them, PipX, the transcriptional co-activator of NtcA, was identified as the PII-dependent regulator protein mediating the transcriptional regulation of acclimation to nitrogen availability. It might be possible that among the unknown targets of SbtB displayed in Fig. 6, a protein could exist that mediates an interaction of SbtB with a transcriptional factor as it is known for GlnB. However, we found that Δ*sbtB* cells exhibited altered expression of several transcription factors, including NdhR, one of the master regulators of C_i acclimation (Wang *et al.*, 2004). Still, only a few genes directly involved in the CCM were differentially regulated in Δ*sbtB* compared to WT cells, making it difficult to explain how Δ*sbtB* C_i affinity was altered due to changes affecting the CCM. It is possible that some of the as yet not functionally annotated hypothetical proteins that were differentially expressed in Δ*sbtB* may play more important roles in C_i acclimation than is presently recognized. Like the mutation of *glnB* that encodes the canonical PII protein (Schwarz *et al.*, 2014), the absence of SbtB had a marked impact on the proper C_i-induced downregulation of genes encoding proteins involved in N assimilation and metabolism, also resulting in an altered glutamate to glutamine ratio (Fig. 5). However, in contrast to the mutation of *glnB*, the absence of SbtB additionally affected the expression of photosynthesis-associated genes, which are also impacted on by the mutation of the gene encoding CyAbrB2 (Orf *et al.*, 2016a). This finding is consistent with reports that PSI and its interactions with NDH1 in the cyclic electron flow are important for

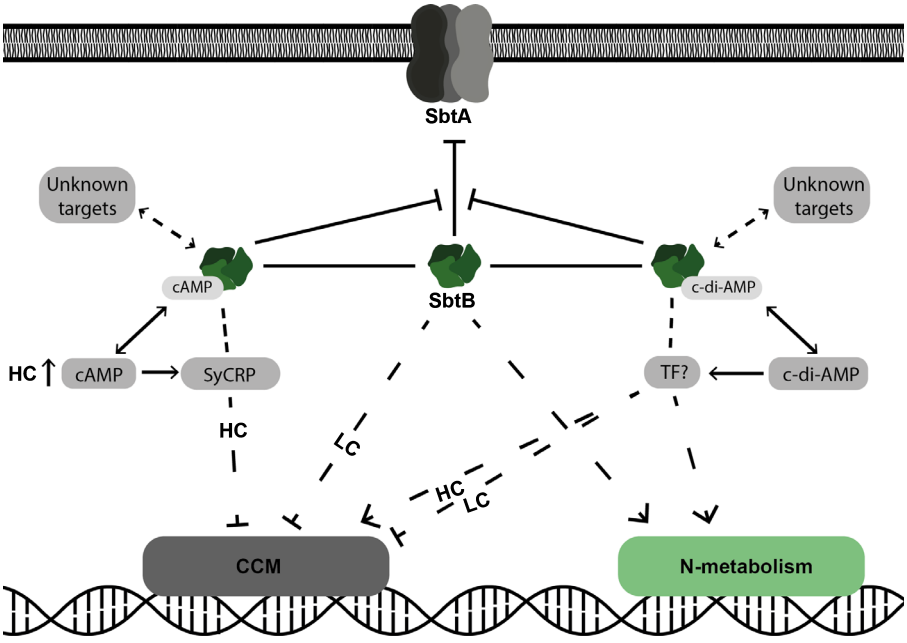

Fig. 6 Possible consequences of the absence of SbtB, cAMP or c-di-AMP on inorganic carbon-regulated expression of genes encoding proteins involved in the inorganic carbon-concentrating mechanism (CCM) or nitrogen metabolism in *Synechocystis* sp. PCC 6803. In its native state or when bound to AMP, SbtB interacts with the transport activity of SbtA, but this interaction is not possible when bound by cAMP or c-di-AMP. Independently on the two second messengers, SbtB influences the cell gene expression level by repressing (CCM) related genes under low CO_2 (0.04%, low inorganic carbon (LC)) conditions and inducing nitrogen-metabolism related genes. Both second messengers can influence gene expression as well, whether through SbtB or independently. The expression of CCM-related genes is downregulated by cAMP, whereas c-di-AMP upregulates those genes at high CO_2 (5%, high inorganic carbon (HC)) but underregulate some of them under LC conditions. Moreover, SbtB and c-di-AMP downregulate genes for proteins related to nitrogen-metabolism. The effect of cAMP is likely exhibited through the specific transcription factors SyCRP, while the effects of SbtB (when interacting or not with either second messenger) and of c-di-AMP are mediated through the interaction with yet undiscovered transcription factor(s) (TF?). Among the other c-di-AMP targets, recently the GlnB protein has been identified (Selim *et al*., 2021). (Blunt ended arrows indicate repression; normal arrows indicate activation.)

acclimation to fluctuating C_i concentrations (Battchikova *et al.*, 2011).

The second most prominent impact on C_i-regulated gene expression was observed for Δ*dacA*, which also had a larger overlap in C_i-regulated gene expression with Δ*sbtB* than the Δ*cya1* mutant. Interestingly, several CCM-related genes, especially those encoding the BCT1 transporter, were markedly overexpressed in Δ*dacA* (Fig. 6). Despite these expression changes, the photosynthetic CO_2 affinity of Δ*dacA* was not significantly different to that of the WT (Fig. 4). It should be noted that none of the genes encoding proteins involved in compatible solute biosynthesis or transport, or potassium homeostasis, which are thought to be associated with c-di-AMP in bacteria (Nelson *et al.*, 2013; Agostoni *et al.*, 2018; Selim *et al.*, 2021), showed significant alterations in expression in Δ*dacA* compared to WT. However, the expression of other genes such as *nhaS6*, *hliA*, *hliB*, or *sll1483*, which had been previously shown to be transcriptionally regulated following salt stress in *Synechocystis* (Kanesaki *et al.*, 2002; Klähn *et al.*, 2021), was different in Δ*dacA* compared to WT in the present study. Furthermore, the gene *slr0753*, which was shown to be regulated by the c-di-AMP-dependent riboswitch in the present study (Fig. 3), may be involved in chloride transport (Kobayashi *et al.*, 2006). These expression changes are therefore consistent with the recently reported low osmotic stress tolerance of Δ*dacA* (Selim *et al.*, 2021).

The second messenger cAMP is regarded as an HC signal as its binding releases SbtB from SbtA under HC conditions (Selim *et al.*, 2018; Fang *et al.*, 2021), whereas it has lower impact at LC. Consistently, we found many more gene expression changes comparing Δ*cya1* and WT under HC than under LC conditions (Fig. 1). However, compared to mutant Δ*sbtB*, the overlap with C_i-regulated genes identified from studies on WT cells was lower for Δ*cya1*. A possible explanation could be that Cya1 is the principal but not the only adenylate cyclase in *Synechocystis*. Previously published data (Terauchi & Ohmori, 1999) show that only *c.* 4% of WT cAMP levels are present in the Δ*cya1* mutant. This amount of cAMP may be sufficient to act as a HC signal for SbtB in the Δ*cya1* mutant, because its cAMP affinity is high (K_d of the highest affinity binding site = 2.1 μM, Selim *et al.*, 2018) compared to other cAMP-binding proteins such as SyCRP (K_d = 2.8 μM, Yoshimura *et al.*, 2000). However, the absence of Cya1 influences the expression of many genes, including several previously reported to be regulated by the cAMP receptor SyCRP (Yoshimura *et al.*, 2002). Moreover, the expression of genes encoding proteins involved in the biosynthesis of extracellular sulfated polysaccharides (Maeda *et al.*, 2021) was altered in Δ*cya1* cells, which indicates that cAMP may influence the lifestyle of cyanobacteria. Finally, the concerted upregulation of many transposase-encoding genes in mutant Δ*cya1* points at an important role of this adenylate kinase and/or cAMP in the maintenance of genome stability in *Synechocystis*.

Collectively, our results indicate that the lack of SbtB impacts a subset of LC acclimation genes, while c-di-AMP, and especially cAMP, appear to influence gene expression, especially during times of HC availability.

Acknowledgements

The authors thank Klaudia Michl (University of Rostock) for technical assistance in strain cultivation and sample preparation. The project was funded by grants from the German Research Foundation (DFG) as part of the priority research program (SPP1879) to M Hagemann (HA 2002/24-1) and to KF (Fo195/18-1). Work of WRH was also funded by the DFG (HE 2544/15-2, AOBJ: 680666). LC–MS/MS systems at the Department of Plant Physiology were supported through the German Research Foundation (DFG) (grant no. INST 264/125-1 FUGG). Open access funding enabled and organized by ProjektDEAL.

Author contributions

OM and M Hagemann designed the study, OM performed most experiments, VR performed transcriptomics, FPH performed qPCR, KAS and M Haffner constructed mutants and performed ATP measurements, KAS, KF, WRH and M Hagemann supervised experiments and evaluated data, OM and M Hagemann wrote manuscript with the input from all authors.

ORCID

Karl Forchhammer https://orcid.org/0000-0003-3199-8101
Martin Hagemann https://orcid.org/0000-0002-2059-2061
Wolfgang R. Hess https://orcid.org/0000-0002-5340-3423
Oliver Mantovani https://orcid.org/0000-0003-0999-3988
Viktoria Reimann https://orcid.org/0000-0002-9643-4553
Khaled A. Selim https://orcid.org/0000-0002-2974-9483

Data availability

The full transcriptome datasets for the wild-type and mutants Δ*sbtB*, Δ*dacA* and Δ*cya1* are accessible from the GEO database (https://www.ncbi.nlm.nih.gov/geo/) with the following accession numbers: GSE185294 (*Synechocystis* sp. PCC 6803 wild-type and Δ*sbtB* mutant), GSE185296 (*Synechocystis* sp. PCC 6803 wild-type and Δ*cya1* mutant), and GSE185297 (*Synechocystis* sp. PCC 6803 wild-type and Δ*dacA* mutant). Metabolome and many other data are supplied in the Supporting Information.

References

Agostoni M, Logan-Jackson AR, Heinz ER, Severin GB, Bruger EL, Waters CM, Montgomery BL. 2018. Homeostasis of second messenger cyclic-di-AMP is critical for cyanobacterial fitness and acclimation to abiotic stress. *Frontiers in Microbiology* **9**: 1121.

Battchikova N, Eisenhut M, Aro EM. 2011. Cyanobacterial NDH-1 complexes: novel insights and remaining puzzles. *Biochimica et Biophysica Acta* **1807**: 935–944.

Bolay P, Rozbeh R, Muro-Pastor MI, Timm S, Hagemann M, Florencio FJ, Forchhammer K, Klähn S. 2021. The novel PII-interacting protein PirA controls flux into the cyanobacterial ornithine-ammonia cycle. *mBio* **12**: e00229-21.

Brandenburg F, Klähn S. 2020. Small but smart: on the diverse role of small proteins in the regulation of cyanobacterial metabolism. *Life* **10**: 322.

Cann MJ, Hammer A, Zhou J, Kanacher T. 2003. A defined subset of adenylyl cyclases is regulated by bicarbonate ion. *Journal of Biological Chemistry* **278**: 35033–35038.

Daley SME, Kappell AD, Carrick MJ, Burnap RL. 2012. Regulation of the cyanobacterial CO_2-concentrating mechanism involves internal sensing of $NADP^+$ and α-ketogutarate levels by transcription factor CcmR. *PLoS ONE* **7**: e41286.

Doello S, Burkhardt M, Forchhammer K. 2021. The essential role of sodium bioenergetics and ATP homeostasis in the developmental transitions of a cyanobacterium. *Current Biology* **31**: 1606–1615.

Du J, Förster B, Rourke L, Howitt SM, Price GD. 2014. Characterisation of cyanobacterial bicarbonate transporters in *E. coli* shows that SbtA homologs are functional in this heterologous expression system. *PLoS ONE* **9**: e115905.

Fang S, Huang X, Zhang X, Zhang M, Hao Y, Guo H, Liu LN, Yu F, Zhang P. 2021. Molecular mechanism underlying transport and allosteric inhibition of bicarbonate transporter SbtA. *Proceedings of the National Academy of Sciences, USA* **118**: e2101632118.

Flügel F, Timm S, Arrivault S, Florian A, Stitt M, Fernie AR, Bauwe H. 2017. The photorespiratory metabolite 2-phosphoglycolate regulates photosynthesis and starch accumulation in Arabidopsis. *Plant Cell* **29**: 2537–2551.

Forchhammer K, Selim KA. 2020. Carbon/nitrogen homeostasis control in cyanobacteria. *FEMS Microbiology Reviews* **44**: 33–53.

García-Domínguez M, Reyes JC, Florencio FJ. 1997. Purification and characterization of a new type of glutamine synthetase from cyanobacteria. *European Journal of Biochemistry* **244**: 258–264.

Hagemann M, Kern R, Maurino VG, Hanson DT, Weber APM, Sage RF, Bauwe H. 2016. Evolution of photorespiration from cyanobacteria to land plants considering protein phylogenies and acquisition of carbon concentrating mechanisms. *Journal of Experimental Botany* **67**: 2963–2976.

Hagemann M, Song S, Brouwer EM. 2021. Chapter 1: Inorganic carbon assimilation in cyanobacteria: mechanisms, regulation, and engineering. In: Hudson P, Lee SY, Nielsen J, eds. *Cyanobacteria biotechnology, Wiley-Blackwell biotechnology series*. Weinheim, Germany: Wiley-Blackwell, 1–31.

Hammer A, Hodgson DR, Cann MJ. 2006. Regulation of prokaryotic adenylyl cyclases by CO_2. *Biochemical Journal* **396**: 215–218.

Hein S, Scholz I, Voß B, Hess WR. 2013. Adaptation and modification of three CRISPR loci in two closely related cyanobacteria. *RNA Biology* **10**: 852–864.

Jablonsky J, Papacek S, Hagemann M. 2016. Different strategies of metabolic regulation in cyanobacteria: from transcriptional to biochemical control. *Scientific Reports* **6**: 33024.

Jesser R, Behler J, Benda C, Reimann V, Hess WR. 2019. Biochemical analysis of the Cas6-1 RNA endonuclease associated with the subtype I-D CRISPR-Cas system in *Synechocystis* sp. PCC 6803. *RNA Biology* **16**: 481–491.

Jiang Y-L, Wang X-P, Sun H, Han S-J, Li W-F, Cui N, Lin G-M, Zhang J-Y, Cheng W, Cao D-D *et al.* 2018. Coordinating carbon and nitrogen metabolic signaling through the cyanobacterial global repressor NdhR. *Proceedings of the National Academy of Sciences, USA* **115**: 403–408.

Kanesaki Y, Suzuki I, Allakhverdiev SI, Mikami K, Murata N. 2002. Salt stress and hyperosmotic stress regulate the expression of different sets of genes in *Synechocystis* sp. PCC 6803. *Biochemical Biophysical Research Communications* **290**: 339–348.

Klähn S, Mikkat S, Riediger M, Georg J, Hess WR, Hagemann M. 2021. Integrative analysis of the salt stress response in cyanobacteria. *Biology Direct* **16**: 26.

Klähn S, Orf I, Schwarz D, Matthiessen JKF, Kopka J, Hess WR, Hagemann M. 2015. Integrated transcriptomic and metabolomic characterization of the low-carbon response using an *ndhR* mutant of *Synechocystis* sp. PCC 6803. *Plant Physiology* **169**: 1540–1556.

Klotz A, Georg J, Bučinská L, Watanabe S, Reimann V, Januszewski W, Sobotka R, Jendrossek D, Hess WR, Forchhammer K. 2016. Awakening of a dormant cyanobacterium from nitrogen chlorosis reveals a genetically determined program. *Current Biology* **26**: 2862–2872.

Kobayashi M, Katoh H, Ikeuchi M. 2006. Mutations in a putative chloride efflux transporter gene suppress the chloride requirement of photosystem II in the cytochrome c550-deficient mutant. *Plant Cell Physiology* **47**: 799–804.

Liu XY, Hou WT, Wang L, Li B, Chen Y, Chen Y, Jiang YL, Zhou CZ. 2021. Structures of cyanobacterial bicarbonate transporter SbtA and its complex with PII-like SbtB. *Cell Discovery* **7**: 63.

Maeda K, Okuda Y, Enomoto G, Watanabe S, Ikeuchi M. 2021. Biosynthesis of a sulfated exopolysaccharide, synechan, and bloom formation in the model cyanobacterium *Synechocystis* sp. strain PCC 6803. *eLife* **10**: e66538.

Nelson JW, Sudarsan N, Furukawa K, Weinberg Z, Wang JX, Breaker RR. 2013. Riboswitches in eubacteria sense the second messenger c-di-AMP. *Nature Chemical Biology* **9**: 834–839.

Nishimura T, Takahashi Y, Yamaguchi O, Suzuki H, Maeda SI, Omata T. 2008. Mechanism of low CO_2-induced activation of the *cmp* bicarbonate transporter operon by a LysR family protein in the cyanobacterium *Synechococcus elongatus* strain PCC 7942. *Molecular Microbiology* **68**: 98–109.

Oren N, Timm S, Frank M, Mantovani O, Murik O, Hagemann M. 2021. Red/far-red light signals regulate the activity of the carbon-concentrating mechanism in cyanobacteria. *Science Advances* **7**: eabg0435.

Orf I, Schwarz D, Kaplan A, Kopka J, Hess WR, Hagemann M, Klähn S. 2016a. CyAbrB2 contributes to the transcriptional regulation of low CO_2 acclimation in *Synechocystis* sp. PCC 6803. *Plant and Cell Physiology* **57**: 2232–2243.

Orf I, Timm S, Bauwe H, Fernie AR, Hagemann M, Kopka J, Nikoloski Z. 2016b. Can cyanobacteria serve as a model of plant photorespiration? – a comparative analysis of metabolite profiles. *Journal of Experimental Botany* **67**: 2941–2952.

Rae BD, Long BM, Badger MR, Price GD. 2013. Functions, compositions, and evolution of the two types of carboxysomes: polyhedral microcompartments that facilitate CO_2 fixation in cyanobacteria and some proteobacteria. *Microbiology Molecular Biology Reviews* **77**: 357–379.

Raven JA, Beardall J, Sánchez-Baracaldo P. 2017. The possible evolution and future of CO_2-concentrating mechanisms. *Journal of Experimental Botany* **68**: 3701–3716.

Reinholdt O, Schwab S, Zhang Y, Reichheld JP, Fernie AR, Hagemann M, Timm S. 2019. Redox-regulation of photorespiration through mitochondrial thioredoxin. *Plant Physiology* **181**: 442–457.

Rippka R, Deruelles J, Waterbury JB, Herdman M, Stanier RY. 1979. Generic assignments, strain histories and properties of pure cultures of cyanobacteria. *Journal of General Microbiology* **111**: 1–61.

Rubin BE, Huynh TN, Welkie DG, Diamond S, Simkovsky R, Pierce EC, Taton A, Lowe LC, Lee JJ, Rifkin SA *et al.* 2018. High-throughput interaction screens illuminate the role of c-di-AMP in cyanobacterial nighttime survival. *PLoS Genetics* **14**: e1007301.

Schwarz D, Orf I, Kopka J, Hagemann M. 2014. Effects of inorganic carbon limitation on the metabolome of the *Synechocystis* sp. PCC 6803 mutant defective in *glnB* encoding the central regulator PII of cyanobacterial C/N acclimation. *Metabolites* **4**: 232–247.

Selim KA, Haase F, Hartmann MD, Hagemann M, Forchhammer K. 2018. PII-like signaling protein SbtB links cAMP sensing with cyanobacterial inorganic carbon response. *Proceedings of the National Academy of Sciences, USA* **115**: E4861–E4869.

Selim KA, Haffner M, Burkhardt M, Mantovani O, Neumann N, Albrecht R, Seifert R, Krüger L, Stülke J, Hartmann MD *et al.* 2021. Diurnal oscillation of cyanobacteria requires perception of second messenger signaling molecule c-di-AMP by the carbon-control protein SbtB. *Science Advances* **7**: eabk0568.

Sigalat C, de Kouchkovsky Y. 1975. Fractionnement et characterisation de l'appareil photosynthetique de l'algue bleue unicellulaire *Anacystis nidulans*. I. Obtention de fractions par lyse osmotique et analyse pigmentaire. *Physiologie Végétale* **13**: 243–258.

Song K, Baumgartner D, Hagemann M, Muro-Pastor AM, Maaß S, Becher D, Hess WRH. 2022. AtpΘ is an inhibitor of F_0F_1 ATP synthase to arrest ATP hydrolysis during low-energy conditions in cyanobacteria. *Current Biology* **32**: 136–148.

Spät P, Barske T, Maček B, Hagemann M. 2021. Alterations in the CO_2 availability induce alterations in the phospho-proteome of the cyanobacterium *Synechocystis* sp. PCC 6803. *New Phytologist* **231**: 1123–1137.

Stülke J, Krüger L. 2020. Cyclic di-AMP signaling in bacteria. *Annual Reviews in Microbiology* **74**: 159–179.

Tamoi M, Kurotaki H, Fukamizo T. 2007. Beta-1,4-glucanase-like protein from the cyanobacterium *Synechocystis* PCC6803 is a beta-1,3–1,4-glucanase and functions in salt stress tolerance. *Biochemical Journal* **405**: 139–146.

Tcherkez GGB, Farquhar GD, Andrews TJ. 2006. Despite slow catalysis and confused substrate specificity, all ribulose bisphosphate carboxylases may be nearly perfectly optimized. *Proceedings of the National Academy of Sciences, USA* **103**: 7246–7251.

Terauchi K, Ohmori M. 1999. An adenylate cyclase, Cya1, regulates cell motility in the cyanobacterium *Synechocystis* sp. PCC 6803. *Plant and Cell Physiology* **40**: 248–251.

Wang HL, Postier BL, Burnap RL. 2004. Alterations in global patterns of gene expression in *Synechocystis* sp. PCC 6803 in response to inorganic carbon limitation and the inactivation of *ndhR*, a LysR family regulator. *Journal of Biological Chemistry* **279**: 5739–5751.

Yoshimura H, Hisabori T, Yanagisawa S, Ohmori M. 2000. Identification and characterization of a novel cAMP receptor protein in the cyanobacterium *Synechocystis* sp. PCC 6803. *Journal of Biological Chemistry* **275**: 6241–6245.

Yoshimura H, Yanagisawa S, Kanehisa M, Ohmori M. 2002. Screening for the target gene of cyanobacterial cAMP receptor protein SYCRP1. *Molecular Microbiology* **43**: 843–853.

Supporting Information

Additional Supporting Information may be found online in the Supporting Information section at the end of the article.

Fig. S1 Principal component analysis of microarray data.

Fig. S2 Venn diagrams showing the overlap of CO_2-regulated gene expression after 3 h LC.

Fig. S3 Absorbance spectra between 400 and 800 nm (normalized to the value at 750 nm).

Fig. S4 Comparison of the expression of selected C_i-regulated genes 3 h after the shift to LC.

Fig. S5 Verification of microarray data by qRT-PCR for selected genes.

Fig. S6 Mean cell diameter of the different strains grown under either HC or LC conditions.

Fig. S7 Bicarbonate dependent photosynthetic activity measurements.

Methods S1 Details on quantitative pigment analysis.

Table S1 Protein-coding gene expression comparison between wild-type (WT) and Δ*sbtB* mutant.

Table S2 Protein-coding gene expression comparison between wild-type (WT) and Δ*dacA* mutant.

Table S3 Protein-coding gene expression comparison between wild-type (WT) and Δ*cya1* mutant.

Table S4 Genes that are upregulated or downregulated in all strains after growth at high inorganic carbon (HC) conditions.

Table S5 Genes that are upregulated or downregulated in all strains after shift to low inorganic carbon (LC) for 24 h.

Table S6 Metabolome data set.

Please note: Wiley Blackwell are not responsible for the content or functionality of any Supporting Information supplied by the authors. Any queries (other than missing material) should be directed to the *New Phytologist* Central Office.

The redox-sensitive R-loop of the carbon control protein SbtB contributes to the regulation of the cyanobacterial CCM

Mantovani O, Haffner M, Walke P, Elshereef AA, Wagner B, Petras D, Forchhammer K, Selim KA, Hagemann M 2023**.** *ResearchGate* DOI: 10.21203/rs.3.rs-3292191/v1

The redox-sensitive R-loop of the carbon control protein SbtB contributes to the regulation of the cyanobacterial CCM

Oliver Mantovani[1], Michael Haffner[2], Peter Walke[1], Abdalla A. Elshereef[2], Berenike Wagner[2], Daniel Petras[2], Karl Forchhammer[2], Khaled A. Selim[2,3*], Martin Hagemann[1,4*]

1 – Institute of Biosciences, Department of Plant Physiology, University of Rostock, Rostock, Germany

2 – Interfaculty Institute of Microbiology and Infection Medicine Tübingen, University of Tübingen, Tübingen, Germany

3 – Department of Protein Evolution, Max Planck Institute for Biology, Tübingen, Germany

4 – Interdisciplinary Faculty, Department Life, Light and Matter, University of Rostock, Rostock, Germany

***Corresponding authors:** Khaled A. Selim, Interfaculty Institute of Microbiology and Infection Medicine Tübingen, University of Tübingen, Tübingen, Germany, Email: khaled.selim@uni-tuebingen.de; Martin Hagemann, Institute of Biosciences, Department of Plant Physiology, University of Rostock, A.-Einstein-Str. 3, Rostock D-18059, Germany; Tel: +49(0)3814986110; Fax: +49(0)3814986112; Email: martin.hagemann@uni-rostock.de

OM - https://orcid.org/0000-0003-0999-3988

MiH - https://orcid.org/0000-0001-9906-6832

PW – https://orcid.org/0009-0006-8043-183X

DP - https://orcid.org/0000-0002-6561-3022

KF – https://orcid.org/0000-0003-3199-8101

KAS – https://orcid.org/0000-0002-2974-9483

MaH - http://orcid.org/0000-0002-2059-2061

BW - https://orcid.org/0000-0002-7691-7531

Abstract

SbtB is a PII-like protein that regulates the carbon-concentrating mechanism (CCM) in cyanobacteria. SbtB proteins can bind many adenyl nucleotides and possess a characteristic C-terminal redox sensitive loop (R-loop) containing two cysteine residues that allow the formation of a disulfide bridge in response to the diurnal state of the cell. SbtBs also possess an ATPase/ADPase activity that is modulated by the redox-state of the R-loop.

To investigate the functions of the R-loop in the cyanobacterium *Synechocystis* sp. PCC 6803, the site-specific mutants C105A-C110A, unable to form the hairpin and permanently in the reduced state, and Δ104, where the entire R-loop has been truncated, were characterized under different inorganic carbon (C_i) and light regimes. During diurnal rhythm, growth analysis showed a role of the R-loop as sensor for acclimation to changing light conditions. The redox-state of the R-loop was found to impact the binding of the adenyl-nucleotides to SbtB, its membrane association and thereby the CCM regulation, while these phenotypes disappeared after truncation of the R-loop.

Collectively, our data imply that the redox-sensitive R-loop provides an additional regulatory layer to SbtB, linking the C_i-related signaling activity of SbtB with the redox state of cells mainly reporting the actual light conditions. This regulation not only coordinates CCM activity in the diurnal rhythm but also affects the primary carbon metabolism.

Key words

Cyanobacteria, carbon metabolism, CCM, light acclimation, redox regulation, PII superfamily signaling

Introduction

Cyanobacteria evolved the inorganic carbon-concentrating mechanism (CCM) to adapt towards the declining availability of CO_2 and to reduce the occurrence of the competing oxygenation reaction of ribulose-1,5-bisphosphate carboxylase/oxygenase (RuBisCO), the key enzyme of the Calvin–Benson–Bassham (CBB) cycle that is responsible for the fixation of CO_2 in all oxygenic phototrophs (Raven *et al.,* 2017, Hagemann *et al.,* 2018).

The main components of the cyanobacterial CCM consist of up to five uptake systems for inorganic carbon (C_i, the sum of bicarbonate and CO_2) including three bicarbonate transporters, namely SbtA, BicA and BCT1 complex, and the CO_2 hydration system made up of the $NDH1_3$ and $NDH1_4$ complexes. Furthermore, the prokaryotic organelle carboxysome contains all active RuBisCO molecules and carbonic anhydrase (CA). The bicarbonate transporters significantly increase the intracellular bicarbonate concentration, which after entering the carboxysomes is converted by the CA into CO_2, increasing its concentration around RuBisCO and thereby reducing the possibility of the enzyme incorporating O_2. The excess CO_2 that escapes the carboxysomes and the environmental CO_2 that permeates inside the cells through the membrane, is converted to HCO_3^- by the CO_2 hydration system, re-supplying the bicarbonate pool (reviewed by Rae *et al*., 2013; Hagemann *et al*., 2021).

The CCM, apart from greatly reducing the rate of photorespiration, allows cyanobacteria to adapt to fluctuating conditions, whether C_i, light or else (Mantovani *et al*., 2022, Köbler *et al*., 2018). For this reason, the CCM needs to be tightly regulated. The expression of key CCM components especially C_i uptake systems is regulated at transcriptional level, whereas the activity regulation is mostly done by the carbon regulator protein SbtB (reviewed in Mantovani *et al*., 2023). As member of the PII superfamily, this protein forms a homotrimer capable of regulating many components of the CCM and carbon metabolism. SbtB binds to different adenyl-nucleotides, which include ATP, ADP, AMP, cAMP, or c-di-AMP, and thereby can perceive various intracellular signals to modulate its interaction partners accordingly (reviewed by Mantovani *et al.,* 2023). This is achieved by its T-loop, a typical protein part characteristic of the PII superfamily, which can adapt different conformations depending on which nucleotide is found in the binding pocket and thereby modulating the interaction with various target proteins (Forchhammer & Lüddecke, 2016; Forchhammer *et al*., 2022; Forchhammer and Selim, 2020).

Contrary to canonical PII proteins, SbtB can only bind adenyl nucleotides including the two second messengers cAMP and c-di-AMP (Selim *et al*. 2018, 2021). Furthermore, SbtB presents features that are not found in the rest of the superfamily. One of which is its recently discovered apyrase activity, which causes the hydrolysis of ATP and ADP to AMP, thereby modulating the activity of SbtB. Another unique characteristic is the presence of the C-terminal

redox-regulated loop (R-loop) in many cyanobacterial SbtBs, which can form a disulphide bridge and acts as a redox-sensing structure (Selim *et al*., 2023). Among photoautotrophs, the presence of redox-sensitive disulphide bridges is often found in enzymes associated with photosynthesis or light regulation. The light-dependent activation of those proteins is usually mediated by the ferredoxin/thioredoxin system, causing reduction in the light and oxidation in the night (McMarlane *et al*., 2019; reviewed by Foyer and Noctor, 2009). While the role of the R-loop in modulation of the CCM was not investigated yet, it was found to affect the apyrase activity, which is significantly decreased when the loop is unable to form a disulphide bridge and even more when truncated (Selim *et al*., 2023).

Currently, the identified interaction partners of SbtB include the bicarbonate transporter SbtA and the glycogen branching enzyme GlgB (Selim *et al*., 2021; Liu *et al*., 2021). The SbtB-GlgB interaction is modulated through c-di-AMP binding to SbtB, which allows it to regulate glycogen synthesis during diurnal rhythm. However, the primary target of SbtB is SbtA, which it SbtB can interact with in multiple manners depending on the nucleotide bound to it. The binding of AMP or ADP promote a strong interaction between SbtB and SbtA, while ATP, cAMP or c-di-AMP hinder or prevent the binding of SbtB on SbtA (Liu et al. 2021; Fang *et al*., 2021; Selim *et al.,* 2018, 2023). In such a manner, SbtB can regulate SbtA activity by modulating bicarbonate transport when not needed by the cell (Förster *et al*., 2023) and to function as a plug to prevent the back-flow of bicarbonate outside of the cells during darkness, to avoid waste of energy (Haffner *et al*., 2023).

Here, we performed an in-depth investigation into the function of the R-loop in *Synechocystis* sp. PCC 6803 (hereafter *Synechocystis*), in regard to its role as redox-sensing module, its impact on the modulation of the CCM and carbon metabolism, the binding affinity of SbtB to the different adenyl nucleotides and the affinity of SbtB to SbtA.

Materials ad methods

Strains and cultivation

The freshwater cyanobacterium *Synechocystis* sp. PCC 6803 was used as wild type (WT) for this study. The bacterium was cultured in BG11 media (Rippka *et al*., 1979) buffered with TES/KOH, at pH 7.0 for low-carbon (LC) and pH 8.0 for high-carbon (HC) conditions. LC cultures were bubbled with ambient air (0.04% CO_2), while HC cultures with CO_2-enriched air (5%, v/v). Growth on solid media was performed in plates with BG11 and added agar (10 g/L) at 28 °C and constant light of 30 µmol photons m^{-2} s^{-1}. Growth in liquid media was performed in bubbling tubes at 29 °C with a light intensity of 130 µmol photons m^{-2} s^{-1}. Dark incubation was performed with black bubbling tubes.

The *Synechocystis* mutant of the SbtB-encoding ORF *slr1513* (*sbtB* knock-out mutant, named Δ*sbtB*) harbors an erythromycin resistance, whereas the strains SbtB-C105A-C110A and SbtB-Δ104 possess resistance for spectinomycin. These strains were cultivated in the presence of appropriate amounts of the corresponding antibiotics.

Generation of mutants

The *sbtB* mutants in *Synechocystis* have been obtained through homologous recombination. All constructs were generated using pUC19 plasmids, containing the modified *sbtB* coding regions (*slr1513*), a downstream spectinomycin resistance cassette, and the 500 base pairs up- and down-stream flanking regions necessary for recombination. The plasmids used for homologous recombination were obtained as described by (Selim *et al*., 2023).

Cyanobacteria transformation was performed starting with inoculation of a WT culture at an OD ~0.5 then grown over night at LC conditions. The following day 10 mL of the culture were collected and centrifuged. The pellet was resuspended in 500 µL of fresh BG11 media, which was split in two new Eppendorf tubes, one for each transformation. 5 µL of the mutated-*sbtB*-containing pUC19 plasmid were added to each tube, which were then incubated in darkness on a shaker for 3 h at 28 °C. The transformed cultures were then plated on BG11 plates without antibiotics and grown for 3-5 days at 28 °C until the cell growth became visible, after which spectinomycin was added to each plate and the culturing was continued until the appearance of single colonies. The correct integration and segregation of the mutants was verified via PCR (2059 and 2092) and the correct coding sequence via sequencing (PR6) (Supplementary table S1).

Growth rate determination

For the determination of growth rates, cultures were pre-acclimated to the desired carbon/light conditions for 3 days in bubbling tubes. Experiments started with inoculum at an OD_{720} of 0.2 in fresh BG11 media at pH 8.0 for HC or at pH 7.0 for LC Growth at different light and C_i regimes was then performed in Multicultivator MC-1000 (PSI, Czech Republic) that measures the OD_{720} every 15 min.

Glycogen quantification

To determine concentrations of glycogen in *Synechocystis* strains during diurnal cycle, cultures were started with an OD_{750} 1 under HC conditions and grown for 2 days under a 12 h light/12 h dark cycle in the Multicultivator MC-1000 with a light intensity of 100 µmol photons m^{-2} s^{-1}. After the pre-acclimation, 5 mL samples were harvested in triplicates in the middle (6 h) of the light and dark phases, respectively, via centrifugation. Measurements of glycogen concentrations were performed as described previously (Lucius *et al*., 2021).

Bicarbonate-dependent oxygen production

In vivo affinity for bicarbonate of HC- or LC-acclimated cultures of the *Synechocystis* strains used in this study was determined by the measurement of C_i-dependent photosynthetic activity through a Clarke-type oxygen electrode (Hansatech). Cultures were re-suspended in fresh BG11 pH 8.0 medium at an OD_{750}=3. Measurements were performed on 3 mL of the culture, illuminated with 300 µmol photons m^{-2} s^{-1} and increasing amounts of HCO_3^-. Oxygen evolution rates were used to calculate the affinities to C_i of each strain as function of K_m values.

Heterologous expression and purification of TrxA protein

The pET15b plasmid carrying the gene for the His-Tagged TrxA, generated in Tübingen, was used for the heterologous expression and purification of TrxA. The *E. coli* strain carrying the plasmid was inoculated from an LB agar plate to 5 mL LB medium containing 50 µg/mL ampicillin, and grown over-night (ON) at 37 °C. The pre-culture was then used the following day for the inoculation of 200 mL LB medium without antibiotics and grown on a shaker at 37 °C until it reached an OD_{600} between 0.6 and 0.8. IPTG 50 µg/mL was then added for induction of protein expression and the culture was left in incubation on a shaker ON at room temperature (RT). Afterwards, the cells were collected by centrifugation for 15 min at 4 °C and 9000 rpm, then re-suspended in 5 mL homogenization buffer (20 mM Tris, 50 mM NaCl, pH 7.8). The cells were lysed with four cycles of sonication of 30 s with a BANDELIN sonoplus HD70 sonicator at 70 % of the maximum output, interspersed with 30 s cooling on ice.

His-tagged purification was achieved via affinity chromatography with Ni-NTA column (Bio-Rad) as described previously (Selim *et al*., 2020), pre-equilibrated with 5 mL homogenization buffer twice. After loading the lysate, collecting the flow-through, and washing the column twice with washing buffer (Tris 20 mM, NaCl 300 mM, pH 7.8), TrxA was eluted with elution buffer (Tris 20 mM, NaCl 500 mM, Imidazole 300 mM, DTT 2 mM, pH 7.8).

Immuno-blotting for determining cellular localization of SbtB

Whole cell extracts were performed as in (Selim *et al*., 2018), after adding ~200 µL of 200 µL glass beads (Sigma) with a diameter of 465-600 µm, using a Retsch MM400 beads beater with a speed of 30 beats/s with 2 cycles of 30 s, interspersed with incubation on ice for 30 sec. The membrane and soluble fractions were separated by centrifugation at 21.000 x g for 30 min at 4 °C. Total protein content was determined with the Roti-Nanoquant Bradford assay (Roth). 10 µg of total protein extracts were separated via SDS 15% poly-acrylamide gel electrophoresis, which were then transferred to PVDF membranes (BIO-RAD) via semi-dry blot transfer. The membranes were blocked with a 5 % milk 1x TBS buffer for 1 h and then incubated ON at 4 °C with the polyclonal anti-SbtB antibody (1:1000). Subsequently, the membranes were incubated with a goat anti-rabbit antibody coupled with a horseradish peroxidase (BIO-RAD)

(1:5000). Images were developed by incubation with ECL Bright (Agrisera) and taken with a C-DiGit (LI-COR).

Recombinant SbtB protein purification and Isothermal titration calorimetry (ITC)

All the plasmids and primers used in this study are listed in (Table S1). The recombinant N- or C-terminal StrepII-tagged SbtB or it's R-loop variants were expressed and purified on strep-tactin column (IBA) as described previously (Selim *et al*., 2018, 2023). The ITC experiments were conducted as described previously (Lapina *et al.,* 2018 and Selim *et al.,* 2019) using a MICROCal PEAQ-ITC SYSTEM (Malvern, UK) microcalorimeter or a VP-ITC microcalorimeter (MicroCal, LCC). Sample solutions were prepared by dialyzing the SbtB proteins, including SbtB-WT or its variants (SbtB-C105S, SbtB-C110S, SbtB-C105S-C110S, SbtB-C105A-C110A, SbtB-Δ104, and SbtB-Δ109), separately in a buffer of 50 mM Tris (pH 7.8), 150 mM KCl and 150 mM NaCl at 25°C. Nucleotides (ATP, ADP, cAMP, and AMP) were used as ligand solutions. To ensure successful ITC runs, both protein and ligand solutions were prepared in the same buffer and condition to minimize heat changes arising from solution mismatches during mixing. Heat isotherms of the ligand dilution in the cell buffer were collected as blank runs for each experiment in the absence of protein.

For determining ligand binding isotherms of SbtB WT and its variants, 30 μM protein solutions (trimer concentration) were titrated against 1.5 or 2 mM of ligand solutions. The binding isotherms were calculated from the received data and fitted using one set of binding sites model with the MicroCal PEAG-ITControl Software (Malvern, UK) to calculate the dissociation constant K_D. All titrations were performed in duplicates with different purification batches of recombinant proteins. The baseline subtraction and fitted offset were conducted based on the default control subtraction type of the software. The K_D value for the WT-SbtB protein was re-calculated from (Selim *et al.,* 2018) using a single binding model.

Crystallization

The crystallization screens were done using vapor diffusion method in 96-well sitting-drop plates at 20 °C as described previously (Selim *et al*., 2018, 2023). For co-crystallization of SbtB C105S-C110S variant with cAMP, 2 mM of cAMP was added to the protein solution. The co-crystal was obtained with a reservoir solution composed of 0.1 M MES pH 6.5 and 25% (w/v) PEG 1000. Our previous SbtB structure (PDB: 7R31) in space group $P4_1$ was used as a search model and the structure was solved using difference Fourier method.

Intact Protein Mass Spectrometry Analysis

For denaturing TopDown Proteomics analysis of SbtB redox state, 10 μM SbtB protein (calculated based on the monomeric molecular weight) either in presence or absence of 10

µM TrxA were incubated for 30 min at 28 °C in reaction buffer [50 mM Tris/HCl (pH 8.0); 250 mM NaCl; 0.5 mM EDTA] either without reducing agent or containing 5 mM DTT. Samples were shock frozen in liquid nitrogen and stored at -80 °C upon analysis. Intact protein MS analysis was carried out by injecting 5 µL of SbtB reaction mixture onto a Q Exactive HF hybrid quadrupole-Orbitrap mass spectrometer couple to a Vanquish UHPLC system (Thermo Scientific) using a Supleco C18 BioWide column (150x2mm) with a flow of 0.4 mL/min and a linear gradient ramped over 5 minutes from 5% to 70% acetonitrile/water + 0.1% formic acid. MS1 and MS/MS spectra were acquired in Top3 data dependent acquisition mode. Resolution for both MS1 and MS/MS scans was set to 120,000 at 200 m/z. Data analysis was performed using Xcalibur 4.1 (Thermo Scientific). Deconvolution of the spectra was performed with Xtract using FreeStyle™ 1.8 SP2. Protein spectrum matching of the MS/MS was performed using *ProSight Lite* (Fellers *et al.,* 2015).

Urea-PAGE analysis

For denaturing urea PAGE analysis of the SbtB redox state, 10 µM reduced TrxA were incubated with 10 µM SbtB (calculated based on the monomeric molecular weight) in reaction buffer [50 mM Tris/HCl pH 8.0; 250 mM NaCl; 0.5 mM EDTA] at 28 °C for 30 min. As control, 10 µM SbtB were parallel incubated in reaction buffer that either contained 5 mM or 0.5 mM DTT or without reducing agent. All samples were mixed with and equal volume of two-fold concentrated non-reducing sample buffer [125 mM Tris-HCl, pH 6.8; 20 % glycerol; 4 % SDS; 0.1 % bromophenol blue] and applied to a 14 % 8 M urea-PAGE (Ibrahim *et al*., 2022). The urea-PAGE was pre-run in 1X TBE running buffer [10.8 g/l Tris; 5.5 g/l boric acid; 0.75 g/l EDTA] at 20 V for approx. 30 min, before samples were applied and run at 40 V. SbtB was subsequently identified by western blotting against SbtB, using a specific α-SbtB antiserum (Selim *et al.,* 2018).

Bicarbonate leakage quantification

To determine the back-flow of ^{14}C-labbelled HCO_3^- from *Synechocystis*, each strain was acclimated to LC conditions for 2 days, then, on the day of the experiments, cultures were re-started at an OD_{750}= 1.0 in fresh BG11 pH 7.0 and grown for 2 h. Leakage was determines as described by Haffner *et al*., 2023.

Data Sharing

All raw and processed data from the intact protein MS experiments is available through the MassIVE repository (massive.ucsd.edu) with the identifierMassIVE MSV000090130

Results

The R-loop affects the binding affinity of nucleotides to SbtB

It was previously shown that the C-terminal-loop of SbtB acts as a redox sensor to modulate the apyrase activity of SbtB, where it strongly influences the T-loop conformation. The folded R-loop (oxidized) is therefore incompatible with the correct structuring of the T-loop. When the R-loop is reduced (unfolded) or absent, however, the T-loop becomes folded and wraps around ATP or ADP, protecting them from hydrolysis. By contrast the oxidized R-loop prevents the protecting conformation of the T-loop, inducing the nucleotides-strained conformation and thereby exposing them to hydrolytic attack to form AMP (Selim *et al.,* 2023). Therefore, we assumed that the redox-state of the R-loop could additionally affect the nucleotide-binding affinities of SbtB. To gain deeper insights into the influence of the reduced R-loop on the ligand binding properties of SbtB, we performed isothermal titration calorimetry (ITC) experiments using SbtB variants either lacking the R-loop (Δ104) or mimicking its reduced state using alanine or serine substitutions of both Cys105 and Cys110 (C105A-C110A or C105S-C110S) (Suppl. Fig. S1). Both of the SbtB C105A-C110A and C105S-C110S variants were able to bind ATP with high affinity comparable to the oxidized WT-SbtB protein, while cAMP bound with a slightly lower affinity (Table 1). Notably, the binding of ADP and AMP were strongly impaired (Suppl. Fig. S1), yielding only very weak isotherm signals, for which the Kd values could not be calculated. Surprisingly, the truncated R-loop SbtB variant (Δ104) regained the ability to bind ADP and AMP and increased the binding affinity towards ATP as opposed to cAMP (Table 1). Those results show similarities to the nucleotide-binding properties of *Cyanobium* SbtB, which naturally lacks the R-loop (Kaczmarski *et al*., 2019). To further confirm those finding, we created a single Cys substitution to serine (C105S or C110S) or deletion of the last Cys110 (SbtB-Δ109) and determined their binding affinities with ITC. Again, all those single point mutation variants showed a reduced ADP and AMP binding and preference for ATP and cAMP (Table 1). These results provided strong evidence for the SbtB R-loop to be an element influencing the binding affinities of adenyl-charged nucleotides, such as ATP, ADP and AMP, but not cAMP, in addition to modulating the apyrase activity.

To further support our results, we solved the crystal structure of the SbtB C105S-C110S variant in a complex with cAMP (Fig. 1), confirming its ability to retain a high affinity to cAMP, indicating that the reduced state of SbtB does not influence the binding of cAMP. The crystal space group of the C105S-C110S variant in a complex with cAMP was $P4_{1,}$ similar to what was previously observed for the C105A-C110A variant in complex with ATP (PDB: 7R31), in which the R-loop was disordered (Selim *et al.,* 2023). In the structure of the SbtB C105S-C110S:cAMP complex, both T- and R-loops were disordered, resembling the *Anabaena variabilis* SbtB structure (PDB: 3DFE), showcasing a cAMP-binding mode almost identical to the previous structure of the

oxidized *Synechocystis* WT-SbtB (PDB: 5O3Q) (Selim *et al.,* 2018). Since the structure did not provide further insights, it was not regarded further.

***Table 1**: Dissociation constants (Kd) in (µM) for the adenyl nucleotides ATP, ADP, AMP, and cAMP to SbtB variants with exchanged cysteine residues (C105A-C110A, C105S-C110S, C105S, S110S) or truncated R-loop (Δ109, Δ104). UND: undetermined.*

	***SbtB* WT (oxidized)** (calculated from Selim *et al.*, 2018)		***SbtB*-C105A-C110A**		***SbtB*-C105S-C110S**		***SbtB*-C105S**		***SbtB*-C110S**		***SbtB*-Δ109**		***SbtB*-Δ104**	
	Binding	**K_d (µM)**	**Binding**	**K_d (µM)**	**Binding**	**K_d (µM)**	**Binding**	**K_d (µM)**	**binding**	**K_d (µM)**	**binding**	**K_d (µM)**	**Binding**	**K_d (µM)**
ATP	Binding	62.5 ± 16.6	Binding	29.8 ± 14.1	Binding	47.6 ± 21.3	Binding	40.5 ± 75.9	Binding	60.1 ± 6.7	Binding	32.5 ± 17.9	Binding	35.0 ±7.1
ADP	Binding	55.8 ± 7.7	very weak Binding	UND	very weak Binding	UND	very weak Binding	UND	very weak Binding	UND	very weak Binding	UND	Binding	79.2 ±55.1
AMP	Binding	87.4 ± 3.7	very weak Binding	UND	very weak Binding	UND	very weak Binding	UND	very weak Binding	UND	very weak Binding	UND	Binding	78.2 ±6.0
cAMP	Binding	30.3 ± 5.0	Binding	106 ± 42.4	Binding	52.8 ± 34.7	Binding	36.2 ± 46.8	Binding	53.2 ± 35.3	Binding	70.2 ± 28.9	Binding	68.1 ±10.1

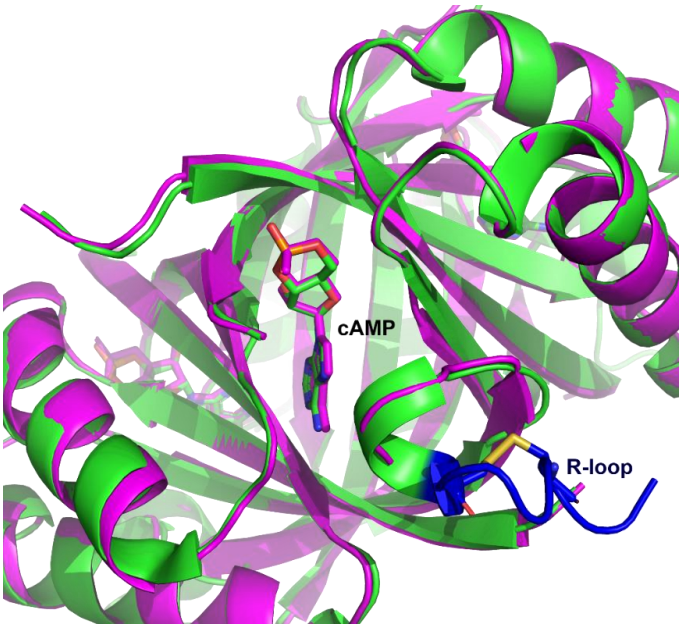

Figure 1**: **Reduced R-loop does not influence on cAMP binding. Alignment of oxidized *Synechocystis* WT-*SbtB*:cAMP (Green; PDB: 5O3Q) and *SbtB*-C105S-C110S:cAMP complex (Magenta) structures. cAMP molecules are visible in the middle of binding sites. The oxidized R-loop is highlighted in blue.

The R-loop functions as a redox sensor

As all point mutation variants behaved similarly in respect to their sensory properties, we focused our efforts to obtain *Synechocystis* R-loop mutants Δ*sbtB*::*sbtB*-C105A-C110A

(hereafter C105A-C110A), where the cysteines were replaced with alanine to simulate a permanent open structure of the reduced R-loop, and Δ*sbtB*::*sbtB*-Δ104 (hereafter Δ104), where the entire R-loop was truncated. To further investigate the physiological role of redox sensing by SbtB through its R-loop, different growth experiments were performed with the R-loop mutants compared to Δ*sbtB* mutant.

The growth of these strains was first compared under ambient CO_2 (0.04%, low C_i, LC) and continuous light (Fig. 2a). Under these conditions, no significant growth difference was observed between the strains with mutated R-loop compared to WT, whereas the mutant Δ*sbtB* showed slower growth, consistent with our earlier finding (Selim *et al.,* 2018). The growth rate of the strains under high CO_2 (5%, high C_i, HC) conditions and continuous light was measured as well (Suppl. Fig. S2), showing again no significant difference. The relevance of the redox-sensing R-loop became only apparent, when the *sbtB* mutants were exposed to diurnal cycles (12 h day/12 h night) under LC (Fig. 2b) as well as HC (Fig. 2c) conditions. In the diurnal cycle, the photosynthesis and CCM activity needs to be activated when light turns on and is switched off upon onset of darkness. Under LC conditions, all *sbtB* mutants demonstrated a significantly impaired growth, with the most heavily impacted being Δ*sbtB*, followed by Δ104 and C105A-C110A, demonstrating that not only the presence of SbtB but also the redox sensing of the R-loop is relevant for acclimation to the diurnal rhythm. While under HC conditions, the R-loop mutants showed a growth similar to WT, the lack of SbtB still caused slower growth. Those phenotypes are likely caused by the influence of SbtB on glycogen metabolism (Selim *et al.,* 2021, 2023), indicating that the regulatory functions of SbtB during the diurnal cycle are not limited to those mediated by the redox-sensitive R-loop.

To further investigate the redox-sensing capability of the R-loop, the growth of the *sbtB* mutants was studied under fluctuating light with periods of standard growth light (3 h 100 µmol photons m^{-2} s^{-1}) or high light (3 h 500 µmol photons m^{-2} s^{-1}) in LC conditions (Fig. 2d). The WT strain experienced an approximately two-fold higher growth rate in high light (HL) periods than standard light (SL) periods, whereas all *sbtB* mutants appeared to have lost the ability to adapt to fluctuating light intensity, showcasing similar growth rates between HL and LL periods, with the Δ*sbtB* mutant performing the worst.

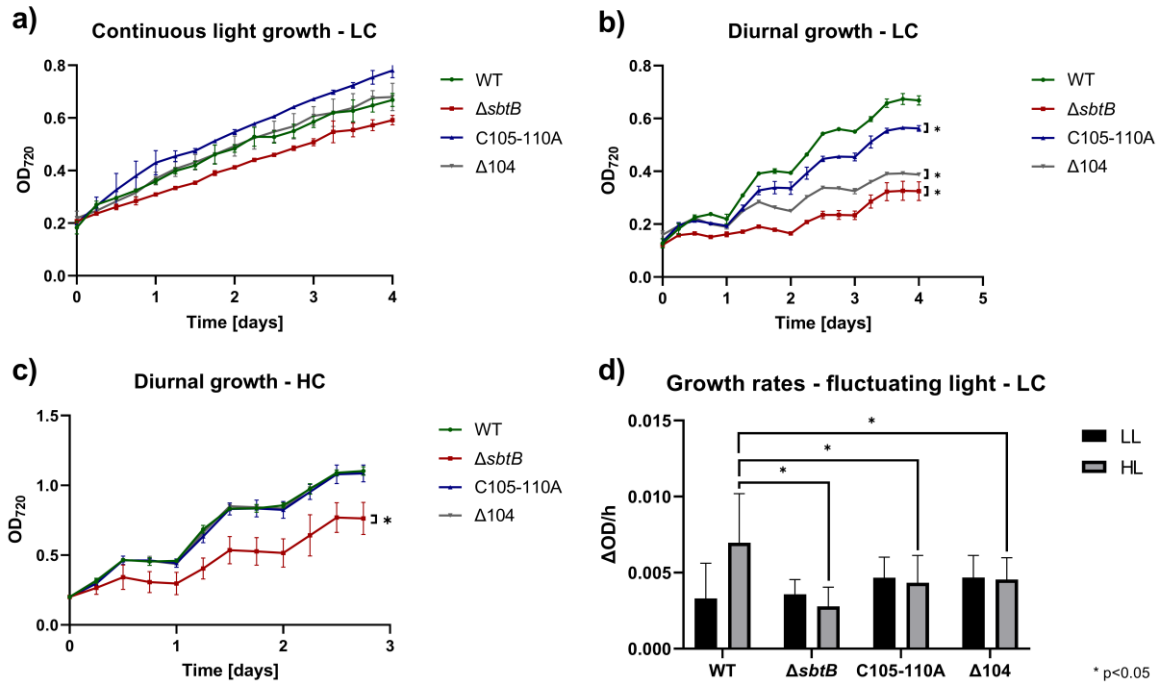

Figure 2: Impact of R-loop mutations on growth under different C_i and light conditions. Growth experiments using the *Synechocystis* WT strain and mutants Δ*sbtB*, C105A-C110A, Δ104 were performed in the Multicultivator MD1000. **a)** Growth under continuous light in LC conditions. **b)** growth in 12 h light, 12 h darkness diurnal rhythm under HC conditions. **c)** growth in 12 h light, 12 h darkness diurnal rhythm under LC conditions. **d)** Growth rates (ΔOD_{720}/h) under 6 cycles of fluctuating light conditions (LL: 3 h 100 µmol photons m^{-2} s^{-1}, HL: 3 h 500 µmol photons m^{-2} s^{-1}) at LC. Number of replicates (n) ≥ 3.

The R-loop barely affects glycogen turnover during diurnal rhythm under HC conditions

As previously observed (Selim *et al*., 2021, 2023), SbtB plays a direct role in controlling glycogen metabolism under diurnal conditions via interaction with the glycogen branching enzyme GlgB. The R-loop was also shown to be relevant in the interaction between SbtB and GlgB under LC conditions. To determine whether it is also important in the regulation of glycogen anabolism and/or catabolism under HC conditions, the glycogen concentrations in the cells of WT, Δ*sbtB* and R-loop mutant strains were determined during the light and dark phase of diurnal growth (Fig. 3).

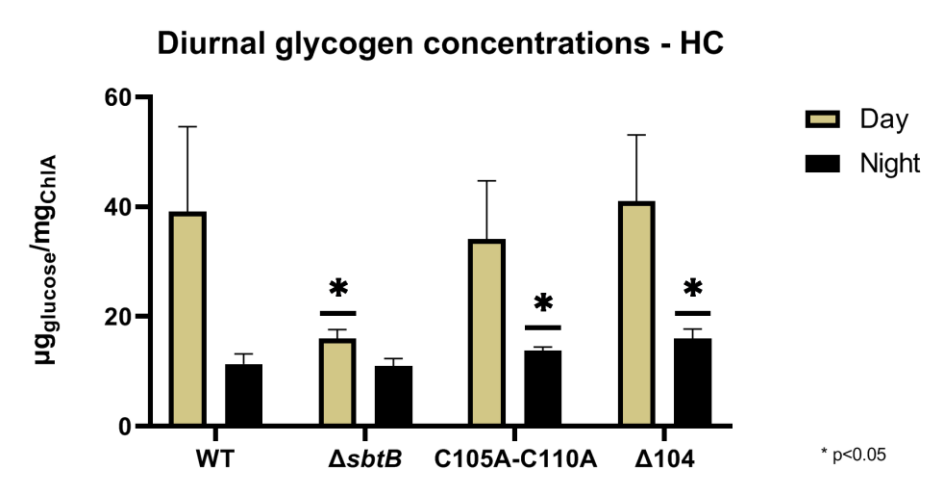

Figure 3**: **Effect of sbtB mutations on glycogen concentrations during diurnal rhythm and HC conditions. Glycogen concentration in the *Synechocystis* sp. PCC 6803 strains WT and mutants Δ*sbtB*, C105A-C110A and Δ104 were measured during growth under diurnal rhythm (12 h light, 12 h darkness). Samples were taken in the middle of the day (Yellow) or night (Black) phases. n = 6.

The knock-out of *sbtB* was once again confirmed to greatly impact glycogen metabolism, causing a more than two-fold decrease in the glycogen concentration during the day and almost no glycogen breakdown during the night when compared to WT. The R-loop modulation of SbtB also appears to be slightly involved in the regulation of glycogen metabolism under HC conditions. The mutants accumulated similar amounts of glycogen during the day as WT cells, implying that under HC conditions, the R-loop does not influence glycogen synthesis. Consistent with the ability of SbtB R-loop variants to interact with GlgB (Selim *et al.,* 2023). However, less glycogen was consumed during the night, as the two R-loop mutants showed slightly higher glycogen concentrations during the dark phase compared to the WT cells. These findings indicate that the R-loop mutants are moderately affected in the glycogen catabolism.

The R-loop influences the CCM activity

In addition to glycogen turnover, SbtB has been shown to heavily impact many parts of the CCM (Mantovani *et al*., 2022) and because of this, we have studied the effect of R-loop mutations on CCM activity by determining the bicarbonate-dependent oxygen evolution. To this end, the C_i-dependent photosynthetic activity of WT, Δ*sbtB*, C105A-C110A and Δ104 mutants was compared in cells acclimated to either HC or LC conditions. From the measured C_i/photosynthesis curves (Suppl. Fig. S3) the affinity to bicarbonate was calculated (Fig. 4).

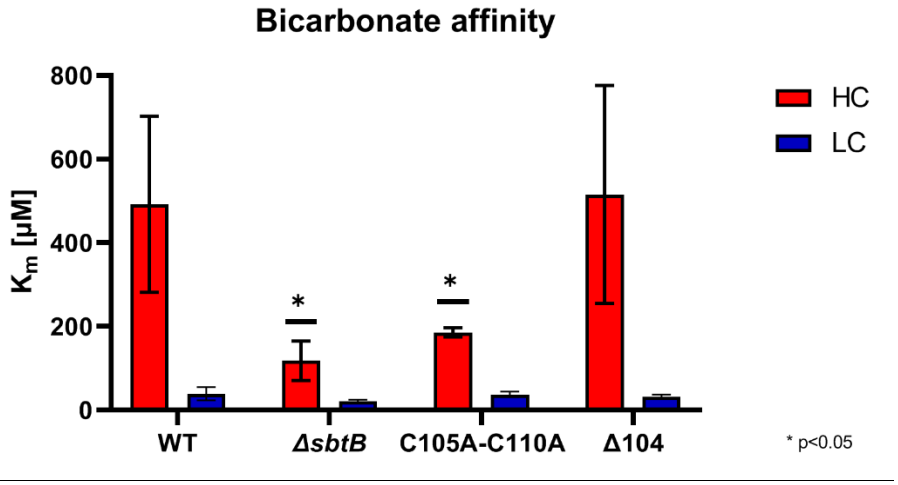

Figure 4**: **Impact of the sbtB R-loop mutations on CCM activity. Whole cell affinity to bicarbonate is expressed as average K_m values of µM bicarbonate of an oxygen evolution experiment using the *Synechocystis* strains WT, Δ*sbtB*, C105A-C110A, and Δ104. Cells were acclimated to either HC (Red) or LC (Blue) conditions. n ≥ 3.

As previously seen (Selim *et al.*, 2018; Mantovani *et al.*, 2022), the knocking-out of *sbtB* caused a significantly higher affinity to C_i under HC conditions, but comparable affinity under LC conditions. Surprisingly, the permanently open conformation mimicking the reduced state of the hairpin-loop in the C105A-C110A mutant caused a strong increase in the affinity to bicarbonate for HC-grown cultures, comparable to the Δ*sbtB* strain. Interestingly, the complete truncation of the R-loop (Δ104) reverted the bicarbonate affinity of HC cultures back to a WT-like state. Like the total absence of SbtB in the mutant Δ*sbtB*, changes in the R-loop had no significant impact on C_i affinity in cells acclimated to LC conditions.

The TrxA reduces SbtB R-loop and thereby influencing the affinity of SbtB to SbtA

The discovery of the R-loop playing a role in the affinity of SbtB to second messengers caused us to re-evaluate the membrane association of SbtB under LC conditions as previously done for the native SbtB (Selim *et al.*, 2018). According to the results shown in Table 1, ADP and AMP are not bound to SbtB when the R-loop is reduced, for example during the day. This observation might indicate that the observed association of SbtB to SbtA under LC conditions could be affected by the oxidation of the R-loop.

We previously suggested that SbtB R-loop is reduced through an interaction with the thioredoxin TrxA (Selim *et al.,* 2023), therefore we first determined the ability of TrxA to reduce SbtB through mass spectrometry (MS). Using a C-terminal Strep-tagged SbtB variant, intact protein MS analysis indicates that recombinant *Synechocystis* TrxA reduces SbtB, with a calculated mass of 13065.59 Da, compared to the oxidized SbtB with mass of 13063.55 Da (Fig. 5 and Suppl. Fig. S4). However, incubation of SbtB with the reducing agent DTT (5 mM) only led to a partial reduction of SbtB, suggesting that the C-terminal Strep-tag could provide

extra protection for the R-loop. The experiment was therefore repeated using an N-terminal Strep-tagged SbtB variant, in which 5 mM DTT was able to efficiently reduce SbtB completely with a mass of 13912.86 Da compared to the oxidized SbtB with 13910.86 Da. To further confirm those results and determine the degree of SbtB reduction, we performed an Urea-PAGE experiment as described previously (Ibrahim *et al*., 2022). Incubation of equimolar concentrations of SbtB with DTT or TrxA in presence or absence of 5 mM DTT led to the appearance of a band shift towards the reduced state of SbtB. However, at lower DTT concentrations (0.5 mM), DTT alone was not able to reduce SbtB completely (Suppl. Fig. S5). These results further suggest the ability of TrxA to reduce SbtB more efficiently than other tested reducing agents. Collectively, these results imply firstly that TrxA is able to efficiently reduce SbtB even if the R-loop is protected, and secondly that *in vivo,* the native untagged SbtB would be more prone to reduction in response to the fluctuation of the redox state of the cell. Notably, similarly to SbtB, TrxA responds to the fluctuation of redox and diurnal state of the cell (Pérez-Pérez *et al*., 2009).

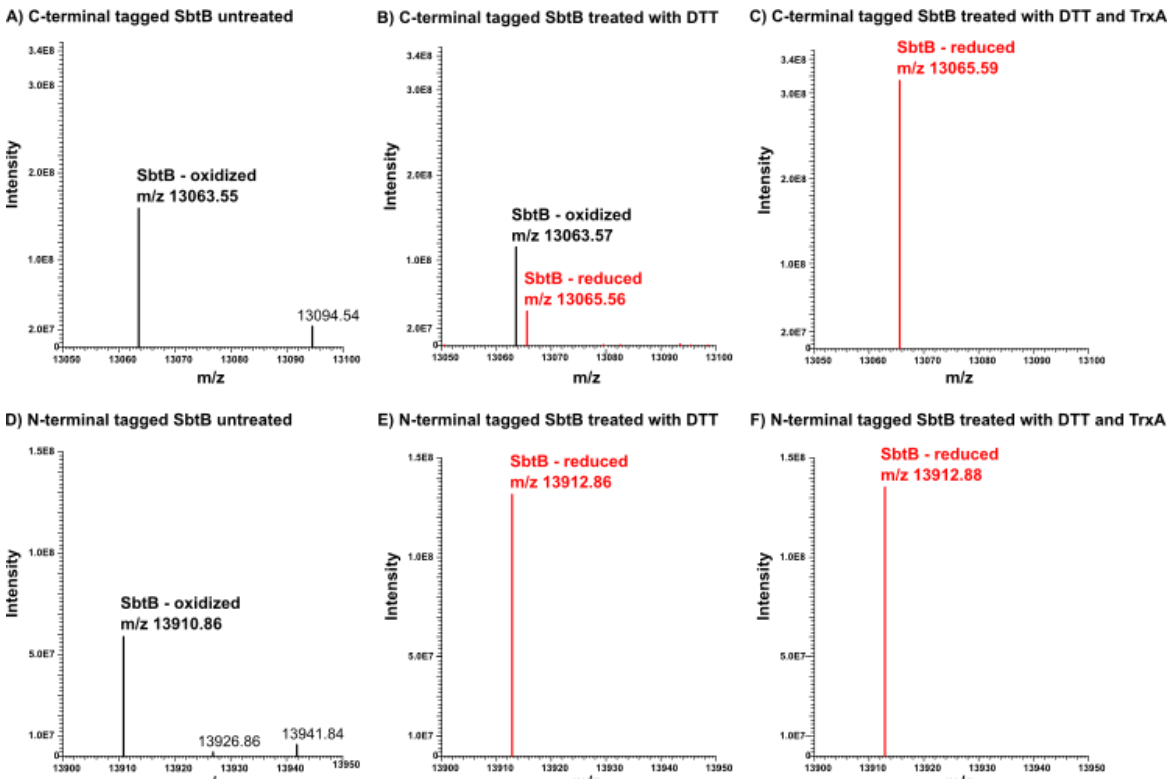

Figure 5*: *Intact protein mass spectrometry analysis indicating the redox status of* Synechocystis *SbtB without and after addition of reducing agents DTT and TrxA. Deconvoluted mass spectra of C-terminally (A-C) or N-terminally (D-F) tagged SbtB, either untreated (A, D), treated with 5 mM DTT (B, E), or with equimolar amounts of TrxA (C, F). Formation of a disulfide bond is labeled as "oxidized" and depicted in black. Reduction of the disulfide bond was observed as a mass shift by two protons (2 Da; depicted in red). C-terminal tagged SbtB treated with DTT was found in both redox states in the measurement displayed in Figure 5B (also shown in Figure S4).

Thereafter, to investigate the membrane association of SbtB in *Synechocystis*, cell extracts of WT samples after treatment either with 5 mM DTT or with equimolar TrxA (Fig. 6a), were subjected to immune-blotting using specific α-SbtB antibody. To this end, soluble and membrane fractions were compared to estimate the relative SbtB amounts in these fractions under oxidized or reduced conditions (Fig. 6b).

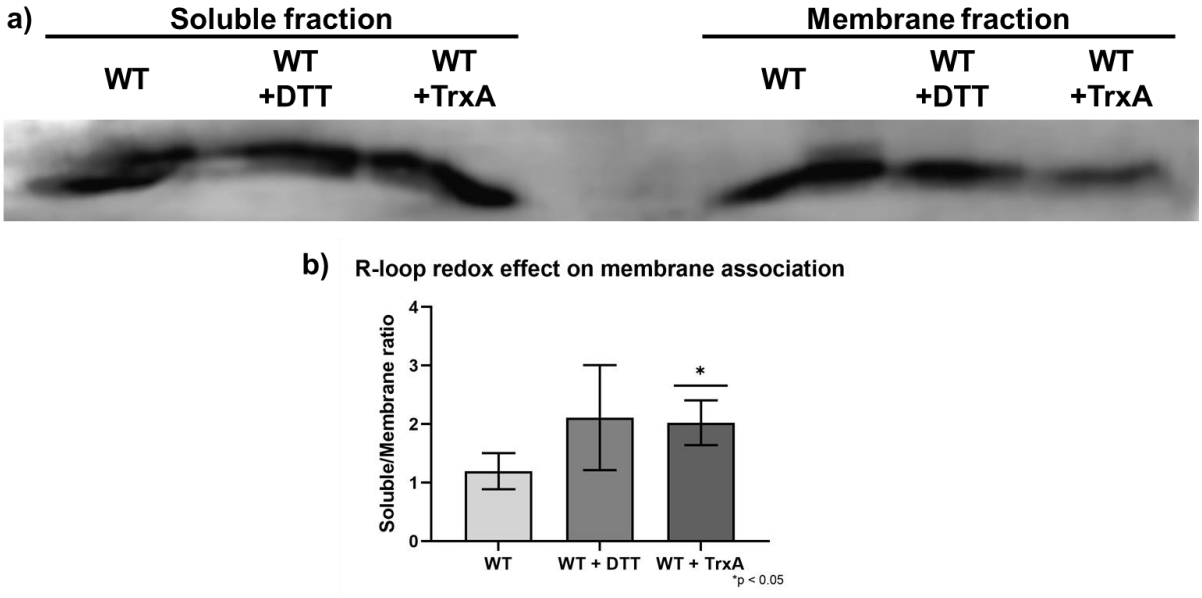

***Figure 6**: **Impact of the redox state of SbtB on membrane association in* Synechocystis.** The membrane association of SbtB was determined by immune-blotting using an anti-SbtB antibody in two experiments in which soluble and membrane fractions were separated by high speed centrifugation. **a)** Immuno-blot of membrane (M) and soluble (S) fractions of WT cells from LC conditions, either untreated, or incubated with either 5 mM DTT or equimolar TrxA. **b)** Ratio of relative membrane-associated SbtB to soluble in WT samples from immuno-blots shown in panel a). n = 3.

These experiments revealed that the treatment of the cell extracts with either DTT and especially TrxA caused a significant decrease in the amount of SbtB associated to the membrane, compared to the untreated samples. The difference was more pronounced in the TrxA-treated samples, showing once more its role in the reduction of SbtB. This result suggests that under oxidizing conditions, the membrane association of SbtB is clearly promoted, as the affinity of SbtB towards AMP would increase and induction of its apyrase activity, which altogether promote the membrane localization to SbtA.

Truncation of R-loop affects the function of SbtB as a plug for SbtA

Finally, as highlighted by Haffner *et al*., 2023, the interaction of SbtB with SbtA is not limited to the regulation of SbtA-mediated bicarbonate uptake, but presents more complex regulatory functions, such as plugging SbtA to prevent the leakage of bicarbonate when the CCM is not

active. After discovering that mutations in the R-loop impact the affinity to adenyl nucleotides and/or the association of SbtB to the membrane, a C_i leakage experiment using ^{14}C-labelled bicarbonate was performed (Fig. 7) to determine the influence of the R-loop of SbtB and the redox-state of the cell on the plug function of SbtB.

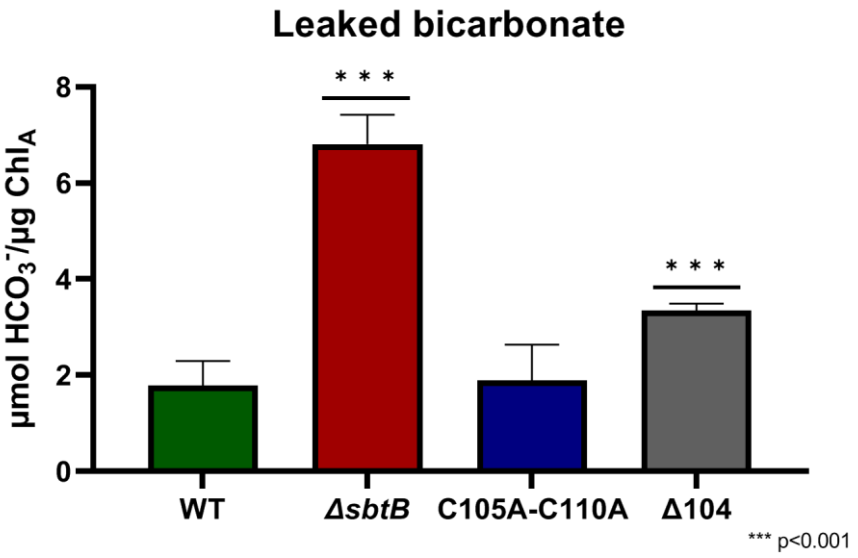

***Figure 7: Role of the R-loop on the plug function of SbtB in* Synechocystis.** Concentration of radio-labelled bicarbonate per amount of Chlorophyll A leaked from cells of strains WT, Δ*sbtB*, C105A-C110A and Δ104 strains is shown. n ≥ 6.

The experiment revealed, as seen before (Haffner *et al*., 2023), that the absence of SbtB causes a significantly higher amount of bicarbonate to be leaked during the dark incubation. The C105A-C110A mutation did not affect the leakage, whereas truncation of the R-loop in the Δ104 mutant caused a significantly increased leakage, albeit still almost two-fold inferior to what the knocking-out of *sbtB* caused.

Discussion

During the last years, our and other groups provided evidence that the SbtB protein plays important roles in the regulation of the CCM and other aspects of the acclimation of the carbon metabolism to changing C_i amounts among cyanobacteria (reviewed in Mantovani *et al*., 2023). The structural investigations of SbtB (Selim *et al*., 2018, 2021, 2023; Kaczmarski *et al*., 2019) and the super-complex of SbtB with SbtA (Fang *et al*., 2021; Liu *et al*., 2021) showed that SbtB harbours different domains, which fulfil specific tasks in binding of adenyl nucleotides, interaction with the bicarbonate transporter SbtA, and redox sensing. The latter function is attributed to the R-loop, which harbours two redox-sensitive cysteine residues. A bioinformatic investigation of 460 different cyanobacterial SbtBs (Suppl. Fig. S6) revealed that the R-loop is

present in roughly 50% of all SbtBs, with a high degree of conservation. It always contains the two conserved cysteines, which can form a disulphide bridge under oxidative conditions that significantly impacts the apyrase activity of SbtB (Selim *et al*., 2018, 2023).

To reveal the physiological roles of the R-loop of SbtB in cyanobacterial cells, we investigated the Δ*sbtB*, C105A-C110A and Δ104 mutants of the model cyanobacterium *Synechocystis*. The likely role of the R-loop as a redox-responsive module, agrees with the general impact of SbtB mutations on the general physiology of *Synechocystis* during acclimation to different light and C_i regimes, which are known to impact the cellular redox homeostasis in cyanobacteria as in eukaryotic phototrophs. Our results imply an important role of the R-loop in the regulation of the CCM during diurnal growth and moreover, under conditions of fluctuating light intensities. These phenotypic alterations were more pronounced, when cells were grown under LC conditions, when the CCM is more highly induced and active (Mantovani *et al*., 2022). The observed effect of the R-loop on glycogen synthesis under LC conditions (Seilm *et al*., 2023) could at least partially explain the observed growth phenotypes for the mutants, while measurement of glycogen concentrations during diurnal rhythm under HC conditions shows that the R-loop appears to play a more moderate role in the regulation of glycogen catabolism.

An oxygen evolution experiment provided insight into the role of the R-loop on SbtB's regulation of the CCM as a whole under constant conditions, revealing that the open conformation in the C105A-C110A mutants caused a Δ*sbtB*-like phenotype (Selim *et al*., 2018; Mantovani *et al*., 2022), with significantly higher affinity to C_i for cultures acclimated to HC conditions. Surprisingly, the truncation of the R-loop in the Δ104 mutant caused the phenotype to revert to a WT-like state. This phenotype correlates with the loss of affinity of the SbtB variant C105A-C110A towards ADP and AMP, as the greatly reduced binding of the nucleotides would strongly impact the functionality of SbtB on the regulation of SbtA (Liu *et al*., 2021; Fang *et al*., 2021) and the CCM (Mantovani *et al*., 2022)., This is further supported by the study of the truncated R-loop SbtB mutant, which displayed nucleotide affinities reverting to a WT-like state similar to those cyanobacteria that possess an SbtB without an R-loop, such as *Cyanobium* sp. PCC 7001 (Kaczmarski *et al*., 2019), with ATP showcasing the highest binding affinity, instead of cAMP as is the case for *Synechocystis*. Oxidation of the R-loop with consequent generation of the SbtB-AMP state, that stimulates binding to SbtA, might promote the membrane associated state of SbtB. In agreement, we found diminished amounts of membrane-bound SbtB after treatment with reducing agents, especially TrxA that very efficiently can convert the oxidized R-loop in the open reduced conformation *in vitro*. Thereafter, the role of the R-loop on the activity of SbtB as a plug for SbtA to prevent back-flow of bicarbonate outside the cells (Haffner *et al*., 2023) was investigated. Contrary to expectations, the open reduced R-loop conformation in mutant C105A-C110A did not seem to

influence the leakage of bicarbonate, but its truncation caused more bicarbonate to flow out of the cells possibly due to its smaller plug size. This result suggests that while the binding of the different adenyl nucleotides is more relevant for the general regulatory properties of SbtB on the CCM, in regard to its ability to plug SbtA, either the steric encumbrance is more relevant, or a still undiscovered regulation of SbtB comes into play.

Altogether, it seems that R-loop is an extra element acquired during the evolution of SbtB to fine tune the nucleotide-binding affinity and to modulate the SbtB apyrase activity. The physiological meaning behind this regulation would be, during the day, for SbtB to always be in a reduced state and respond to fluctuation of C_i levels. Under LC, the increase in AMP levels could drive partial localization of SbtB to SbtA to prevent the back-flow of accumulated HCO_3^- (Selim *et al.,* 2018; Haffner *et al.,* 2023), while under HC conditions SbtB would remain localized in the cytoplasm. However, the system appears to also possess a “stand-by” state, where once it gets oxidized by sudden light changes, for example, the apyrase activity would promote the SbtA-B complex formation. On the other hand, the SbtB variants lacking the R-loop would only respond to changes in the adenylate charge, with drops in the adenylate charge, for example during the night, shifting the equilibrium towards the SbtA-B complex. In agreement with this proposal, a recent study showed that the cyanobacterial SbtB proteins, lacking the R-loop, are responding mainly to energy state of the cell (Förster *et al*., 2023). Therefore, the R loop addition made SbtB more versatile to integrate cellular energy and redox state than the basal SbtB without R-loop.

From our structural and ITC analysis of different R-loop variants, it also became obvious that the R-loop does not influence at all cAMP binding, but is only needed to fine tune the ADP/AMP affinity and regulate hydrolysis of ATP/ADP. Overall, this study provided evidence that the R-loop of SbtB, provides an additional layer of regulation to the protein, which allows a finer regulation of the CCM in coordination with the entire photosynthetic Ci fixation for further adaptability to fluctuating conditions.

Acknowledgments

We thank Klaudia Michl (University of Rostock) and Heinz Grenzendorf (Tübingen University) for technical assistance in strain cultivation and samples preparation. The authors are also grateful to Reinhard Albrecht and Marcus Hartmann (Max Planck Institute for Biology, Tübingen) for crystallographic sample preparation and assistance with diffraction data collection, the staff of SLS beamline, and to Heike Brötz-Oesterhelt for facilitating the ITC usage.

Funding information

The project was funded by grants from the German Research Foundation (DFG) as part of the priority research program (SPP1879) to MHagemann (HA 2002/24-1) and to KF (Fo195/18-1), and by the Federal Ministry of Education and Research (BMBF) and the Baden-Württemberg Ministry of Science as part of the Excellence Strategy of the German Federal and State Governments to KAS (Projektförderung: PRO-SELIM-2022-14). LC-MS/MS systems at the Department of Plant Physiology were supported through the German Research Foundation (DFG) grant No. INST 264/125-1 FUGG). The infrastructural support by the Cluster of Excellence “Controlling Microbes to Fight Infections” (EXC 2124–390838134) of the DFG to DP, KF and KAS, and through the and exploratory research grant through the DFG collaborative research center "CellMap” (TRR 261) to DP.

Author contributions

OM, MaH and KAS designed the study; OM performed the growth, glycogen, membrane association and leakage experiments; PW determined bicarbonate affinity; KAS created all recombinant proteins used in this study and performed crystallographic and ITC analysis with AE; BW, DP and MiH performed SbtB-TrxA reduction experiments. KAS, KF and MaH supervised experiments and evaluated data. OM, MaH and KAS wrote the manuscript with the input from all authors.

References

Du J, Förster B, Rourke L, Howitt SM, Price GD 2014. Characterisation of cyanobacterial bicarbonate transporters in *E. coli* shows that SbtA homologs are functional in this heterologous expression system. *PLoS One* **9**: e115905. doi: 10.1371/journal.pone.0115905.

Fang S, Huang X, Zhang X, Zhang M, Hao Y, Guo H, Liu LN, Yu F, Zhang P 2021. Molecular mechanism underlying transport and allosteric inhibition of bicarbonate transporter SbtA. *Proceedings of the National Academy of Sciences USA* **118**: e2101632118.

Fellers RT, Greer JB, Early BP, Yu X, LeDuc RD, Kelleher NL, Thomas PM 2015. ProSight lite: graphical software to analyze top-down mass spectrometry data. *Proteomics*.;15(7):1235–1238. doi: 10.1002/pmic.201570050

Forchhammer K, Lüddecke J 2016. Sensory properties of the PII signalling protein family. *FEBS Journal* **283**: 425-437.

Forchhammer K, Selim KA, Huergo LF. 2022. New views on PII signaling: from nitrogen sensing to global metabolic control. *Trends in Microbiology* **30**: 722-735.

Forchhammer K, Selim KA. **2020.** Carbon/nitrogen homeostasis control in cyanobacteria. *FEMS Microbiology Reviews* **44**: 33-53.

Förster B, Mukherjee B, Rourke LM, Kaczmarski JA, Jackson CJ, Price GD 2023. Adenylnucleotide-mediated binding of the PII-like protein SbtB contributes to controlling activity of the cyanobacterial bicarbonate transporter SbtA *eLife* **12**: RP88488

Foyer CH, Noctor G 2009. Redox regulation in photosynthetic organisms: signaling, acclimation, and practical implications. *Antioxidants and Redox Signalling; Mary Ann Liebert* **11**: 861-905. doi: 10.1089/ars.2008.2177. PMID: 19239350.

Haffner M, Hou WT, Mantovani O, Walke PR, Hauf K, Liu XY, Borisova M, Hagemann M, Zhou CZ, Forchhammer K, Selim KA. 2023. Binding of adenyl nucleotides allows PII superfamily signaling proteins to act as a valve plug to control bicarbonate and ammonia homeostasis among different bacterial phyla. *Bioarchives*

Hagemann M, Kern R, Maurino VG, Hanson DT, Weber APM, Sage RF, Bauwe H. 2016. Evolution of photorespiration from cyanobacteria to land plants considering protein phylogenies and acquisition of carbon concentrating mechanisms. *Journal of Experimental Botany* **67:** 2963-2976.

Hagemann M, Song S, Brouwer EM. 2021. Inorganic carbon assimilation in cyanobacteria: Mechanisms, regulation, and engineering. In Hudson P, Lee SY, Nielsen J (eds.) *Cyanobacteria Biotechnology, Wiley-Blackwell Biotechnology Series*, Chapter 1, 1-31.

Ibrahim IM, Rowden SJL, Cramer WA, Howe CJ, Puthiyaveetil S 2022. Thiol redox switches regulate the oligomeric state of cyanobacterial Rre1, RpaA and RpaB response regulators. *FEBS Letters* **596**: 1533-1543. doi: 10.1002/1873-3468.14340.

Kaczmarski JA, Hong NS, Mukherjee B, Wey LT, Rourke L, Förster B, Peat TS, Price GD, and Jackson CJ 2019. Structural Basis for the Allosteric Regulation of the SbtA Bicarbonate Transporter by the PII-like Protein, SbtB, from *Cyanobium* sp. PCC7001 *Biochemistry* **58**: 5030-5039 DOI: 10.1021/acs.biochem.9b00880

Köbler C, Schultz S-J, Kopp D, Voigt K. and Wilde A. 2018. The role of the Synechocystis sp. PCC 6803 homolog of the circadian clock output regulator RpaA in day–night transitions. *Molecular Microbiology*; 110: 847-861. https://doi.org/10.1111/mmi.14129

Lapina T, Selim KA, Forchhammer K. and Ermilova E. 2018. The PII signaling protein from red algae represents an evolutionary link between cyanobacterial and Chloroplastida PII proteins. *Scientific Reports* 8, 790. https://doi.org/10.1038/s41598-017-19046-7

Liu XY, Hou WT, Wang L, Li B, Chen Y, Chen Y, Jiang YL, Zhou CZ 2021. Structures of cyanobacterial bicarbonate transporter SbtA and its complex with PII-like SbtB. *Cell Discovery*; **7**: 63. doi: 10.1038/s41421-021-00287-w.

Lucius S, Makowka A, Michl K, Gutekunst K, Hagemann M 2021. The Entner-Doudoroff pathway contributes to glycogen breakdown during high to low CO_2 shifts in the cyanobacterium *Synechocystis* sp. PCC 6803. *Frontiers in Plant Science* **12:** 787943. doi: 10.3389/fpls.2021.787943.

Mantovani O, Reimann V, Haffner M, Herrmann FP, Selim KA, Forchhammer K, Hess WR, Hagemann M 2022. The impact of the cyanobacterial carbon-regulator protein SbtB and of the second messengers cAMP and c-di-AMP on CO_2-dependent gene expression. *New Phytologist* **234:** 1801-1816. doi: 10.1111/nph.18094.

Mantovani O, Haffner M, Selim KA, Hagemann M, Forchhammer K 2023. Roles of second messengers in the regulation of cyanobacterial physiology: the carbon-concentrating mechanism and beyond *Microlife* 4: uqad008. doi: 10.1093/femsml/uqad008.

McFarlane CR, Shah NR, Kabasakal BV, Echeverria B, Cotton CAR, Bubeck D, Murray JW 2019. Structural basis of light-induced redox regulation in the Calvin-Benson cycle in cyanobacteria. *Proceedings of the National Academy of Sciences* USA **116:** 20984-20990. doi: 10.1073/pnas.1906722116.

Pérez-Pérez ME, Martín-Figueroa E, Florencio FJ 2009. Photosynthetic regulation of the cyanobacterium Synechocystis sp. PCC 6803 thioredoxin system and functional analysis of TrxB (Trx x) and TrxQ (Trx y) thioredoxins. *Molecular Plant* **2:** 270-283. doi: 10.1093/mp/ssn070.

Rae BD, Long BM, Badger MR, Price GD. 2013. Functions. compositions. and evolution of the two types of carboxysomes: polyhedral microcompartments that facilitate CO_2 fixation in cyanobacteria and some proteobacteria. *Microbiology Molecular Biology Reviews* **77:** 357-379.

Raven JA, Beardall J, Sánchez-Baracaldo P. 2017. The possible evolution and future of CO2- concentrating mechanisms. *Journal of Experimental Botany* **68**: 3701–3716.

Rippka R, Deruelles J, Waterbury JB, Herdman M, Stanier RY. 1979. Generic assignments. strain histories and properties of pure cultures of cyanobacteria. *Journal of General Microbiology* **111:** 1-61.

Selim KA, Haase F, Hartmann MD, Hagemann M, Forchhammer K. 2018. PII-like signaling protein SbtB links cAMP sensing with cyanobacterial inorganic carbon response. *Proceedings of the National Academy of Sciences USA* **115:** E4861-E4869.

Selim KA, Haffner M, Burkhardt M, Mantovani O, Neumann N, Albrecht R, Seifert R, Krüger L, Stülke J, Hartmann MD, Hagemann M, Forchhammer K 2021. Diurnal metabolic control in cyanobacteria requires perception of second messenger signaling molecule c-di-AMP by the carbon control protein SbtB. *Science Advances* **7**: eabk0568.

Selim KA, Haffner M, Mantovani O, Albrecht R, Zhu H, Hagemann M, Forchhammer K, Hartmann MD 2023. Carbon signaling protein SbtB possesses atypical redox-regulated apyrase activity to facilitate regulation of bicarbonate transporter SbtA. *Proceedings of the National Academy of Sciences USA* **120**: e2205882120. doi: 10.1073/pnas.2205882120.

Selim KA, Haffner M, Watzer B, Forchhammer K 2019. Tuning the in vitro sensing and signaling properties of cyanobacterial PII protein by mutation of key residues. *Scientific Reports* 9, 18985. https://doi.org/10.1038/s41598-019-55495-y

Selim KA, Lapina T, Forchhammer K, Ermilova E 2020. Interaction of N-acetyl-l-glutamate kinase with the PII signal transducer in the non-photosynthetic alga Polytomella parva: Co-evolution towards a hetero-oligomeric enzyme. *FEBS Journal* **287**: 465-482. doi: 10.1111/febs.14989.

PII signal transduction superfamily acts as a valve plug to control bicarbonate and ammonia homeostasis among different bacterial phyla.

***Haffner M, *Hou WT, *Mantovani O,** Walke PR, Hauf K, Liu XY, Borisova M, Hagemann M, Zhou CZ, Karl Forchhammer, Khaled A. Selim 2023**.** *Bioarchives*

* First authors

PII signal transduction superfamily acts as a valve plug to control bicarbonate and ammonia homeostasis among different bacterial phyla

Authors: Michael Haffner[1,#], Wen-Tao Hou[2,#], Oliver Mantovani[3,#], Peter R. Walke[3], Ksenia Hauf[1], Marina Borisova[1], Martin Hagemann[3], Cong-Zhao Zhou[2], Karl Forchhammer[1,*], Khaled A. Selim[1,*]

[1] Interfaculty Institute for Microbiology and Infection Medicine, Organismic Interactions Department, Cluster of Excellence 'Controlling Microbes to Fight Infections', Tübingen University, Auf der Morgenstelle 28, 72076 Tübingen, Germany

[2] Division of Life Sciences and Medicine, University of Science and Technology of China, Hefei, Anhui, China.

[3] Plant Physiology Department, Institute of Biological Sciences, Rostock University, 18059 Rostock, Germany

[#] Shared first authors (those authors contributed equally)

[*] Corresponding authors: K Forchhammer (karl.forchhammer@uni-tuebingen.de) & KA Selim (khaled.selim@uni-tuebingen.de)

Abstract

Life on Earth relies on carbon and nitrogen assimilation by RubisCO and GS-GOGAT enzymes, respectively, whose activities depend on a constant supply of inorganic carbon (C_i) and nitrogen (N). Members of the PII signal transduction superfamily are among the most ancient and widespread cell signaling proteins in nature. One of their most highly conserved functions is controlling C_i- and N-transporters, a feature found in different phyla of the Archaea and in both Gram-positive and Gram-negative bacteria. Recently, we identified the PII-like protein SbtB as C_i-sensing module, mainly controlling the HCO_3^- transporter SbtA in cyanobacteria. Similar to canonical PII proteins, SbtB is able to bind the adenine nucleotides ATP and ADP. Unlike those, it also binds AMP and preferentially binds the second messenger cAMP and c-di-AMP. The functional significance of the binding of different adenyl-nucleotides to SbtB has remained elusive, particularly in the context of the interaction of SbtB with SbtA. By a combination of structural, biochemical and physiological analysis, we revealed that by binding to SbtA, SbtB acts as unidirectional valve, preventing the reverse transport of intracellular enriched bicarbonate. This mechanistic principle holds true for the PII protein from *Bacillus* acting on the ammonium transporter AmtB, suggesting an evolutionary conserved role for PII superfamily proteins in controlling unidirectional flow of different transporters.

Keywords: Cyanobacteria; *Bacillus subtilis*; Carbon concentrating mechanisms; PII signaling superfamily; bicarbonate transporter SbtA; Ammonium transporter AmtB

Introduction

The PII signaling superfamily comprises the most ancient and widespread signal transduction proteins found in all domains of life (Forchhammer et al. 2022; Wheatley et al. 2016; Selim et al. 2018, 2021). The well-studied canonical PII proteins, which are involved in the regulation of carbon/nitrogen homeostasis, are characterized by a highly conserved trimeric structure with ferredoxin-like fold (Forchhammer & Selim 2020; Selim et al. 2020). Despite the similar 3D structures, PII-like proteins show restricted amino acid sequence conservation and evolved to fulfill diverse, yet not completely understood cellular functions.

Cyanobacteria are oxygenic phototrophs that assimilate CO_2 into organic compounds using water and light energy. For efficient CO_2 fixation, cyanobacteria evolved an efficient carbon concentrating mechanism (CCM) that employs high affinity inorganic carbon (C_i; referring to CO_2 and HCO_3^-) uptake systems to augment intracellular C_i levels (Forchhammer & Selim 2020; Hagemann et al. 2021). The sodium-dependent bicarbonate transporter SbtA is an important component of the cyanobacterial CCM and becomes highly expressed under C_i limitation from the *sbtA-sbtB* operon, which also encodes the conserved PII-like protein SbtB (Mantovani et al. 2022). Similar to canonical PII proteins, SbtB is able to bind the adenine nucleotides ATP and ADP, but unlike those, it also binds AMP. Moreover, SbtB preferentially binds the second messengers cAMP (Selim et al. 2018), which is known as carbon-status indicator (Chen et al. 2000; Steegborn et al. 2005), and c-di-AMP, which is involved in global cellular homeostasis (Selim et al. 2021; Mantovani et al. 2022, 2023).

Detailed structural characterization of various cyanobacterial SbtB homologues showed that they display typical PII-protein characteristics, being homo-trimeric proteins with three characteristic loop regions (T-, B- and C-loops) (Selim et al. 2018, 2021, 2023; Kaczmarski et al. 2019). These loop regions are located near the inter-subunit clefts and play a major role in ligand binding and intramolecular signaling. Intriguingly, the structures of *Synechocystis* SbtB:AMP (PDB: 5O3R) and SbtB:cAMP (PDB: 5ORQ) complexes did not reveal any conformational changes on the flexible surface-exposed T-loop, the protein interaction module of PII superfamily proteins that usually responds to effector molecule binding. Another striking feature of many SbtB proteins, including *Synechocystis* SbtB (hereafter *Sc*SbtB), is a C-terminal extension (referred to as R-loop) with a conserved C_{105}GPxGC_{110} motif to which we ascribed a redox-regulatory function due to a disulfide bond formation between C_{105} and C_{110} (Selim et al. 2023).

In summary, we revealed that *Sc*SbtB acts as C_i-sensor module by integrating the energy/redox-state of the cell and second messengers cAMP and c-di-AMP, and thereby it

plays a central role in the regulation of the entire CCM, similar to the role of the canonical PII protein in controlling carbon/nitrogen balance in central metabolism (Forchhammer et al. 2022; Selim et al. 2018, 2021; Mantovani et al. 2022). While the evolutionary conserved role of cAMP/AMP as indicators of cellular carbon status is well understood (Steegborn et al. 2005; Selim et al. 2018; Fang et al. 2021), the specific function of ATP/ADP adenyl-nucleotide binding to SbtB has remained unresolved. Several studies assigned SbtB to the regulation of SbtA through direct protein-protein interaction (Du et al. 2014; Selim et al. 2018, 2023; Liu et al. 2021), in analogy to the canonical PII member GlnK-mediated inhibition of the ammonium transporter AmtB in Gram-negative bacteria under nitrogen excess conditions to prevent an over-accumulation of ammonium (Conroy et al. 2007; Gruswitz et al. 2007; Boogerd et al. 2011; Forchhammer et al. 2022). Recently, we showed that SbtB displays an unusual slow ATP/ADP apyrase (diphosphohydrolase) activity that is controlled by the C-terminal R-loop in response to the redox-state of the cell (Selim et al. 2023). The SbtB apyrase activity leads to a conformational change in the surface-exposed T-loop, hence the ATP/ADP binding could act as a molecular switch that drives a conformational change in the T-loops. Although its physiological role has remained obscure, the redox-regulated apyrase activity of SbtB may link the photosynthetic electron transport to the regulation of SbtA mediated bicarbonate transport.

Recently, we and others solved the structures of SbtA and SbtA:SbtB complex (Fang et al. 2021; Liu et al. 2021). We showed that SbtA is a secondary-active transporter and operates by an elevator-type mechanism, with alternating outward and inward open substrate transport sites (Liu et al. 2021). Furthermore, these studies revealed symmetric binding of the trimeric SbtB to a trimeric SbtA. In the SbtA:SbtB complex, the SbtB T-loops lock SbtA in the inward-facing state, thereby assumed to inhibit the SbtA bicarbonate transporter activity (Fang et al. 2021). This strongly implies that SbtB exerts a direct regulatory function on SbtA in response to the metabolic state of the cell through binding to various adenine nucleotides, which may induce conformational changes in the SbtA-interacting T-loop in analogy to canonical PII proteins (Forchhammer & Selim 2020; Forchhammer et al. 2022). In fact, it was demonstrated that the conformation of the T-loop in the SbtA:SbtB complex is favored by AMP binding but is sterically incompatible with cAMP binding (Selim et al. 2018, 2023; Fang et al. 2021). The conclusion of an inhibitory SbtA:SbtB complex is, however, in conflict with the fact that the complex forms when high bicarbonate uptake activity is required. It also conflicts with the phenotype of Δ*sbtB* deficient mutants, which showed growth impairment under low C_i supply (Selim et al. 2018), suggesting that SbtB is indeed required for efficient C_i uptake.

Deeper insights in the mechanism, how SbtB affects the SbtA transporter can be obtained by

comparing different snapshots from recent structural studies (Fang et al., 2021; Liu et al. 2021). In absence of AMP, SbtB is still able to interact with SbtA in the cytoplasmic inward-facing state, although the SbtB T-loop was disordered (PDB: 7EGL). In this the structure, the HCO_3^- substrate was clearly defined toward the cytoplasm (Fang et al. 2021). We also revealed that the SbtB in the AMP state induces the cytoplasmic inward-open conformation of SbtA by separating the SbtA core-domain from the gate-domain, where the structured SbtB T-loop only partially locks the HCO_3^- exit tunnel of SbtA, leaving SbtA in an inward-open conformation (PBD: 7CYF) (Liu et al. 2021). This implies that SbtB within the SbtA:SbtB complex remains in dynamic to regulate the SbtA transport activity in response to the concentrations of intracellular adenyl-nucleotides and the redox-state of the cell. Another important aspect, so far not considered, is the fact that the transport mechanism of the secondary-active transporter to which SbtA belongs, is reversible (Sauer et al. 2022).

This work aimed to gain a deeper understanding of the mechanism of how SbtB affects transport activity of SbtA in *Synechocystis*. We show that formation of the SbtA:SbtB complex doesn't inhibit the HCO_3^- uptake but rather blocks leakage of bicarbonate in response to the energy state of the cell, suggesting a novel function of PII-like proteins as unidirectional valve in transport complexes preventing reverse transport of the substrate along the concentration gradient to the outside. We also expanded our model by reexamining the effect of the canonical PII protein in *Bacillus subtilis*, GlnK, on ammonium transport. The paradigm of a purely inhibitory action of PII-proteins on transporters, as derived from studies on GlnK-AmtB interaction in Gram-negative bacteria (Gruswitz et al. 2007), conflicts also with the finding that the homologue GlnK:AmtB complex in *B. subtilis* is strongly expressed under conditions of nitrogen-limitation, where active ammonium uptake is required (Detsch & Stülke 2003; Heinrich et al. 2006; Kayumov et al. 2011). Here we show that *B. subtilis* GlnK also acts as a valve to prevent ammonium leakage through AmtB, suggesting that this mechanism is a widely occurring feature among members of the PII superfamily**.**

Results

SbtB nucleotides diphosphohydrolase (apyrase) activity requires T-loop arginines and an oxidized R-loop

In our previous structural characterization of *Sc*SbtB (Selim et al. 2023), we observed that SbtB possesses a novel type of diphosphohydrolase (apyrase) activity, which is redox-dependent, converting either ATP or ADP to AMP. In summary, in the oxidized SbtB state, when the R-loop is folded via the C_{105}-C_{110} disulfide bridge (PDBs: 7R2Y, 7R2Z and 7R30), the adenine

nucleotides (ATP or ADP) are prone to hydrolysis due to a steric conflict of the oxidized R-loop with the T-loop, which forces the β- and γ-phosphates of ATP/ADP into a highly strained conformation, exposing the phosphates to hydrolytic attack. By contrast, *Sc*SbtB in the reduced state displays an unfolded R-loop, which allows the T-loop to adopt an ATP/ADP binding conformation, in which these nucleotides are protected from hydrolysis (PDBs: 7R31 and 7R32). Moreover, the T-loop arginine residues R_{43} and R_{46} were shown to be important for both ADP and ATP binding, as they coordinate the β- and γ-phosphates and K_{40} is situated close to the metal ion coordinating the β- and γ-phosphates (Selim et al. 2023). To experimentally validate the function of those residues, we created variants of SbtB, in which the T-loop residues K_{40}, R_{43} and R_{46} were substituted to alanine. Using isothermal titration colorimetry (ITC), we tested the ability of the protein variants to bind adenyl nucleotides (cAMP, AMP, ADP and ATP). In comparison to wildtype *Sc*SbtB, all the T-loop variants were strongly impaired in ADP and ATP binding as indicated by high K_d values, but less impaired in AMP or cAMP binding (Fig. 1A, Fig. S1, and Table 1), a property that was most prominently seen in the SbtB-R_{46}A variant.

Next, we selected the SbtB-R_{46}A variant to analyze in depth the stepwise nucleotide hydrolysis via high-performance liquid chromatography-mass spectrometry (HPLC-MS) (Fig. 1B,C, and Fig. S2). Whereas the wildtype SbtB protein converted ATP efficiently into AMP with a very small detectable amount of ADP, the apyrase activity of the SbtB-R_{46}A variant was strongly impaired similar to the mutated SbtB R-loop variant (C_{105}S+C_{110}S), which acts as a control for weak apyrase activity (Selim et al. 2023). By contrast, ADP was turned over by both SbtB-R_{46}A and the SbtB-C_{105}S+C_{110}S variants as efficiently as by wildtype *Sc*SbtB (Fig. 1C).

Together, the *in vitro* characteristics of the SbtB variants demonstrate the importance of the T-loop residues for both ADP and ATP binding and hydrolysis, and highlight the critical role of R_{46} in ATP binding and breakdown, and further confirm a role for the R-loop in tuning nucleotide hydrolysis.

Table 1: Dissociation constants for the binding of the adenyl nucleotides ATP, ADP, AMP, and cAMP to the WT-SbtB protein (Selim et al. 2018) and its variants as measured by ITC. NT: Not tested

Titrant/Protein	K_d **(μM) for** SbtB-WT	K_d **(μM) for** SbtB-K_{40}A	K_d **(μM) for** SbtB-R_{43}A	K_d **(μM) for** SbtB-R_{46}A
ATP	47.0	357.1	212.7	No binding
ADP	33.9	877.1	471.6	434.7
AMP	53.5	NT	NT	94.34
cAMP	21.3	66.9	83.3	31.3

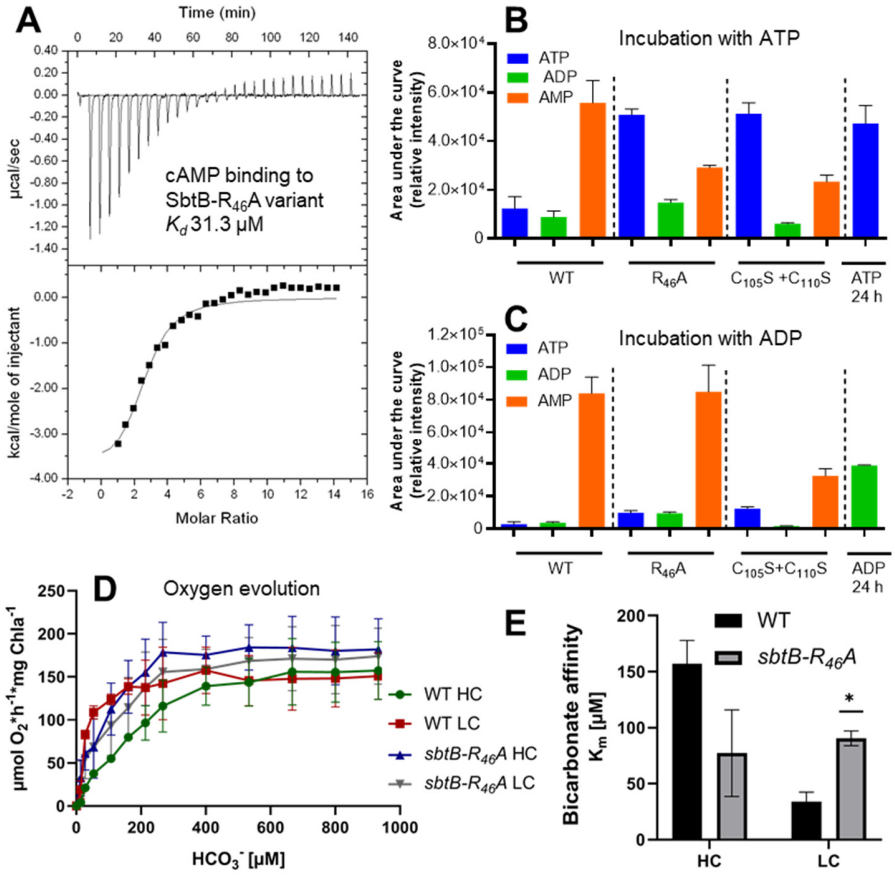

Fig. 1: Characterization of SbtB T- and R-loop variants. (A) Isothermal titration calorimetry (ITC) shows that SbtB-R_{46}A variant can still bind cAMP efficiently. (B,C) Nucleotide hydrolysis by SbtB wildtype and its variants (R_{46}A and C105S+C110S [+ve control]) were incubated with ATP (B) or ADP (C) for 24 h. In addition, equal amounts of ATP and ADP were incubated with the reaction buffer (without protein) for 24 h and indicated as 24 h of ATP or ADP, respectively. The obtained relative intensity for ATP is shown in blue, for ADP in green and for AMP in orange. (D,E) Phenotypic characterization of the *sbtB-R46A* mutant. (D) Bicarbonate-dependent photosynthetic rates per chlorophyll a (Chla) of WT and the *sbtB-R46A* mutant as a function of increasing HCO_3^- concentrations. Cells were acclimated to either high carbon (HC) or low carbon (LC) conditions (n = 3). (E) Bicarbonate affinity represented by the K_m (HCO_3^-) values of *Synechocystis* wild type (WT) and the *sbtB-R46A* mutant under either high carbon (HC; black bars) or low carbon (LC; gray bars) regimes. *: p<0.05.

Impact of SbtB apyrase activity on *Synechocystis* physiology

To further reveal the impact of ATP/ADP binding and hydrolysis on *Sc*SbtB function, we chose to characterize the SbtB-R_{46}A variant *in vivo* as this variant was most strongly impaired in ATP/ADP binding and hydrolysis *in vitro*. Therefore, we generated a *Synechocystis* strain in which the wildtype *sbtB* gene was replaced by a gene encoding the *sbtB-R46A* variant. Then, we measured the bicarbonate-dependent photosynthetic oxygen-evolution of this mutant (Fig. 1D) to determine the bicarbonate affinity (Fig. 1E). The wildtype cells exhibited low bicarbonate

affinity when adapted to high ambient C_i conditions (5% CO_2; indicated by HC), whereas they displayed high bicarbonate affinity when cultivated under C_i-limiting ambient conditions (0.04% CO_2; indicated by LC), in accord with a fully induced CCM. In our previous work, we showed that an SbtB-deficient mutant exhibited constitutive high bicarbonate affinity, even when acclimated to HC conditions. In low C_i-grown Δ*sbtB* cells, the maximal photosynthetic rate was lower than in wildtype cells, indicating an impaired function of the Calvin-Benson-Bassham (CBB) cycle (Selim et al. 2018), in agreement with the recently discovered additional function of SbtB in regulating entire CCM and glycogen synthesis in c-di-AMP dependent manner (Selim et al. 2021; Mantovani et al. 2022). Similar to the phenotype of the Δ*sbtB* mutant, the *sbtB-R*$_{46}$*A* mutant was unable to change its overall bicarbonate affinity in response to the changing C_i conditions. Irrespective of LC- or HC-conditions, the *sbtB-R*$_{46}$*A* cells displayed an affinity for bicarbonate in between the LC- and HC-acclimated wildtype cells, respectively. However, in contrast to the Δ*sbtB* mutant, the maximal photosynthetic rate of the *sbtB-R*$_{46}$*A* mutant at saturating C_i conditions was as high as in the wildtype (Fig. 1D), implying that SbtB-R_{46}A could complement the pleiotropic effect on the CBB-cycle, in agreement with its unimpaired ability to bind c-di-AMP (Fig. S3A). Immunoblot analyses also revealed that the *sbtB-R*$_{46}$*A* variant could still be partially recovered from the cytoplasmic membrane under HC conditions, indicating that its interaction with SbtA was not completely abrogated (Fig. S3). Furthermore, the *R*$_{46}$*A SbtB* variant complemented the defect of the Δ*sbtB* mutant in diurnal growth (Fig. S3B), which further suggests that this variant is able to fulfill additional functions of SbtB in accord with its ability to still bind c-di-AMP. Altogether, the *sbtB-R*$_{46}$*A* mutant appeared specifically impaired in its ability to change the CCM activity in response to the ambient C_i-supply, which involves SbtA function. This indicates that the ATP-binding and/or the stepwise hydrolysis by SbtB plays a crucial role in the regulation of SbtA activity.

SbtB acts as valve plug to prevent bicarbonate leaking out of the cells

Recently, it was reported that immediately after light to dark shifts, the uptake activity of SbtA ceases, independent of the presence of SbtB (Förster et al. 2023). This argues against a role for SbtB in rapidly switching off SbtA-mediated bicarbonate uptake. The assumption that the formation of SbtA:SbtB complex is required to allosterically inhibit bicarbonate uptake is also in conflict with the observation that a tight SbtA:SbtB-AMP complex is formed under LC conditions when AMP levels increase (Selim et al., 2018; Liu et al. 2021; Fang et al. 2021; Förster et al. 2023). Rather, under LC-conditions, cells require maximum bicarbonate uptake activity and should not inhibit the activity of the main bicarbonate transporter, SbtA. The assumption of SbtB

inhibiting SbtA activity under LC conditions is also inconsistent with the phenotype of the SbtB-deficient mutant, which showed growth impairment under LC (Selim et al. 2018, 2023). Our recent discovery that the nucleotide-bound states of SbtB are not static but may be interconverted via apyrase activity provides alternative explanations for the function of SbtB.

A so far overlooked possibility is that SbtB might serve as a dynamic valve plug to close the reverse diffusion of bicarbonate through SbtA, since it belongs to the secondary-active transporters, which operate by a reversible, bidirectional mechanism (Sauer et al. 2022). The cells invest much energy to maintain a Na^+-motif force at the cytoplasmic membrane, which is required for the Na^+-dependent HCO_3^- transporters, SbtA and BicA, to accumulate bicarbonate approximately 100-1000 times against the gradient under C_i-limiting conditions (Hagemann et al. 2021). According to these considerations, it should be beneficial for the cells to prevent HCO_3^- backward diffusion. To verify this assumption, first, we measured the intracellular ATP levels within *Synechocystis* cells after shifting cells from HC (2% CO_2) to LC conditions. During the first 3 h after the shift, the ATP levels dropped by 10%, whereas under prolonged C_i-limitation (24 h) the ATP levels dropped to almost 50% of the original ATP levels under HC condition (Fig. 2A), in agreement with increasing AMP levels under LC conditions (Selim et al. 2018). Next, to test our hypothesis whether SbtB could act as a safety-valve, we checked the leakage of ^{14}C-bicarbonate. Therefore, cells were loaded with ^{14}C-bicarbonate in the light, then cells were washed and incubated in bicarbonate-free medium in the dark for 5 min to measure leaked ^{14}C in the supernatant. In fact, the leakage of HCO_3^- in the Δ*sbtB* mutant was almost 50% higher than the wildtype cells (Fig. 2B).

All previous structural and biochemical data imply that the ATP-bound state of SbtB destabilizes the SbtA:SbtB interaction, while the AMP bound state stabilizes the interaction (Selim et al. 2018, 2023; Fang et al. 2021; Liu et al. 2021). Therefore, we assumed that the *sbtB-*R_{46}*A* variant would be preferentially in the AMP-bound state, based on its inability to bind and hydrolyze ATP (Fig. 1B, Fig. S1, and Table 1). To test how this affects bicarbonate leakage in the *sbtB-*R_{46}*A* mutant, we performed the ^{14}C-bicarbonate leakage assay. As expected, the *sbtB-*R_{46}*A* strain showed less HCO_3^- leakage than the wild type, implying that the SbtB-R_{46}A variant more efficiently prevents the backward diffusion of HCO_3^- through the SbtA tunnel, consistent with the constitutive AMP bound state of SbtB-R_{46}A and its inability to bind and hydrolyze ATP (Fig. 1B, and Fig. S1). These results are also in accordance with the membrane localization of SbtB-R_{46}A variant (Fig. S3C). Collectively, these results generally support our hypothesis that SbtB prevents backwards HCO_3^- transport. Moreover, the leakage experiments suggest that SbtB in wildtype cells dynamically changes between different states of interaction with SbtA

depending on the adenyl-nucleotide bound state, which would influence the T-loop conformations to regulate the HCO_3^- tunnel but not the transport activity of SbtA.

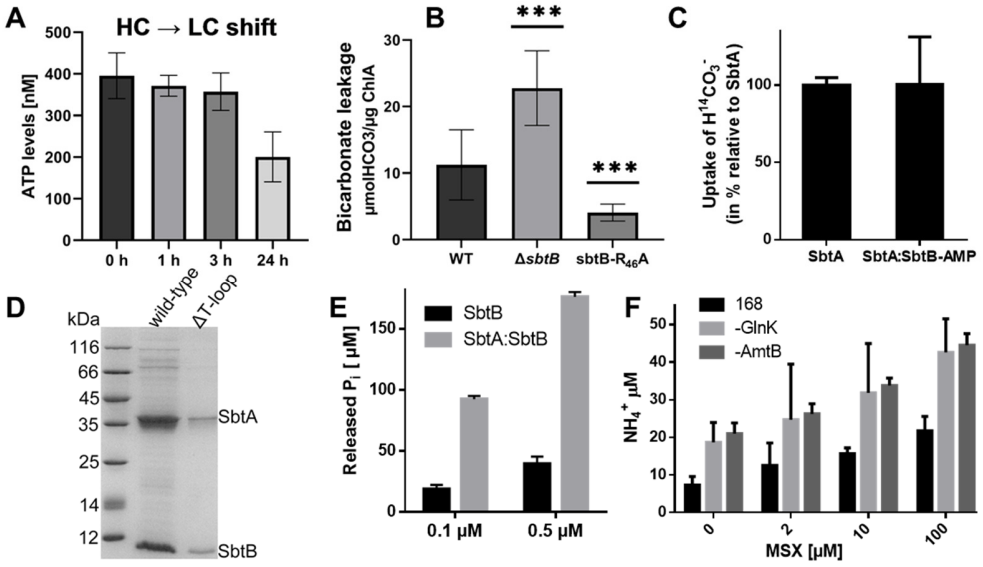

Fig. 2: Functional characterization of PII superfamily proteins *Sc*SbtB and *Bs*GlnK. (A) Intracellular ATP levels in *Synechocystis* cells after shift from HC (0) to LC (1, 3 and 24 h) conditions. (B) Physiological investigation of SbtB function as a plug. Levels of leaked ^{14}C-bicarbonate from WT, Δ*sbtB* and *sbtB-R$_{46}$A* mutant cells. ***:p<0.001. (C) Transport activity assays of SbtA or SbtA:SbtB complex in the presence of 1 mM AMP. The assays were performed in *E. coli* membrane vesicles using ^{14}C-bicarbonate. The vesicles from *E. coli* transformed by the empty pET28a plasmid were used as the negative control. (D) Interaction of SbtB ΔT-loop with SbtA compared to WT-SbtB. (E) Apyrase activity of SbtB alone or in complex with SbtA via phosphate release assay at 0.1 and 0.5 µM. (F) Level of leaked NH_4^+ from *B. subtilis* WT (strain 168), Δ*glnK* and Δ*amtB* mutants after treating the cells for 5 min with different concentrations of MSX, as indicated, to inhibit the GS activity to increase the intracellular levels of ammonia. For all graphs, the means and standard deviations were calculated and the data are presented as means ± SD.

SbtB does not influence the SbtA transport activity negatively

Recently, we revealed the mode of action of SbtA transport in presence of SbtB (PDB: 7CYF), which resembles an elevator alternating-access transport mechanism. In the SbtA:SbtB complex, when the SbtB T-loop is inserted into the inter-domain cleft of SbtA, it partially blocks the cytoplasmic substrate exit tunnel of SbtA and induces the cytoplasmic inward open conformation of SbtA by causing the SbtA subunits (core and gate domains) to undergo a significant rigid-body movement against each other (Liu et al. 2021). Intriguingly, the SbtB T-loop residue R_{46} has a dual function in stabilizing both SbtB-ATP and SbtA:SbtB interactions (Fang et al. 2021; Selim et al. 2023; Fig. S1). Based on the ability of the *sbtB-R$_{46}$A* variant to localize to the membrane (Fig. S3C), we assumed that SbtB would still interact partially with

SbtA even when the SbtB T-loop cannot be inserted firmly in SbtA. This complex would resemble the SbtA:SbtB complex with SbtB in the ATP bound state, and would correspond to either an SbtA-occluded conformation, in which the substrate tunnel is inaccessible from the intracellular or extracellular space, or to SbtA in fully open conformation, allowing HCO_3^- leakage. By contrast, when the SbtB T-loop is deeply inserted in SbtA and the SbtA:SbtB interaction is stabilized via AMP or ADP, the SbtB-AMP or SbtB-ADP bound states would not influence the inward transport activity but rather prevent the back-flux of accumulated HCO_3^-. Those assumptions were further validated experimentally by performing *in vitro* transport activity assays in membrane vesicles containing either SbtA alone or SbtA:SbtB complex in presence of AMP to promote the SbtA-inward state (Liu et al. 2021). The activity assays showed that the SbtB-AMP state in the complex does not influence on the HCO_3^- transport activity (Fig. 2C), compared to that of free SbtA, supporting our conclusions that SbtB doesn't block bicarbonate import by SbtA but only prevents the backward HCO_3^- flux (Fig. 2B). Also, we tested a T-loop variant (SbtB ΔT-loop), in which we deleted the entire T-loop so that the T-loop cannot be inserted into SbtA to determine whether the SbtB ΔT-loop variant can still interact with SbtA, resembling either the SbtA-occluded or the HCO_3^- leakage state(s). Indeed, the SbtB ΔT-loop variant was still able to complex with SbtA, despite its weak interaction compared to wildtype *Sc*SbtB (Fig. 2D). This further explains a previous result showing that in absence of AMP, SbtB was able to complex with SbtA in the inward active state, where the HCO_3^- substrate was clearly defined in SbtA when the SbtB T-loop was disordered (PDB: 7EGL) (Fang et al. 2021).

Structural bases for the role of SbtB in preventing the leakage

In order to get deeper insights into the T-loop independent SbtB:SbtA complex, which likely could resemble the weak SbtA:SbtB-ATP complex, we solved the structure of SbtA:SbtB ΔT-loop complex at 3.1 Å resolution by cryo-EM (Fig. S4). In the SbtA:SbtB ΔT-loop structure SbtA, forms a membrane-localized homotrimer with symmetric orientation towards the homotrimeric SbtB ΔT-loop facing from the cytoplasmic side (Fig. 3A). Without the T-loop, SbtB can still interact primarily with the cytoplasmic phase of SbtA via van der Waals' interactions to form a heterohexameric complex of trimer-trimer interphase, but the interactions are restricted mainly to TM2 and TM9 of SbtA and two loops of SbtB. Specifically, a salt bridge between Arg_{333} on TM9 and Glu_{13} on the loop between α1 and β1 of SbtB, as well as a hydrogen bond between Arg_{333} and Tyr_{87} on the loop between α2 and β4 (B-loop) could be found in the complex. In addition, Lys_{14} between α1 and β1 of SbtB could also form a salt bridge with Glu_{40} on TM2 of SbtA (Fig. 3A). It is noteworthy that this salt bridge is formed due to the more condensed

architecture of SbtA:SbtB ΔT-loop complex, which cannot be found in our previously reported SbtA:SbtB-AMP complex (PDB: 7CYF), where the T-loop is ordered and inserted into SbtA.

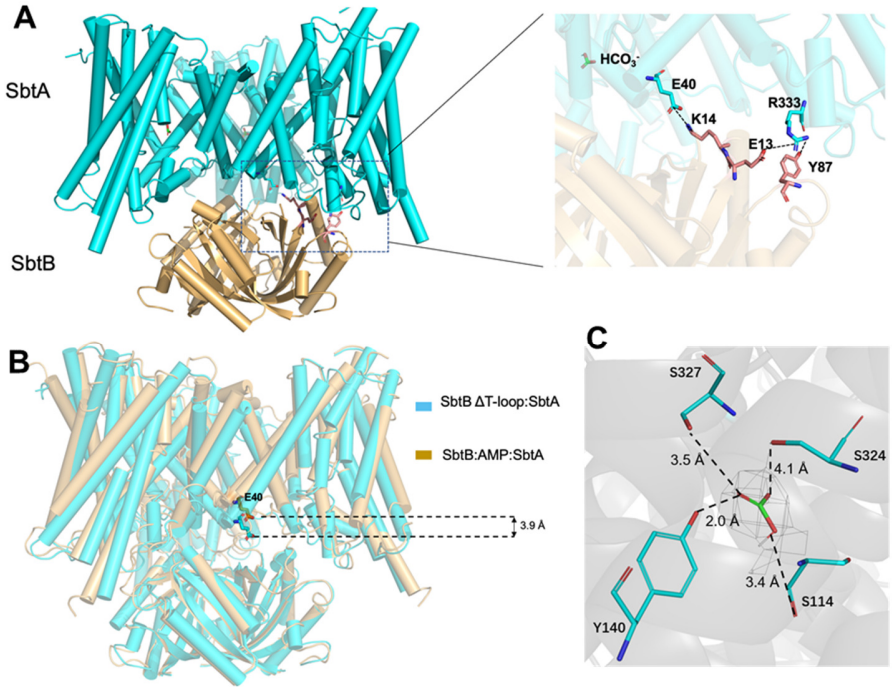

Fig. 3: cryo-EM structure of SbtA:SbtB ΔT-loop complex. (A) Overall structure of SbtA:SbtB ΔT-loop complex. SbtA is colored cyan and SbtB is colored brown. Inset in (A): A zoom-in displaying the interface of SbtA and SbtB. Interacting residues are shown as sticks. The salt bridge and hydrogen bonds are indicated as dotted line. (B) Superposition of SbtA:SbtB ΔT-loop complex and SbtA:SbtB-AMP complex (PDB:7CYF). SbtB ΔT-loop approaches to SbtA for ~3.9 Å measuring E_{40}. (C) The HCO_3^- binding site. The HCO_3^- molecule is shown as sticks and colored by atoms. The polar interactions are indicated by dashed lines. The cryo-EM density map of HCO_3^- is shown in gray mesh at 5 σ.

In fact, superposition of the two complexes yield an RMSD of 2.19 Å. While SbtB could almost be perfectly superposed to the previously obtained structure, SbtB ΔT-loop is approaching to SbtA by only about 3.9 Å (measuring Glu_{40}), which seems more compact and reminds of the elevator mechanism (Fig. 3B), probably due to the absence of the T-loop. This approach of SbtB ΔT-loop toward SbtA led to the relative shift between the gate domain and the core domains of SbtA. This shift causes the core domain of SbtA within the SbtA:SbtB ΔT-loop complex to be uplifted, while the gate domain in this complex (TM6b and the loop between TM6b-TM7) was immobile and superimposed perfectly with our previous SbtA:SbtB-AMP complex (PDB: 7CYF) (Fig. 4A). As a result, the HCO_3^- and Na^+ binding sites are relatively elevated by about 4.1 Å (measuring Ser_{114}) and 3.6 Å (measuring Phe_{110}), respectively.

Surprisingly, near the SbtA Ser_{114}, which was reported to form the HCO_3^- binding site (Liu et al. 2021; Fang et al. 2021), a clear electron density that perfectly matches HCO_3^- was observed (Fig. 3C, and Fig. S4E), despite the fact that no HCO_3^- was added during the purification. Although our buffer contained 300 mM Na^+, the Na^+-binding site did not appear occupied, supporting the notion that SbtA indeed possesses higher affinity towards HCO_3^- than to Na^+. The bicarbonate binding cavity is located at the interface between the gate domain and the core domain and interacts with Ser_{114}, Tyr_{140}, Ser_{324}, Ser_{327} (Fig. 3C).

We recently showed that the structure of free SbtA represents an occluded conformation (Liu et al. 2021). The superimposition of SbtA:SbtB ΔT-loop complex over the free SbtA (PDB: 7CYE) showed little difference and yielded an RMSD of 0.8 Å, indicating that the SbtA:SbtB ΔT-loop complex is also in the occluded conformation, where HCO_3^- binding site is inaccessible from either intracellular or extracellular side and the HCO_3^- molecule is trapped inside the SbtA tunnel. Moreover, the superimposition of SbtA:SbtB ΔT-loop complex over the SbtA:SbtB-AMP (PDB: 7CYF) complex, where the HCO_3^- binding site is accessible from the intracellular space, revealed that the gate and core domains of SbtA in the SbtA:SbtB-AMP complex undergo a significant rigid-body movement against each other. As a result, the core and gate domains of SbtA in the SbtA:SbtB-AMP complex (PDB: 7CYF) separate from each other keeping the complex in an inward-open conformation toward the cytoplasm (Fig. 4A). By contrast, the SbtA:SbtB ΔT-loop complex returns back to the original occluded state exhibited by free SbtA (PDB: 7CYE) (Fig. 4). Therefore, the SbtA:SbtB ΔT-loop complex structure could represent a snapshot of the leaked HCO_3^- trapped inside the SbtA tunnel when the SbtB T-loop is disordered. In this structure representing the occluded SbtA conformation of the HCO_3^- transport cycle, the intermolecular interactions within the complex are restricted to the SbtA core domain due to the absence of the SbtB T-loop (Fig. 3A). Of note, a close examination of the SbtA:SbtB complex (PDB: 7EGL) solved in absence of AMP by X-ray crystallography, where the SbtB T-loop was also disordered, revealed SbtA in an inward facing state and the HCO_3^- binding site in an accessible state from the intracellular space. Moreover, we simulated a tunnel starting from the binding site of HCO_3^- in this complex (PDB: 7EGL), and the tunnel is clearly blocked by the loop between TM6a and TM6b of SbtA in SbtA:SbtB ΔT-loop complex (Fig. 4B). This strongly supports that SbtB undergoes dynamic structural changes in the complex to regulate the SbtA transport activity. This interpretation solves the paradox of SbtA:SbtB complex formation under low C_i-conditions: instead of inhibiting bicarbonate uptake, SbtB prevents its leakage, as in the SbtA:SbtB-AMP complex, the cytoplasmic HCO_3^- tunnel entry of SbtA is partially closed (PDB: 7CYF).

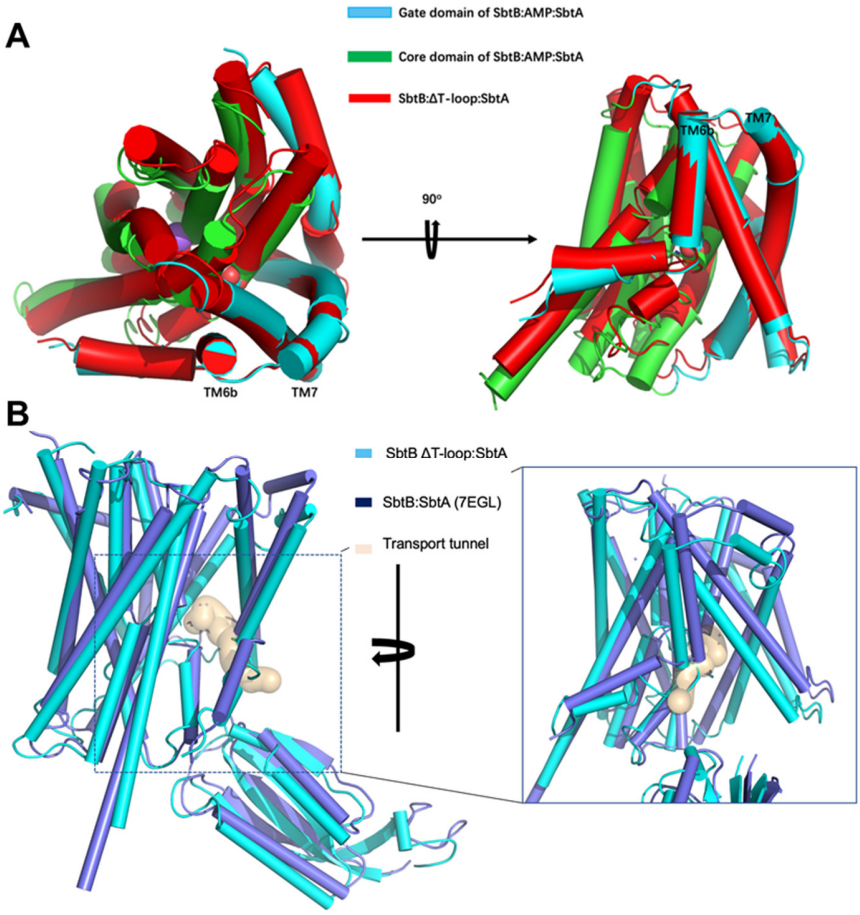

Fig. 4: Structural comparison between current and previous SbtA:SbtB complexes. (A) Superposition of SbtA from SbtA:SbtB ΔT-loop complex and SbtA:SbtB-AMP complex (PDB:7CYF), respectively. The core domain and gate domain of SbtA (7CYF) are colored differently as indicated. (B) A simulated tunnel starting from the binding site of HCO3- in SbtB:SbtA complex (PDB:7EGL). The superposition revealed that this tunnel is blocked by the loop between TM6a and TM6b of SbtA in the SbtA:SbtB ΔT-loop complex. The tunnel is simulated by Mole 2.

The presence of oxidized SbtB in the SbtA:SbtB complex further supports SbtB's apyrase activity

In light of the above results and their implications, the redox-regulated nucleotide hydrolysis activity of SbtB makes perfect sense, as it induces the tight SbtA:SbtB-AMP complex in the oxidized (dark) state. Within all reported SbtA:SbtB complexes (PDBs: 7CYF, 7EGL and 7EGK), the R-loop of SbtB forms the disulfide bridge including our recent SbtA:SbtB ΔT-loop complex (PDB: 7X1Q). We used the phosphate release assay to test the possibility that the apyrase activity of the oxidized SbtB might be further modulated by the interaction with SbtA. Indeed, we observed ≈ 4 fold increased phosphate release for SbtB in complex with SbtA as compared to SbtB alone (Fig. 2E). Finally, we assessed whether the reduced form of SbtB would still interact

with SbtA. The experiments demonstrated that the reduced state mimicking variants (SbtB-Δ104 and SbtB-C_{110}S) could still interact with SbtA in presence of AMP and dissociate in presence of ATP similar to wildtype SbtB (Fig. S5).

These results imply that the SbtB-redox switch does not influence the interaction with SbtA but rather accelerates the hydrolytic activity of SbtB in response to the cellular redox-state. Altogether, the formation of weak complexes of SbtB with SbtA in presence of ATP or of the SbtB ΔT-loop variant (Fig. 2) suggests that a fraction of SbtB is always close to SbtA in a sort of stand-by to open/close the SbtA tunnel.

GlnK is a valve plug for AmtB in *Bacillus subtilis*

Intriguingly, a paradox similar to what is described here for SbtA:SbtB interaction was previously reported for the canonical PII protein GlnK in *Bacillus subtilis*. In *E. coli*, GlnK was shown to interact and inhibit the ammonium transporter AmtB (Conroy et al. 2007). In *B. subtilis, Bs*GlnK is highly expressed when grown with a poor nitrogen source, for example, with nitrate as sole nitrogen source, which is slowly reduced to ammonia for its assimilation by glutamine synthetase (GS) (Heinrich et al. 2006; Forchhammer et al. 2022; Forchhammer & Selim 2020). Localization experiments revealed that *Bs*GlnK is AmtB-associated under poor nitrogen supply (Detsch & Stülke 2003; Kayumov et al. 2011), when the AmtB transporter should support maximum ammonium transport. When nitrate ions are reduced to ammonia/ammonium (which are in a pH dependent equilibrium), the membrane permeable ammonia molecules may diffuse out of the cells before being assimilated by GS. Hence under nitrogen-limiting conditions, a highly active ammonium transport is required to recuse ammonia/ammonium molecules that leaked out of the cells, and therefore, GlnK and AmtB are highly induced and interact (Heinrich et al. 2006). In light of the above results, instead of inhibiting ammonia uptake, *Bs*GlnK could also act as a valve plug to prevent the leakage of ammonium through the AmtB ammonia pore, similar to the action of SbtB on SbtA.

To proof this hypothesis, we first showed that *Bs*GlnK indeed localizes to the membrane in an AmtB-dependent manner (Fig. S6) by fusing YFP to the C-terminus of *Bs*GlnK and analyzing its localization under nitrate growing conditions. In an AmtB-deficient mutant (Δ*amtB*), the *Bs*GlnK-YFP was solely cytoplasmic localized and never found membrane-associated, while in *amtB+* strain the *Bs*GlnK-YFP was found to be membrane localized, which indicates that AmtB is required for recruiting *Bs*GlnK to the membrane. Next, ammonium leakage experiments were performed with *B. subtilis* strains deficient in either *glnK* or *amtB*. To further trigger intracellular ammonium formation in nitrate-growing cells, samples were treated with increasing

concentrations of the GS inhibitor methionine sulfoximine (MSX) to prevent ammonium assimilation by GS. GlnK- and AmtB-deficient cells displayed significantly higher extracellular ammonium levels than wildtype cells, clearly indicating ammonia leakage (Fig. 2F). The increased extracellular ammonium levels in AmtB-deficient cells illustrates the contribution of AmtB in counteracting ammonium leakage. Since in GlnK-deficient cells the same amount of extracellular ammonium was found as in the AmtB mutant, we can safely assume that in the absence of GlnK, AmtB cannot contribute to efficient ammonium scavenging. Apparently, in the absence of GlnK, the net uptake of AmtB is zero, which is the case if uptake equals the outward diffusion.

Discussion

Recently, we have shown that in addition to linear-adenine nucleotides, SbtB also binds the cyclic nucleotides cAMP and c-di-AMP, and that by sensing cAMP, SbtB modulates C_i uptake and metabolism (Selim et al. 2018, 2021). During the day, the cells incur high-energy costs to intracellularly accumulate elevated concentrations of bicarbonate under C_i-limiting conditions and to maintain the Na^+-homeostasis required for HCO_3^- transport to support efficient CO_2 assimilation and to synthesize glycogen as an energy reservoir for the night phases. The present work has established another important role for SbtB especially during dark periods or prolonged C_i-limitation. Our results clearly support the necessity of SbtB for the maintenance of high intracellular bicarbonate levels through its interaction with SbtA by preventing the outflux of the energetically expensive HCO_3^-. This also reduces energetically unfavorable Na^+ influx, which is counteracted by secondary active sodium-proton antiport activity, under conditions when no further bicarbonate is needed. Hence, SbtB is able to simultaneously play multiple roles, reminiscent of the multitasking PII signaling proteins (Forchhammer et al. 2022; Forchhammer & Selim 2020; Mantovani et al. 2023). Our results further indicate that the apyrase activity of *Sc*SbtB stabilizes AMP-bound SbtB at the membrane (Selim et al. 2023), in a process whereby the R-loop of SbtB senses the differential redox-state between periods of dark and light. This prevents backward diffusion of bicarbonate (and Na^+) out of the cells especially during night.

From the essence of the now available data on SbtB and its interaction partners, we propose the following refined model for the control of bicarbonate uptake through the SbtA:SbtB complex. In the light, when the R-loop is in a reduced state, there is competitive binding of adenine nucleotides to SbtB. During active photosynthesis, ATP is by far more abundant than AMP and ADP, whereas the concentration of cAMP depends on the CO_2 supply to the cells

rather than on the uptake of HCO_3^- by CCM (Hammer et al. 2006). *In vitro*, cAMP, known as a high-C_i signal, has the highest affinity for *Sc*SbtB and the cAMP-bound state prevents binding of AMP, which is known as low-C_i signal (Selim et al. 2018). This adenyl-nucleotide competition is able to activate/inactivate the SbtA transport activity according to the C_i availability. At high C_i, cyanobacteria accumulate high ATP and low AMP, while ATP levels drop and AMP levels increase under prolonged C_i-limitation (Fig. 2A; and Selim et al. 2018). Therefore, it seems plausible that during the day, most of SbtB is either in the ATP-bound state or in the soluble cAMP-bound state at high CO_2, while under prolonged C_i-limitation SbtB accumulates in the ADP/AMP-bound state and localizes to the membrane (Selim et al. 2018). Under those conditions of C_i-limitation and with help of SbtB, SbtA adapts an elevator alternating-access transport mechanism, as follows:

First, in the outward-open conformation, SbtA takes up the substrates HCO_3^- and Na^+. Binding of substrate seems to induce an SbtA-occluded conformation, as seen in our previous free SbtA structure (PDB: 7YCE), with bound Na^+-ion. Subsequently, in the presence of AMP-bound SbtB, the SbtB T-loop inserts deeply into the inter-domain cleft of SbtA forming the SbtA:SbtB-AMP complex (PDB: 7CYF). In this complex, upon SbtB binding, the SbtA core domains move toward the cytoplasmic space against the immobile SbtA gate domains, causing the SbtA-substrate tunnel to be in an inward-open conformation toward the cytoplasm, and accordingly facilitating the release of substrates into the cytoplasm. At the same time, the SbtB T-loop partially blocks the SbtA-substrate tunnel exit, preventing the backward transport activity but not the inward transport, in agreement with our transport assays of SbtA:SbtB-AMP complex and the ^{14}C-flux analysis of *ΔsbtB* mutant under C_i-limitation (Fig. 2B,C). When low C_i-acclimated cells are exposed to darkness, the ATP levels further drop and the SbtB apyrase activity, which seems to be even accelerated in the SbtA:SbtB complex (Fig. 2E), is further stimulated by the oxidation of the R-loop. This results in an increased population of ADP- and AMP-bound SbtB states, preventing the leakage of the HCO_3^- accumulated during the day through the cytoplasmic substrate tunnel entry. The subsequent rise in ATP levels and ATP binding to SbtB reorients the SbtB T-loop in another conformation incompatible with SbtA, causing SbtA to return back to its original occluded conformation, where the HCO_3^- molecule could be trapped inside the SbtA tunnel, as seen in the SbtA:SbtB ΔT-loop complex (PBD: 7X1Q). Altogether, this clearly supports our previous assumption that the transport model of SbtA is reminiscent of the elevator alternating-access transport mechanism (Liu et al. 2021), in which SbtB plays dual functions by inducing the inward conformation of the transporter and preventing the backward flux of the substrate from the cytoplasm (Fig. 5).

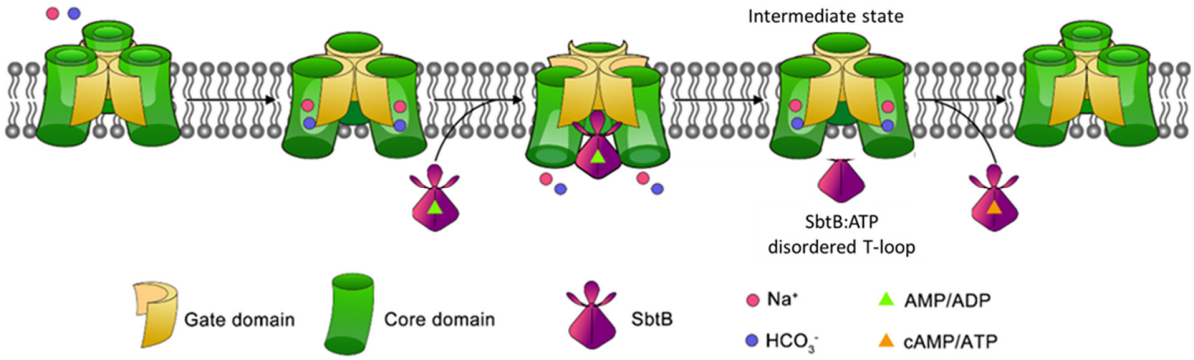

Fig. 5: A proposed elevator mechanism of trimeric Na^+-dependent HCO_3^- transporter SbtA. SbtA in an outward-open conformation recruits the substrates Na^+ and HCO_3^- from the extracellular space This is followed by a rigid-body movement of the core domain against the immobile gate domains upon SbtB binding, a process that is stabilized by binding of AMP to SbtB, presumable also by ADP. Afterwards, the substrates are released into the cytoplasm followed by the turnover of SbtA into the resting state. SbtB can also prevent the backward flux of HCO_3^- from the cytoplasm. When the T-loop of SbtB is in an incompatible conformation with SbtA, such as in ATP-bound SbtB (i.e. SbtB ΔT-loop), HCO_3^- can escape from the cytoplasm as seen trapped in the tunnel of SbtA.

The structural similarity of SbtB with canonical PII proteins suggest that other proteins of the PII family might play similar roles in controlling transport tunnels. Indeed, examination of ammonium leakage by *Bacillus* clearly showed that both AmtB and GlnK are required to prevent ammonia leakage when cells are grown with poor N-source such as nitrate. The enhanced leakage in the absence of GlnK can only be reasonably explained assuming that GlnK closes the cytoplasmic face of the ammonia transporter. However, this model necessarily requires that such a complex should be dynamic like a valve plug (Fig. S7). When ammonium ion binds to the outer face of AmtB, GlnK should not rigidly block the uptake. Like in a valve-plug, the T-loop should transiently flip away from the closing position. Possibly, the previously reported ATP-ADP turnover of PII proteins (Radchenko et al. 2013) plays a role in such a valve plug activity of GlnK. The identification of a similar mechanism in the regulation of two different uptake systems in phylogenetically distant bacteria, namely, SbtA in cyanobacteria and AmtB in firmicutes, points towards a conserved function of PII superfamily proteins in the control of substrate transport. However, further research is required to solve the details of such a process.

Modelling studies revealed that reintroduction of cyanobacterial CCM, especially of the HCO_3^--transporters SbtA and BicA, into plant chloroplasts could improve the carbon-assimilation rate and yield by 36-60%. However, the failure of reinstalling functional HCO_3^- transporters, in particularly SbtA alone, demonstrated a lack of understanding of how those bicarbonate transporters work. In our study, we highlight the importance of considering the simultaneous

reintroduction of regulatory factors such as SbtB. Remarkably, the strategy of co-expressing the *sbtAB* operon was shown to rescue the growth defect of *Corynebacterium glutamicum* carbonic anhydrase mutant under ambient air, and even more provided the wildtype cells with a growth advantage (Kirsch 2014), in contrast to *E. coli* (Du et al. 2014). In this regard, it is important to mention that the physiological meaning of SbtA:SbtB interaction in heterologous systems should be interpreted cautiously as the bioenergetics of *E. coli*, for example, is quite different from that in cyanobacteria.

Altogether, our study provides new insights into the signaling function of the PII superfamily and highlights the plasticity of PII proteins among different bacterial phyla. This is, for example, demonstrated by the ability of canonical PII to inhibit ammonium uptake and/or prevent ammonium leakage in phylogenetically distant bacteria *E. coli* and *Bacillus*, respectively.

Material and methods

Generation and purification of recombinant proteins

Plasmids and primers primers used in this study are listed in Supplementary (Table S1). The recombinant SbtB (wildtype or different variants [K_{40}A, R_{43}A, R_{46}A, and C_{105}S+C_{110}S]) proteins from *Synechocystis* sp. PCC 6803 (*Sc*SbtB) were expressed and purified as previously described (Selim et al. 2018; Lapina et al. 2018). Truncated C-terminal *Sc*SbtB protein (SbtB-ΔC), lacking the last 6 amino acids (C_{105}GPEGC_{110}) at the C-terminus, was constructed as described previously (Selim et al. 2023). The *Sc*SbtB-Δ104 plasmid was used as a DNA template to generate the *Sc*SbtB-C105S+C110S and *Sc*SbtB-C110S plasmids using primer pairs contain the C_{105}+C_{110} or C_{110} substitution into serine. For generation of *Sc*SbtB-K_{40}A, *Sc*SbtB-R_{43}A, and *Sc*SbtB-R_{46}A, we used the wildtype *Sc*SbtB plasmid as a DNA template and primer pairs contain the K_{40}, R_{43} or R_{46} substitution into alanine.

Generation of Mutants

The unicellular, freshwater cyanobacterium *Synechocystis sp.* PCC 6803 was used as a reference wildtype strain in this study. The Δ*sbtB-*R_{46}*A* mutants were generated with homolog recombination using the natural competence of *Synechocystis*, as described previously (Selim et al. 2018). For generation of Δ*sbtB-*R_{46}*A* mutant, in which the arginine 46 (R46) is replaced by alanine (designated *sbtB-*R_{46}*A*), a synthetic DNA fragment encoding *sbtB-R46A* with upstream and downstream regions of *slr1513* and spectinomycin resistant cassette (gBlock, IDT, USA) was cloned into BamHI-digested pUC19 vector using the Gibson assembly. The Δ*sbtB-*R_{46}*A* mutant was selected on BG_{11} plates supplemented with spectinomycin and verified by PCR. Plasmids and primers used in this study are listed in Supplementary (Table S1).

Protein expression and purification of SbtA-SbtB (ΔT-loop)

The codon-optimized genes *sbtA-sbtB* were synthesized by Genewiz Biotech and cloned into pET-28a (YouBio) carrying an N-terminal 6×His-tag on SbtA. The T-loop (Arg43-Ser52) truncation variant of SbtB (SbtB ΔT-loop for short) was constructed using a standard two-step PCR. The plasmids were transformed into *E. coli* C43 (WeidiBio), growing at 37°C in Luria Bertani (LB) culture medium, supplemented with 30 μg mL^{-1} kanamycin. Protein expression was induced by adding 0.4 mM isopropyl-β-D-thiogalactoside (IPTG, BioFroxx) when the OD_{600} nm reached 1.1~1.3 for 4 h at 37°C. Next, the cells were collected and resuspended in the lysis buffer containing 25 mM Tris-HCl pH 8.0, 300 mM NaCl, 5% glycerol and stored at -80°C before use.

For purification of SbtA-SbtB (ΔT-loop) complex, the collected cells were resuspended in the lysis buffer and lysed by AH-1500 High Pressure Homogeniser (ATS, inc.) with 5 passes at 700~800 bar. Cell debris was removed by centrifugation at 17,300 × g for 20 min. The supernatant was ultra-centrifuged at 200,000 × g for 1 h. The membrane was collected and solubilized by adding 1% (w/v) dodecyl-β-D-maltopyranoside (DDM, Bluepus) and 1% (w/v) Lauryl Maltose Neopentyl Glycol (LMNG, Anatrace) for 1 h at 4°C in the lysis buffer. After ultracentrifugation at 200,000 × g for 0.5 h, the supernatant was loaded onto a Ni-NTA resin (GE Healthcare), washed with the buffer containing 25 mM Tris-HCl pH 8.0, 300 mM NaCl, 5% glycerol, 40 mM imidazole, 0.02% (w/v) glyco-diosgenin (GDN, Anatrace) and then eluted with the same buffer supplemented with 300 mM imidazole. The eluate was then concentrated to about 1 mL by concentrators with a relative molecular mass cut-off of 10 KDa, and was applied to a Superdex 200 Increase 10/300 gel filtration column (GE Healthcare) equilibrated in the buffer containing 25 mM Tris-HCl pH 8.0, 300 mM NaCl, 5% glycerol, 0.02% (w/v) GDN. The peak fractions were collected for further procedures.

Cryo-EM sample preparation, data collection and processing

Aliquots of 3.5 μL SbtA-SbtB (ΔT-loop) samples (~6 mg/mL) were applied to the glow-discharged grids (Quantifoil holey carbon Cu R1.2/1.3 grid). Grids were blotted for 4.5 sec and plunge-frozen in liquid ethane vitrified by liquid nitrogen using Vitrobot Mark IV (FEI Company) at 8°C and 100% humidity.

The cryo-EM grids of SbtA-SbtB (ΔT-loop) were loaded into a Titan Krios transmission electron microscope (ThermoFisher Scientific) operating at 300 KeV with a Gatan K3 Summit direct electron detector. Totally 3,056 movie stacks were collected in a super-resolution mode with a defocus range from -1.2 to -2.0 μm. Each movie stack of 32 frames was exposed for 3.5 sec under a dose rate of 16 e/pixel/sec, resulting in a total dose of ~55 e $Å^{-2}$. All Krios data were collected using FEI EPU and then processed by cryoSPARC. After motion correction and contrast transfer function (CTF) estimation, a total of 1,787,952 particles were auto-picked and extracted at a 2-fold binned with a pixel size of 2.14 Å. After multi-rounds of 2D classification, 424,896 particles were used for 3D classification, searching for 3 classes using the references generated by the 3D initial model. 239,801 particles from the best class were re-extracted at a pixel size 1.07 Å without binning and used for Non-uniform 3D refinement yielding a 3.49 Å map. After multi-rounds of 3D classification, 178,612 particles were selected for final 3D refinement yielding a 3.10 Å map (Supplementary Fig. S4).

Model building and refinement

The initial model of SbtA-SbtB complex was built by fitting the SbtA-SbtB complex (PDB: 7CYF) structures into the map using the UCSF Chimera. Then model building and refinement was accomplished manually by Coot. The final structures showed good geometry and were further evaluated using MolProbity. A list of parameters of cryo-EM data collection, processing, structure determination and refinement is provided in the Supplementary (Table S2).

HCO_3^- leakage assay

Low carbon (LC) adapted cells (WT, Δ*sbtB*, and Δ*sbtB*-R46A) were centrifuged and re-suspended in fresh BG11 medium (pH 8.0) at an OD_{750} = 1.0. Two mL of each culture were transferred to 2 mL tubes, to which $H^{14}CO_3^-$ and HCO_3^- were added, each with a final concentration of 200 µM. The tubes were incubated at 30 °C under a constant light with an intensity of 50 µE for 10 minutes, after which 1 mL from each sample was placed in new tubes containing 200 µL of a mix of silicone oil AR20:AR200 (Sigma-Aldrich) with a ratio of 4:1 (to separate the cells from the culture media which contains $^{14C}HCO_3^-$). The samples were then centrifuged at 12.000 rpm for 20 minutes, the supernatant was discarded and the cells re-suspended in 650 µL carbon free BG11 media (pH 8.0), after which they were incubated in darkness for 5 minutes at room temperature (to prevent use of intracellular bicarbonate and allow it to leak from the cells). 250 µL of each sample were transferred into new tubes. The tubes were then centrifuged at 12000 rpm for 1 min to remove the cells and to collect the supernatant (to determine in the supernatant the amount of released ^{14}C outside the cells). In 5 mL scintillation vials (PerkinElmers), from each supernatant sample, 50 µL were added to 200 µL of 10 M formic acid (acid samples; all HCO_3^- and H_2CO_3 are converted to CO_2) and 50 µL were added to 200 µL of 1M NaOH (alkaline samples; all CO_2 and HCO_3^- are converted to H_2CO_3). After mixing, the samples were left to evaporate overnight at 70 °C. Finally, after evaporation, the samples were dissolved in 500 µL ddH_2O, then 5 mL of the scintillation cocktail UltimaGold (PerkinElmers) were added to each tube, and the scintillation counts were measured in a scintillograph (Tri-Carb 2810 TR, PerkinElmers). For calculation, the acid samples were subtracted from the alkaline samples to determine the amount of radioactively labelled C_i that has evaporated from the solutions (which corresponds to the C_i that leaked from the cells). Simplified scheme is presented in (Fig. S8).

High-performance liquid chromatography-mass spectrometry (HPLC-MS) analysis of SbtB ATPase/ADPase activity

Purified SbtB wildtype, $R_{46}A$ and $C_{105}S+C_{110}S$ protein variants were dialyzed overnight at 4°C in Tris-HCl buffer [50 mM Tris/HCl, 200 mM NaCl, 1 mM $MgCl_2$; pH 7.4]. 300 µM of the dialyzed enzyme was then incubated in a rotary shaker with 300 µM ATP or ADP at 28 °C in a total volume of 100 µl (as control 300 µM of either ATP or ADP was incubated in a buffer without enzyme) for 24 h. Next, the proteins were precipitated by addition of 100 µl $CHCl_3$ and centrifuged for 10 min centrifugation at 21000 x g at 4 °C.

Supernatants were taken and dried in a vacuum concentrator at room temperature for 2-4 h. Finally, pellets were solved in 30 µl of Millipore water and analyzed by HPLC-MS.

Nucleotide analysis was performed using an ESI-TOF mass spectrometer (micrO-TOF II, Bruker) operated in negative ion mode (mass range 85-900 m/z) and connected to an UltiMate 3000 HPLC system (Dionex). Five µl of each sample or standards (ATP, AMP or AMP) were injected into the SeQuant ZIC-pHILIC column (Merck, PEEK 150 × 2.1 mm, 5 µm) and the HPLC system was run with a flow rate of 0.2 ml/min as previously described (Kästle et al. 2015; Gratani et al. 2018) with only modified 35-minute gradient program: 5 minutes of 82% buffer A (CH_3CN) and 18% buffer B (100 mM $(NH_4)_2CO_3$, pH 9); 20 minutes of a linear gradient from 82% to 42% buffer A; and finally, 10 minutes of 82% buffer A. The nucleotide analysis was done using the program UmetaFlow (Kontou et al. 2023) by calculating the area under the curve (relative intensity) of the extracted ion chromatograms for ATP (505.989 m/z), ADP (426.022 m/z) and AMP (346.056 m/z). HPLC-MS experiment was performed in three biological replicates and presented in GraphPad Prism 8.4.3 as mean ±SD.

Preparation of membrane vesicles

The right-side-out membrane vesicles were prepared according to the previous report (Liu et al. 2021). Briefly, the process was started with the preparation of osmotically sensitive *E. coli* cells. The empty plasmid or plasmids carrying SbtA or SbtA:SbtB were transformed into *E. coli* C43. Then cells were cultured in M63 medium (2 g $(NH_4)_2SO_4$, 13.6 g KH_2PO_4, 0.5 mg $FeSO_4 \cdot 7H_2O$, 0.246 g $MgSO_4 \cdot 7H_2O$, 4.2 g KOH, 0.2% glucose, 0.1% casamino acids and 0.1 ml 0.5% vitamin B_1 per liter) and induced with 0.4 mM IPTG at 37 °C for 4 h. The culture was centrifuged at 16000 × g to harvest the cells and the pellet was washed twice with 10 mM Tris-HCl, pH 8.0 on ice. The cells were weighted and resuspended with 30 mM Tris-HCl, pH 8.0, and 20% sucrose, and flash-frozen with liquid nitrogen.

Next, the thawed cells were diluted with 30 mM Tris-HCl, pH 8.0, and 20% sucrose (1g wet weight, per 80 mL) supplemented with 10 mM EDTA-KOH, pH 7.0 and 0.5 mg/mL lysozyme, and swirled for 30 min by means of a magnetic stirrer at room temperature. The protoplast suspensions were centrifuged at 16,000 × g for 15 min and the pellet was resuspended in 10 mL buffer containing 0.1M KH_2PO_4/K_2HPO_4, pH 6.6, 20 mM $MgSO_4$ and homogenized by ULTRA-TURRAX (IKA). The suspension was poured directly into 300-fold volumes of 50 mM KH_2PO_4/K_2HPO_4, pH 6.6 supplemented with 100 µg/mL DNase and 100 µg/mL RNase. The lysate was incubated for 15 min at 37°C with vigorous swirling. Then, 10 mM EDTA-KOH was supplemented and the lysate was incubated for another 15 min. Afterwards, 15 mM $MgSO_4$ was supplemented in the lysate. In the end, the lysate was centrifuged at 16,000 g for 30 min and the pellet was centrifuged at 45,000 × g for 30 min to isolate the membranes.

The isolated membranes were homogenized in a solution of 0.1 M KH_2PO_4/K_2HPO_4, pH 6.6, containing 10 mM EDTA on ice. Then, the suspension was centrifuged at 800 × g until the supernatant fluid was clear. The pellet was washed 4~6 times by centrifugation at 45,000 × g for 30 min in the solution of 0.1 M KH_2PO_4/K_2HPO_4, pH 6.6, containing 10 mM EDTA on ice. Finally, the obtained membrane vesicles were

resuspended by homogenization in the transport assay buffer[5] (50 mM CHES-KOH pH 9.0, 0.3 mM $MgSO_4$, 0.26 mM $CaCl_2$, 0.22 mM K_2HPO_4) at a concentration of 5 mg/mL (wet weight), frozen in small aliquots in liquid nitrogen and stored in -80°C before use within a week for the best performance. The amounts of proteins in the membrane vesicles for each preparation were quantified by purifying the proteins from the same batch of cells by Coomassie brilliant blue staining.

Transport activity assays

For each assay sample, 50 µL of membrane vesicles were thawed. The substrates of 12 mM NaCl and 0.1 nCi ^{14}C labeled $NaHCO_3$ (~12 µM, American Radiolabled Chemicals) were added in the system supplemented with the transport assay buffer (50 mM CHES-KOH pH 9.0, 0.3 mM $MgSO_4$, 0.26 mM $CaCl_2$, 0.22 mM K_2HPO_4) to 100 µL. All reactions were performed at 30 4°C for 30 s and terminated by rapid filtration on a glass filter (25 mm GF/F, Whatman) by suction, followed by immediate wash of the filter with 10 mL of the washing buffer (the transport assay buffer supplemented with 120 mM $NaHCO_3$ to prevent back flow). The filters were soaked in 3 mL ULTIMA Gold (PerkinElmer) overnight before liquid scintillation counting. The vesicles prepared with induced *E. coli* transformed by the empty plasmid pET-28a were tested as the control group.

ATPase activity assays

ATPase activities were measured using the ATPase colorimetric Assay Kit (Innova Biosciences) in 96-well plates at OD_{630} nm. The protein was added in the reaction buffer consisting of 25 mM Tris–HCl pH 8.0, 50 mM KCl, 2 mM $MgCl_2$, and 2 mM ATP (Sigma) to 80 µL as one reaction sample. Reactions were performed at 37°C and the amount of released phosphate group (P_i) was quantitatively measured using a SpectraMax iD5 Multi-Mode Microplate Reader (Molecular Devices). The control groups in the absence of proteins were subtracted as background for each data point.

Isothermal titration calorimetry (ITC)

ITC experiments were performed as previously described (Selim et al. 2018, 2019) at 20°C using a VP-ITC microcalorimeter (MicroCal) or Malvern-Microcal PEAQ-ITC in Tris-HCl buffer pH 7.9 and 150 mM NaCl buffer pH 8.0. For determination of binding isotherms, *Sc*SbtB wildtype or mutant variants (30 µM trimeric concentration) were titrated against ATP, ADP, AMP, and cAMP, as indicated.

ATP quantification

For quantification of intracellular ATP levels, *Synechocystis* sp. PCC 6803 cells were cultivated under high CO_2 (HC, 2% CO_2) bubbling. A shift to low CO_2 (LC, 0.04% CO_2) was achieved by replacing CO_2 with ambient air bubbling. 2 ml samples were taken at each time point and disrupted in three consecutive boiling-freezing cycles. Thereby, cells were frozen in liquid nitrogen followed by an immediate heated to 99°C under 1400 rpm agitation. After lysis, cell debris was pelleted by centrifugation at 25.000g at 4°C for

1 min. The ATP content of the supernatant was immediately measured using the ATP Determination Kit (A22066) [Molecular Probes™] according to manufacturer's instructions. Standard curves were generated using a dilution series (0 – 1000 nm) of ATP.

NH_4^+ leakage assay

The release NH4+ into media was measured for wildtype *B. subtilis*, and both Δ*glnK* and Δ*amtB* mutants (Detsch & Stülke 2003; Kayumov et al. 2011) using either glutamate dehydrogenase (GDH) assay and phenol-hypochlorite (PH) assay. The results of both assays were comparable. In the GDH assay, GDH converts ammonia with α-ketoglutaric acid and NADPH to form L-glutamate and $NADP^+$. The decrease in absorbance at 340 nm, due to the oxidation of NADPH to $NADP^+$, is proportional to the ammonia concentrations in the media. The assay was performed using 200 µl of media supernatant in 100 mM phosphate buffer pH 7.4. For PH assay, a reaction mixture of 1:1:1 of solution I (10 mg sodium nitroprusside dissolve in 95.33 ml H_2O add 4.67 ml liquefied Phenol [1.07 g/ml]), solution II (25 ml of 2.5 M NaOH, 0.7 ml NaClOH [150-180 g/liter], 74.3 ml H_20), and samples (media supernatant), was incubated for 15 min at room temperature and the change of the color at 625 nm was recorded and correlated to a calibration curve of standard HN_4^+ solutions.

References

1. Boogerd FC, Ma H, Bruggeman FJ, van Heeswijk WC, García-Contreras R, Molenaar D, Krab K, Westerhoff HV. AmtB-mediated NH3 transport in prokaryotes must be active and as a consequence regulation of transport by GlnK is mandatory to limit futile cycling of NH4(+)/NH3. FEBS Lett. 2011 Jan 3;585(1):23-8. doi: 10.1016/j.febslet.2010.11.055.
2. Chen Y, Cann MJ, Litvin TN, Iourgenko V, Sinclair ML, Levin LR, Buck J. Soluble adenylyl cyclase as an evolutionarily conserved bicarbonate sensor. Science. 2000 Jul 28;289(5479):625-8. doi: 10.1126/science.289.5479.625.
3. Conroy MJ, Durand A, Lupo D, Li XD, Bullough PA, Winkler FK, Merrick M. The crystal structure of the Escherichia coli AmtB-GlnK complex reveals how GlnK regulates the ammonia channel. Proc Natl Acad Sci U S A. 2007 Jan 23;104(4):1213-8. doi: 10.1073/pnas.0610348104.
4. Detsch C, Stülke J. Ammonium utilization in Bacillus subtilis: transport and regulatory functions of NrgA and NrgB. Microbiology (Reading). 2003;149(Pt 11):3289-3297. doi: 10.1099/mic.0.26512-0.
5. Du J, Förster B, Rourke L, Howitt SM, Price GD. Characterisation of cyanobacterial bicarbonate transporters in E. coli shows that SbtA homologs are functional in this heterologous expression system. PLoS One. 2014 Dec 23;9(12):e115905. doi: 10.1371/journal.pone.0115905.
6. Fang S, Huang X, Zhang X, Zhang M, Hao Y, Guo H, Liu LN, Yu F, Zhang P. Molecular mechanism underlying transport and allosteric inhibition of bicarbonate transporter SbtA. Proc Natl Acad Sci U S A. 2021 Jun 1;118(22):e2101632118. doi: 10.1073/pnas.2101632118.

7. Forchhammer K, Selim KA, Huergo LF. New views on PII signaling: from nitrogen sensing to global metabolic control. Trends Microbiol. 2022 Aug;30(8):722-735. doi: 10.1016/j.tim.2021.12.014.
8. Forchhammer K, Selim KA. Carbon/nitrogen homeostasis control in cyanobacteria. FEMS Microbiol Rev. 2020 Jan 1;44(1):33-53. doi: 10.1093/femsre/fuz025.
9. Förster B, Mukherjee B, Rourke LM, Kaczmarski JA, Jackson CJ, Price DG. Adenylnucleotide-mediated binding of the PII-like protein SbtB contributes to controlling activity of the cyanobacterial bicarbonate transporter SbtA. 2023, *eLife***12**:RP88488. doi: 10.7554/eLife.88488.1
10. Gratani FL, Horvatek P, Geiger T, Borisova M, Mayer C, Grin I, Wagner S, Steinchen W, Bange G, Velic A, Maček B, Wolz C. Regulation of the opposing (p)ppGpp synthetase and hydrolase activities in a bifunctional RelA/SpoT homologue from Staphylococcus aureus. PLoS Genet. 2018 Jul 9;14(7):e1007514. doi: 10.1371/journal.pgen.1007514.
11. Gruswitz F, O'Connell J 3rd, Stroud RM. Inhibitory complex of the transmembrane ammonia channel, AmtB, and the cytosolic regulatory protein, GlnK, at 1.96 A. Proc Natl Acad Sci U S A. 2007 Jan 2;104(1):42-7. doi: 10.1073/pnas.0609796104.
12. Hagemann M, Song S, Brouwer EM. Inorganic carbon assimilation in cyanobacteria: Mechanisms, regulation, and engineering. 2021; In Hudson P, Lee SY, Nielsen J (eds.) Cyanobacteria Biotechnology, Wiley-Blackwell Biotechnology Series, Chapter 1, 1-31, https://doi.org/10.1002/9783527824908.ch1
13. Hammer A, Hodgson DR, Cann MJ. Regulation of prokaryotic adenylyl cyclases by CO2. Biochem J. 2006 Jun 1;396(2):215-8. doi: 10.1042/BJ20060372.
14. Heinrich A, Woyda K, Brauburger K, Meiss G, Detsch C, Stülke J, Forchhammer K. Interaction of the membrane-bound GlnK-AmtB complex with the master regulator of nitrogen metabolism TnrA in Bacillus subtilis. J Biol Chem. 2006 Nov 17;281(46):34909-17. doi: 10.1074/jbc.M607582200.
15. Kaczmarski JA, Hong NS, Mukherjee B, Wey LT, Rourke L, Förster B, Peat TS, Price GD, Jackson CJ. Structural Basis for the Allosteric Regulation of the SbtA Bicarbonate Transporter by the P_{II}-like Protein, SbtB, from *Cyanobium* sp. PCC7001. Biochemistry. 2019 Dec 17;58(50):5030-5039. doi: 10.1021/acs.biochem.9b00880.
16. Kästle B, Geiger T, Gratani FL, Reisinger R, Goerke C, Borisova M, Mayer C, Wolz C. rRNA regulation during growth and under stringent conditions in Staphylococcus aureus. Environ Microbiol. 2015 Nov;17(11):4394-405. doi: 10.1111/1462-2920.12867.
17. Kayumov A, Heinrich A, Fedorova K, Ilinskaya O, Forchhammer K. Interaction of the general transcription factor TnrA with the PII-like protein GlnK and glutamine synthetase in Bacillus subtilis. FEBS J. 2011 May;278(10):1779-89. doi: 10.1111/j.1742-4658.2011.08102.x.
18. Kirsch KM. The impact of CO2 on inorganic carbon supply and pH homeostasis in *Corynebacterium glutamicum*. 2014; PhD thesis; University of Klön. https://kups.ub.uni-koeln.de/5545/

19. Kontou EE, Walter A, Alka O, Pfeuffer J, Sachsenberg T, Mohite OS, Nuhamunada M, Kohlbacher O, Weber T. UmetaFlow: an untargeted metabolomics workflow for high-throughput data processing and analysis. J Cheminform. 2023 May 12;15(1):52. doi: 10.1186/s13321-023-00724-w.
20. Lapina T, Selim KA, Forchhammer K, Ermilova E. The PII signaling protein from red algae represents an evolutionary link between cyanobacterial and Chloroplastida PII proteins. Sci Rep. 2018 Jan 15;8(1):790. doi: 10.1038/s41598-017-19046-7.
21. Liu XY, Hou WT, Wang L, Li B, Chen Y, Chen Y, Jiang YL, Zhou CZ. Structures of cyanobacterial bicarbonate transporter SbtA and its complex with PII-like SbtB. Cell Discov. 2021 Aug 10;7(1):63. doi: 10.1038/s41421-021-00287-w.
22. Mantovani O, Haffner M, Selim KA, Hagemann M, Forchhammer K. Roles of second messengers in the regulation of cyanobacterial physiology: the carbon-concentrating mechanism and beyond. Microlife. 2023 Feb 23;4:uqad008. doi: 10.1093/femsml/uqad008.
23. Mantovani O, Reimann V, Haffner M, Herrmann FP, Selim KA, Forchhammer K, Hess WR, Hagemann M. The impact of the cyanobacterial carbon-regulator protein SbtB and of the second messengers cAMP and c-di-AMP on CO_2 -dependent gene expression. New Phytol. 2022 Jun;234(5):1801-1816. doi: 10.1111/nph.18094.
24. Radchenko MV, Thornton J, Merrick M. P(II) signal transduction proteins are ATPases whose activity is regulated by 2-oxoglutarate. Proc Natl Acad Sci U S A. 2013 Aug 6;110(32):12948-53. doi: 10.1073/pnas.1304386110.
25. Sauer DB, Marden JJ, Sudar JC, Song J, Mulligan C, Wang DN. Structural basis of ion - substrate coupling in the Na^+-dependent dicarboxylate transporter VcINDY. Nat Commun. 2022 May 12;13(1):2644. doi: 10.1038/s41467-022-30406-4.
26. Selim KA, Ermilova E, Forchhammer K. From cyanobacteria to Archaeplastida: new evolutionary insights into PII signalling in the plant kingdom. New Phytol. 2020 Aug;227(3):722-731. doi: 10.1111/nph.16492.
27. Selim KA, Haase F, Hartmann MD, Hagemann M, Forchhammer K. P_{II}-like signaling protein SbtB links cAMP sensing with cyanobacterial inorganic carbon response. Proc Natl Acad Sci U S A. 2018 May 22;115(21):E4861-E4869. doi: 10.1073/pnas.1803790115.
28. Selim KA, Haffner M, Burkhardt M, Mantovani O, Neumann N, Albrecht R, Seifert R, Krüger L, Stülke J, Hartmann MD, Hagemann M, Forchhammer K. Diurnal metabolic control in cyanobacteria requires perception of second messenger signaling molecule c-di-AMP by the carbon control protein SbtB. Sci Adv. 2021 Dec 10;7(50):eabk0568. doi: 10.1126/sciadv.abk0568.
29. Selim KA, Haffner M, Mantovani O, Albrecht R, Zhu H, Hagemann M, Forchhammer K, Hartmann MD. Carbon signaling protein SbtB possesses atypical redox-regulated apyrase activity to facilitate regulation of bicarbonate transporter SbtA. Proc Natl Acad Sci U S A. 2023 Feb 21;120(8):e2205882120. doi: 10.1073/pnas.2205882120.

30. Selim KA, Haffner M, Watzer B, Forchhammer K. Tuning the in vitro sensing and signaling properties of cyanobacterial PII protein by mutation of key residues. Sci Rep. 2019 Dec 12;9(1):18985. doi: 10.1038/s41598-019-55495-y.
31. Selim KA, Tremiño L, Marco-Marín C, Alva V, Espinosa J, Contreras A, Hartmann MD, Forchhammer K, Rubio V. Functional and structural characterization of PII-like protein CutA does not support involvement in heavy metal tolerance and hints at a small-molecule carrying/signaling role. FEBS J. 2021 Feb;288(4):1142-1162. doi: 10.1111/febs.15464.
32. Steegborn C, Litvin TN, Levin LR, Buck J, Wu H. Bicarbonate activation of adenylyl cyclase via promotion of catalytic active site closure and metal recruitment. Nat Struct Mol Biol. 2005 Jan;12(1):32-7. doi: 10.1038/nsmb880.
33. Wheatley NM, Eden KD, Ngo J, Rosinski JS, Sawaya MR, Cascio D, Collazo M, Hoveida H, Hubbell WL, Yeates TO. A PII-Like Protein Regulated by Bicarbonate: Structural and Biochemical Studies of the Carboxysome-Associated CPII Protein. J Mol Biol. 2016 Oct 9;428(20):4013-4030. doi: 10.1016/j.jmb.2016.07.015.

Acknowledgments

The project was funded by grants from the German Research Foundation (DFG) as part of the priority research program (SPP1879) to MHag (HA 2002/24-1) and to KF (Fo195/18-1), and by the Federal Ministry of Education and Research (BMBF) and the Baden-Württemberg Ministry of Science as part of the Excellence Strategy of the German Federal and State Governments to KAS (Projektförderung: PRO-SELIM-2022-14). KF, MB and KAS acknowledge the infrastructural support by the Cluster of Excellence “Controlling Microbes to Fight Infections (CMFI)” (EXC 2124–390838134). This work was supported by the Strategic Priority Research Program of the Chinese Academy of Sciences (grant numbers XDB37020301 and XDA24020302). MB gratefully acknowledge the financial support from the DFG (TRR261: project ID 398967434) and (CMFI: project ID 390838134) to Christoph Mayer. We also thank Dr. Yongxiang Gao (Cryo-EM Center) and Mr. Jishu Ren (Isotope Laboratory) at the University of Science and Technology of China for cryo-EM image acquisition and for the transport assays, respectively. The PhD thesis of PW is supported by the German Academic Scholarship Foundation (Studienstiftung des deutschen Volkes).

Author contributions

KAS and KF conceived, initiated, and supervised the whole research; KAS, WH, MHag CZ and KF designed research; MHaf, WH, OM, RRW, KH, and MB performed research; KAS and WH analyzed data and prepared the figures; and KAS wrote the manuscript with inputs from MHag, WH, and KF. All authors approved the final version of the manuscript.

Competing interests

The authors declare no competing interest.

Author contributions

The impact of the cyanobacterial carbon-regulator protein SbtB and of the second messengers cAMP and c-di-AMP on CO_2-dependent gene expression.

Mantovani O, Reimann V, Haffner M, Herrmann FP, Selim KA, Forchhammer K, Hess WR, Hagemann M 2022**.** *New Phytologist* 234:1801-1816. doi: 10.1111/nph.18094.

- Experiments planning
- Transcriptome analysis
- Pigmentation analysis
- Oxygen evolution experiments
- Metabolome measurements

The redox-sensitive R-loop of the carbon control protein SbtB contributes to the regulation of the cyanobacterial CCM

Mantovani O, Haffner M, Walke P, Elshereef AA, Wagner B, Petras D, Forchhammer K, Selim KA, Hagemann M 2023**.** *ResearchGate* DOI: 10.21203/rs.3.rs-3292191/v1

- Experiments planning
- R-loop mutant strains establishment
- Growth experiments
- Glycogen measurements
- Membrane association experiments
- Bicarbonate leakage measurements

PII signal transduction superfamily acts as a valve plug to control bicarbonate and ammonia homeostasis among different bacterial phyla.

Haffner M, Hou WT**, Mantovani O,** Walke PR, Hauf K, Liu XY, Borisova M, Hagemann M, Zhou CZ, Karl Forchhammer, Khaled A. Selim 2023**.** *bioRxiv* DOI: 10.1101/2023.08.10.552651

- R-loop mutant strains establishment
- Execution of R46A mutant strain experiments
- Planning and execution of bicarbonate leakage experiments

Diurnal metabolic control in cyanobacteria requires perception of second messenger signaling molecule c-di-AMP by the carbon control protein SbtB.

Selim KA, Haffner M, Burkhardt M, **Mantovani O**, Neumann N, Albrecht R, Seifert R, Krüger L, Stülke J, Hartmann MD, Hagemann M, Forchhammer K 2021. *Science Advances*, *7*(50), DOI: 10.1126/sciadv.abk0568

- Oxygen evolution analysis

Red/far-red light signals regulate the activity of the carbon-concentrating mechanism in cyanobacteria.

Oren, N., Timm, S., Frank, M., **Mantovani, O**., Murik, O., & Hagemann, M. (2021). *Science Advances*, *7*(34), DOI: 10.1126/sciadv.abg0435

- *Synechocystis ⊿sbtB* mutant creation
- *Synechocystis* cultures preparation

Carbon signaling protein SbtB possesses atypical redox-regulated apyrase activity to facilitate regulation of bicarbonate transporter SbtA

Selim, K. A., Haffner, M., **Mantovani, O.,** Albrecht, R., Zhu, H., Hagemann, M., Forchhammer, K., & Hartmann, M. D. (2023). *Proceedings of the National Academy of Sciences of the USA*, 120(8), DOI: 10.1073/pnas.2205882120

- *Synechocystis* mutants creation

Scientific curriculum

Personal information

Name: Oliver Mantovani

Date of birth: 06.05.1995 in Tradate (Italy)

Academic work experience

2019 – 2023 PhD Student
Faculty of Mathematics and Natural Sciences
Institute of Biosciences
Department of Plant Physiology
Rostock University
Supervisor: Prof. Dr. Martin Hagemann

Academic education

2014 – 2017 Bachelor of Science. Biological sciences and technologies (Scienze e tecnologie biologiche)
Università degli studi dell'Insubria, Varese, Italy

2017 – 2019 Master of Science. Biotechnology
Uppsala University, Uppsala, Sweden

Theses

BSc *Heterologous expression of chitinases from metagenomic libraries*. (*Espressione eterologa di chitinasi da librerie metagenomiche*).
Department of Fermentation Chemistry and Microbial Biotechnology.
Università degli Studi dell'Insubria, Varese, Italy
Supervisor: Prof. Dr. Flavia Marinelli

MSc *Enhancing terpenoid production yields by over-expression of membrane proteins in Cyanobacteria.*

Ångström Laboratory, Department of Molecular Biomimetics; Microbial Chemistry. Uppsala University, Uppsala, Sweden.
Supervisor: Dr. Dennis Dienst

List of publications

2020 Dienst, D., Wichmann, J., **Mantovani, O**., Rodrigues, J. S., & Lindberg, P. (2020). High density cultivation for efficient sesquiterpenoid biosynthesis in Synechocystis sp. PCC 6803. *Scientific Reports*, 10(1), Article 1, DOI: 10.1038/s41598-020-62681-w

2021 Selim, K. A., Haffner, M., Burkhardt, M., **Mantovani, O.,** Neumann, N., Albrecht, R., Seifert, R., Krüger, L., Stülke, J., Hartmann, M. D., Hagemann, M., & Forchhammer, K. (2021). Diurnal metabolic control in cyanobacteria requires perception of second messenger signaling molecule c-di-AMP by the carbon control protein SbtB. *Science Advances*, *7*(50), DOI: 10.1126/sciadv.abk0568

2021 Oren, N., Timm, S., Frank, M., **Mantovani, O.,** Murik, O., & Hagemann, M. (2021). Red/far-red light signals regulate the activity of the carbon-concentrating mechanism in cyanobacteria. *Science Advances*, *7*(34), DOI: 10.1126/sciadv.abg0435

2022 **Mantovani, O.,** Reimann, V., Haffner, M., Herrmann, F. P., Selim, K. A., Forchhammer, K., Hess, W. R., & Hagemann, M. (2022). The impact of the cyanobacterial carbon-regulator protein SbtB and of the second messengers cAMP and c-di-AMP on CO2-dependent gene expression. *New Phytologist*, 234(5), 1801–1816, DOI: 10.1111/nph.18094

2023 Selim, K. A., Haffner, M., **Mantovani, O.,** Albrecht, R., Zhu, H., Hagemann, M., Forchhammer, K., & Hartmann, M. D. (2023). Carbon signaling protein SbtB possesses atypical redox-regulated apyrase activity to facilitate regulation of bicarbonate transporter SbtA. *Proceedings of the National Academy of Sciences of the USA*, 120(8), DOI: 10.1073/pnas.2205882120

2023 **Mantovani, O**., Haffner, M., Selim, K. A., Hagemann, M., & Forchhammer, K. (2023). Roles of second messengers in the regulation of cyanobacterial physiology: The carbon-concentrating mechanism and beyond. *microLife*, 4, DOI: 10.1093/femsml/uqad008

Pre-prints

2023 **Mantovani O.,** Haffner M., Walke P., Elshereef A.A., Wagner B., Petras D., Forchhammer K., Selim K.A., Hagemann M. (2023) The redox-sensitive R-loop of the carbon control protein SbtB contributes to the regulation of the cyanobacterial CCM**.** *ResearchGate* DOI: 10.21203/rs.3.rs-3292191/v1

2023 Haffner M, Hou WT, **Mantovani O**, Walke PR, Hauf K, Liu XY, Borisova M, Hagemann M, Zhou CZ, Karl Forchhammer, Khaled A. Selim (2023).

PII signal transduction superfamily acts as a valve plug to control bicarbonate and ammonia homeostasis among different bacterial phyla. *bioRxiv* DOI: 10.1101/2023.08.10.552651

2023 Haffner, M., **Mantovani, O**., Spät, P., Maček, B., Hagemann, M., Forchhammer, K., & Selim, K. A. (2023). Diurnal rhythm causes metabolic crises in the cyanobacterial mutants of c-di-AMP signalling cascade (p. 2023.11.14.567006). *bioRxiv* DOI: 10.1101/2023.11.14.567006

Conference posters and presentations

MIKAT Symposium "*Cyanobacteria - From gene and protein functions to biotechnology*" - 12-13 December 2019 - Leipzig, Germany

Poster: Linking second messenger nucleotide signalling with CO_2 homeostasis in cyanobacteria: Photosynthesis and metabolism in *sbtB*-mutants

SPP1879 Progress Meeting 28-29 February 2020 - Göttingen, Germany

Poster: Linking second messenger nucleotide signalling with CO2 homeostasis in cyanobacteria: Photosynthesis and metabolism in *sbtB*-mutants

Virtual SPP1879 Progress Meeting 20 May 2021

Talk: Role of the second messenger c-di-AMP and the carbon-control protein SbtB on diurnal life cycle in cyanobacteria

German-Japanese Meeting on Green Aquatic Biology 02-03 March 2022 – Potsdam, Germany

Talk: The redox-sensitive C-terminal extension in the carbon control protein SbtB adjusts inorganic carbon acclimation towards changing light conditions

SPP1879 International Symposium "*Nucleotide Second Messenger Signalling in Bacteria*" 22–25 May 2022 – Berlin, Germany

Poster: Role of second messengers, carbon control protein SbtB and its C-terminal region in the regulation of carbon metabolism

CCM10 Meeting 6-8 July 2022 – Princeton, USA

Talk: Role of second messengers, carbon control protein SbtB and its C-terminal region in the regulation of carbon metabolism

CYANO2022 "*7th Early Career Researcher Symposium on Cyanobacteria*" – 26-28 September 2022 – Leipzig, Germany

Poster: The role of the redox-sensitive C-terminal extension in the carbon concentrating mechanism protein SbtB

Statutory declaration

I herewith formally declare that I have written this submitted dissertation independently. I have not used any outside source except for those quoted in the manuscript.

I have marked and listed all literary work used for the production of this academic work.

Location/Date Oliver Enrico Mantovani

_____

Special thanks

I want to especially thank my supervisor Prof. Dr. Martin Hagemann for giving me the opportunity to work on this project and for his excellent support during my PhD, providing both the guidance and motivation that I needed.

I want to thank my collaborators of the Plant Physiology group as well, for their help in the lab and for creating an enjoyable work environment. Special thanks also to Karl Forchhammer, Khaled Selim and Michael Haffner from the University of Tübingen for the enjoyable project collaboration. Lastly, I want to thank my parents for their continuous support and for giving me the opportunity to study abroad, which led to me to work on this project.